vegetation parameters cci

CCI+ Vegetation Parameters

Product Validation and Intercomparison Report (CRDP-2)

Fernando Camacho, Jorge Sánchez-Zapero, Enrique Martínez-Sánchez

November 2025

vito remote sensing | UNIVERSITY OF TWENTE. ITC | EOLAB | FastOpt | HYGEOS | Imperial College London | University of Antwerp

Distribution list

Author(s)	:	Fernando Camacho, Jorge Sánchez-Zapero and Enrique Martínez-Sánchez
Reviewer(s)	:	Else Swinnen, Christiaan van der Tol
Approver(s)	:	Marin Tudoroiu
Issuing authority	:	VITO

Change record

Release	Date	Pages	Description of change	Editor(s)/Reviewer(s)
V2.0	22/10/2025	All	First version of CDRP-2	See above
V2.1	22/11/2025	p. 75	Annex VI added after reviewer comments	See above

Executive summary

CCI+ Vegetation Parameters (CCI+ VP) is part of the European Space Agency (ESA) Climate Change Initiative. It aims at the identification, development and improvement of algorithms for the consistent retrieval of vegetation Essential Climate Variables (ECVs) Leaf Area Index (LAI) and fraction of Absorbed Photosynthetically Active Radiation (fAPAR) from multi-platform and multi-mission satellite data and interact with the user community to match their requirements. The work plan includes three cycles, in which different data sources are combined, the algorithms' scientific and operational maturity is increased, and user feedback is incorporated. This Product Validation and Intercomparison Report (PVIR) presents the quality assessment results of the Climate Research Data Package cycle 2 (CRDP-2) LAI and fAPAR products, retrieved using the OptiSail algorithm from multi-sensor input data covering 01/2000 - 12/2020. The dataset was generated over a latitudinal North-South transect and over a selection of sites ensuring global representativeness (LAND VALidation sites, LANDVAL) and supporting validation activities (i.e., sites with available ground data). The validation methodology, described in the Product Validation Plan [VP-CCI_D1.3_PVP_V2.0], follows standardized validation protocols for satellite-based biogeophysical products, fully compliant with the best practices for LAI product validation of the Committee on Earth Observation Satellites Land Product Validation subgroup (CEOS LPV). Several performance criteria were evaluated, including completeness, spatial consistency, temporal consistency, error evaluation (i.e., accuracy, precision and uncertainty), conformity testing and stability, by comparison with ground-based (i.e., CEOS DIRECT 2.1 database, the Ground-Based Observations for Validation (GBOV) V3.4, quality controlled (QC) maps over forest sites, and the *Analyse Multidisciplinaire de la Mousson Africaine* (AMMA) project ground data over grassland sites, and satellite-based (i.e., Copernicus Climate Change Service (C3S) V3, Copernicus Land Monitoring Service (CLMS) 1km V2 and MODIS V6.1) references.

This validation demonstrates overall good quality of the CRDP-2 dataset. The LAI and fAPAR spatial distributions are generally consistent and reliable across most regions, with only some spurious unrealistic values in northern latitudes in winter, but also abnormally low LAI values over equatorial forests; the application of quality layers effectively removes most unrealistic values, but the LOW_QUALITY flag has a strong impact during the mono-sensor years (2000-2006) and also removes large amount of good retrievals. LAI and fAPAR temporal variations are consistent with references and captures both peaks and low values well. CCI VP CRDP-2 shows overall good agreement with ground-based references. As compared with DIRECT 2.1 effective LAI, CRDP-2 largely underestimates LAI (B = -0.69 (-74%)), more than the C3S effective LAI products (B = -0.48, -43%), even though the correlation is slightly better. For fAPAR, CRDP-2 show good results (B = -0.01, RMSD = 0.10) very similar to CLMS (B = -0.02, RMSD = 0.09), and better than C3S (RMSD = 0.13) and MODIS (RMSD = 0.11). Comparison with GBOV V3.4_QC shows good correlations with true LAI (R = 0.92), while for fAPAR, CRDP-2 shows good results (B = -0.06, RMSD = 0.09) slightly worse than CLMS, but outperforming MODIS and C3S products. Over AMMA sites, CRDP-2 underestimates LAIeff (B = -0.12 (-40.2%), RMSD = 0.29) but outperforming C3S, and for fAPAR shows slight overestimation (B = 0.05 (21.5%), RMSD = 0.14), comparable CLMS products and better than C3S and MODIS. Overall, as compared with ground references, CRDP-2 provides low accuracy for effective LAI, but accurate and reliable fAPAR retrievals across in-situ datasets, reducing known issues of C3S and MODIS products for low values. Compared to satellite products, CRDP-2 slightly underestimates C3S LAI (bias = -7.9%, RMSD = 0.34), while for fAPAR it shows good agreement with CLMS (R = 0.96, RMSD = 0.08) and large discrepancies with C3S. By biome, CRDP-2 shows higher LAI than C3S in forests (notably EBF) but slightly lower in crops and herbaceous sites, and fAPAR values close to CLMS but slightly lower for forest sites. CRDP-2 shows improved intra-annual precision compared to C3S and MODIS products, and demonstrates good inter-annual precision, with no apparent impact from the ingestion of new input data, confirming its robustness across different sensors. However, a trend in mean and percentile values over the period, and a change in the bias particularly after 2012 reveals some stability limitations in the later years,

probably linked to the inclusion of some sensors. Therefore, users are advised to exercise caution when using this dataset for interpreting long-term trends.

Table of Contents

List of Acronyms 7
List of Figures 10
List of Tables 13
1 Introduction 14
1.1 Scope of this document 14
1.2 Related documents 14
1.3 General definitions 15
2 Validation methodology 17
2.1 Overall validation procedure 17
2.1.1 Product Completeness 17
2.1.2 Spatial consistency 18
2.1.3 Temporal consistency 18
2.1.4 Error evaluation and conformity testing 18
2.1.5 Stability 20
2.1.6 Summary of validation procedure 21
2.2 Satellite products 23
2.2.1 Evaluated dataset: CCI+VP CRDP-2 23
2.2.2 Reference satellite products 24
2.3 Reference ground datasets 27
2.3.1 CEOS LPV DIRECT 2.1 27
2.3.2 The Ground-Based Observations for Validation V3 (GBOV V3) 28
2.3.3 AMMA – Cycle Atmosphérique et Cycle Hydrologique (CATCH) system 29
3 Results 30
3.1 Product completeness 30
3.2 Spatial consistency 32
3.2.1 Visual inspection of maps 32
3.2.2 Analysis of differences 35
3.3 Temporal consistency 36
3.4 Error evaluation (direct validation) 40
3.4.1 Comparison with DIRECT 2.1 40
3.4.2 Comparison with GBOV V3.4 42
3.4.3 Comparison with AMMA 44
3.5 Error evaluation (product intercomparison) 46
3.5.1 Overall analysis 46
3.5.2 Analysis per biome type 47

3.5.3 Intra-annual precision 49
3.5.4 Inter-annual precision 50
3.6 Stability 51
4 Conclusions 54
5 References 58
Annex I: Additional temporal profiles over the whole period 62
Annex II: Scatterplot between CCI+ VP and reference satellite products per biome type 67
Annex III: Hovmöller plots of the bias with C3S and CLMS fAPAR and over LANDVAL V1.1 sites for BQ retrievals 69
Annex IV: CRDP-2 LAI and fAPAR mean values per biome type across relevant sensor periods 70
Annex V: Temporal evolution of bias between CRDP-2 and MODIS fAPAR products evaluated over LANDVAL V1.1 sites best quality per biome type 72
Annex VI: CRDP-2 vs CRDP-1 LAI, fAPAR product intercomparison 75

LIST OF ACRONYMS

1D	One Dimensional
3D	Three Dimensional
4SAILH	Scattering of Arbitrarily Inclined Leaves, with 4-stream extension and hot-spot
AD	Automatic Differentation
AMMA	Analyse Multidisciplinaire de la Mousson Africaine
ANN	Artificial Neural Network
APU	Accuracy, precision, uncertainty
ATBD	Algorithm Theoretical Basis Document
AVHRR	Advance Very High Resolution Radiometer
B	mean Bias
BQ	Best Quality
BRDF	Bidirectional Reflectance Distribution Function
BRF	Bidirectional Reflectance Factor
C3S	Copernicus Climate Change Service
Cal/Val	Calibration/Validation
CATCHA	Couplage de l'Atmosphère Tropicale et du Cycle Hydrologique
CCI	Climate Change Initiative
CCRS	Canada Centre for Remote Sensing
CDR	Climate Data Record
CRDP	Climate Research Data Package
CEOS - LPV	Committee on Earth Observation Satellites - Land Product Validation subgroup
CGLS	Copernicus Global Land Service
CI	Clumping Index
CLMS	Copernicus Land Monitoring Service
CRDP	Climate Research Data Package
CUL	CULtivated
CYCLOPES	Project acronym: 'satellite products for change detection and carbon cycle assessment at the regional and global scales'
DBF	Deciduous Broadleaf Forest
DIRECT	Database of 3x3 km LAI and fAPAR data for validation
EBF	Evergreen Broadleaf Forest
ECV	Essential Climate Variable
EO	Earth Observation
EPS	EUMETSAT Polar System
ESA	European Space Agency
*f*APAR	fraction of Absorbed Photosynthetically Active Radiation
*f*IPAR	fraction of Intercepted Photosynthetically Active Radiation
*f*COVER	fraction of vegetation COVER
FLO	FLOoded
FPAR	Fraction of absorbed Photosynthetically Active Radiation
FRM4Veg	Fiducial Reference Measurements for Vegetation
FVC	Fraction of Vegetation Cover
GBOV	Ground-Based Observations for Validation

GCOS	Global Climate Observing System
GSD	Ground Sampling Distance
HER	HERbaceous
ICOS	Integrated Carbon Observation System
IER	Institut d'Economie Rurale
ILCA	International Livestock Centre for Africa
ImagineS	Implementation of Multi-scale Agricultural Indicators Exploiting Sentinels
IUPAC	International Union of Pure and Applied Chemistry
JCGM	Joint Committee for Guides in Metrology
LAI	Leaf Area Index
LANDVAL	Land validation sites
LP	Land Product
LPV	Land Product Validation
LSB	Least Significant Bit
MAD	Median Absolute Deviation
MAR	Major axis regression
MD	Median Deviation
MetOp	Meteorological Operational
MODIS	Moderate resolution imaging spectrometer
N	Number of samples
NASA	National Aeronautics and Space Administration
NDVI	Normalized Difference Vegetation Index
NEON	National Ecological Observatory Network
NIR	Near InfraRed
NLF	Needle-Leaf Forest
NOAA	National Oceanic and Atmospheric Administration
OF	Other Forests
OLCI	Ocean and Land Colour Instrument
OLIVE	OnLine Validation Exercise
OLS	Ordinary Least Squares
PAR	Photosynthetically Active Radiation
PDF	Probability Density Function
PQAR	Product Quality Assessment Report
PROBA-V	PRoject for On-Board Autonomy Vegetation instrument
PROSPECT	PROperties of leaf SPECTtra
PUG	Product User Guide
PVIR	Product Validation and Intercomparison Report
PVP	Product Validation Plan
QC	Quality Controlled
R	Correlation coefficient
RM	Reference measurement
RMSD	Root Mean Square Deviation
RTM	Radiative Transfer Model
S2LP	Sentinel-2 Land Processor
SAFARI-2000	Southern African Regional Science Initiative – 2000
SAVS	Surface Albedo Validation Sites

SBA	Sparse vegetated and Bare Areas
SCF_QC	Five level confidence score
SHR	SHRublands
SNPP	Suomi National Polar-orbiting Partnership
SPOT	Système Pour l'Observation de la Terre
STD	Standard deviation
TARTES	Two-streAm Radiative Transfer in Snow
TERN	Terrestrial Ecosystem Research Network
TIP	Two-stream Inversion Package
TOC	Top Of Canopy
TSGF	Temporal Smoothing Gap Filling
VALERI	Validation of Land European Remote sensing Instruments
VIIRS	Visible/Infrared Imager Radiometer Suite
VEGA	VEGetation Algorithm
VIS	VISible
VGT	VEGETATION instrument onboard of SPOT4 & 5
VP	Vegetation Parameters
WGCV	Working Group on Calibration and Validation
WMO	World Meteorological Organization

LIST OF FIGURES

Figure 1: Sensor input data used to generate CCI+VP CRDP-2. 23
Figure 2: Sampling strategy: A) selected sites from LANDVAL, GBOV V3, DIRECT_2.1 and AMMA. B) Latitudinal Transect (see red rectangles) 24
Figure 3: Maps of missing values (computed over LANDVAL sites) during 2000-2020 considering all (left) and best quality (right) pixels. From top to bottom: CCI+ VP, C3S V3 and CLMS V2 fAPAR products. 31
Figure 4: Temporal variation of the percentage of missing values over LANDVAL sites for CCI+VP CRDP-2 (2000–2020), considering different quality flags: bit 8 (RETR_UNTRUSTED, red), bit 9 (RETR_LOW_QUALITY, blue), and pixels with $\chi^2 < 0.5$ (yellow). Pixels excluded by all flags (BQ) are shown in grey. 32
Figure 5: Maps CCI+ VP CRDP-2 LAI over the whole transect for all pixels (top) and best quality pixels (bottom) in mid-February for 2004 (left), 2012 (middle) and 2019 (right). Grey values correspond to missing or low-quality pixels. 33
Figure 6: Maps CCI+ VP CRDP-2 LAI over the whole transect for all pixels (top) and best quality pixels (bottom) in mid-July for 2004 (left), 2012 (middle) and 2019 (right). Grey values correspond to missing or low-quality pixels. 34
Figure 7: Maps CCI+ VP CRDP-2 fAPAR over the whole transect for all pixels (top) and best quality pixels (bottom) in mid-February for 2004 (left), 2012 (middle) and 2019 (right). Grey values correspond to missing or low-quality pixels. 34
Figure 8: Maps CCI+ VP CRDP-2 FAPAR over the whole transect for all pixels (top) and best quality pixels (bottom) in mid-July for 2004 (left), 2012 (middle) and 2019 (right). Grey values correspond to missing or low-quality pixels. 35
Figure 9: Map of differences between CCI+ VP CRDP-2 and C3S V3 LAI products (best quality pixels) over the whole transect in mid-June 2012. 35
Figure 10: Maps of differences between CCI+ VP CRDP-2 and C3S V3, CLMS V2 and MODIS V6.1 fAPAR products (best quality pixels) over the whole transect in mid-June 2012 36
Figure 11: Temporal profiles of BQ retrievals over two selected LANDVAL evergreen broadleaved forest (EBF) sites of CCI+ VP (purple), C3S V3 (green), CLMS V2 (blue) and MODIS V6.1 (orange). Note: CCI+ VP and C3S provide effective LAI values. 37
Figure 12: Same as in Figure 11 but over two selected GBOV deciduous broadleaved forests (DBF). Crosses in GBOV data indicates out-of-range estimates. 37
Figure 13: Same as in Figure 11 but over two selected GBOV needle-leaf forests (NLF). 37
Figure 14: Same as in Figure 11 but over two selected LANDVAL cultivated sites. 38
Figure 15: Same as in Figure 11 but over two selected AMMA herbaceous sites. 38
Figure 16: Same as in Figure 11 but over two selected LANDVAL shrublands sites. 38
Figure 17: Same as in Figure 11 but over two selected LANDVAL sparse and bare areas. 39
Figure 18: Scatter plots between CCI+ VP CRDP-2 (left) and C3S V3 (right) LAI products versus DIRECT 2.1 LAIeff ground-based maps. 'EBF' stands for evergreen broadleaved forests, 'DBF' for deciduous broadleaved forests, 'NLF' for needle-leaf, 'OF' for other forests, 'CUL' for cultivated, 'HER' for herbaceous, 'SHR' for shrublands and 'R' for rice. Green and blue lines stand for goal and threshold levels, respectively. The brown line represents the MAR fit, while the green and blue lines indicate the goal and threshold levels, respectively. 40
Figure 19: Scatter plots between CCI+VP CRDP-2 (top left), C3S V3 (top right), CLMS V2 (bottom left) and MODIS V6.1 (bottom right) fAPAR products versus DIRECT 2.1 fAPAR ground-based maps. 'EBF' stands for evergreen broadleaved forests, 'DBF' for deciduous broadleaved forests, 'NLF' for needle-leaf, 'OF' for other forests, 'CUL' for cultivated, 'HER' for herbaceous, 'SHR' for shrublands and 'R' for rice. The brown line represents the MAR fit, while the green and blue lines indicate the goal and threshold levels, respectively. 41

Figure 20: Scatter plots between CCI+ VP CRDP-2 (left) and C3S V3 (right)LAI products versus GBOV ground-based V3.4_QC LAI. 'DBF' stands for deciduous broadleaved forests, 'NLF' for needle-leaf and 'OF' for other forests. The brown line represents the MAR fit, while the green and blue lines indicate the goal and threshold levels, respectively. 42
Figure 21: Scatter plots between CCI+VP CRDP-2 (top left), C3S V3 (top right), CLMS V2 (bottom left) and MODIS V6.1 (bottom right) fAPAR products versus GBOV ground-based V3.4_QC fAPAR. 'DBF' stands for deciduous broadleaved forests, 'NLF' for needle-leaf and 'OF' for other forests. The brown line represents the MAR fit, while the green and blue lines indicate the goal and threshold levels, respectively. 43
Figure 22: Scatter plots between CCI+ VP CRDP-2 (left) and C3S V3 (right) LAI products versus AMMA LAIeff ground data. The brown line represents the MAR fit, while the green and blue lines indicate the goal and threshold levels, respectively. 44
Figure 23: Scatter plots between CCI+VP CRDP-2 (top left), C3S V3 (top right), CLMS V2 (bottom left) and MODIS V6.1 (bottom right) fAPAR products against AMMA fAPAR ground data. The brown line represents the MAR fit, while the green and blue lines indicate the goal and threshold levels, respectively. 45
Figure 24: Scatter plot between CCI+VP CRDP-2 and C3S V3 satellite LAI products (colorbar represents density of points). Computation over best quality retrievals over LANDVAL sites for years 2004, 2012 and 2019. The brown line represents the MAR fit, while the green and blue lines indicate the goal and threshold levels, respectively. 46
Figure 25: Scatter plots between CCI+VP CRDP-2 and reference satellite C3S V3, CLMS V2 and NASA V6.1 fAPAR products (colorbar represents density of points). Computation over best quality retrievals over LANDVAL sites for years 2004, 2012 and 2019. The brown line represents the MAR fit, while the green and blue lines indicate the goal and threshold levels, respectively. 46
Figure 26: Left: Distribution of LAI values for CCI+ VP CRDP-2 and C3S V3 products per main biome type for years 2004, 2012 and 2019. Right: Violin-plots of the bias between CCI+ VP and C3S V3 products per biome type. In the violin-plots, red horizontal bars indicate median values, horizontal dashed black lines stretch from first and third quartile of the data, and vertical black lines stretch from the lower and upper adjacent value. 47
Figure 27: Left: Distribution of fAPAR values for CCI+ VP CRDP-2, C3S V3, CLMS V2 and NASA MODIS V6.1 products per main biome type for years 2004, 2012 and 2019. Right: Violin-plots of the bias between CCI+ VP CRDP-2 and rest of products per biome type. In the violin-plots, red horizontal bars indicate median values, horizontal dashed black lines stretch from first and third quartile of the data, and vertical black lines stretch from the lower and upper adjacent value. 48
Figure 28: Histograms of delta function (smoothness) of different LAI and fAPAR products: CCI+ VP CRDP-2 (purple), C3S V3 (green), CLMS V2 (blue) and NASA MODIS V6.1 (orange) products over LANDVAL sites for years 2004, 2012 and 2019. In case of LAI, only products providing LAIeff values are displayed. 49
Figure 29: Median absolute deviation (MAD) of the 5th and 95th percentiles between consecutive years (2000-2019 period) over LANDVAL sites for CCI+ VP CRDP-2 (left), C3S V3 (right). 50
Figure 30: Median absolute deviation (MAD) of the 5th and 95th percentiles between consecutive years (2000-2019 period) over LANDVAL sites for CCI+ VP CRDP-2 (top left), C3S V3 (top right), CLMS V2 (bottom left) and NASA V6.1 (bottom right) fAPAR products. 50
Figure 31: Hovmöller plots of the fAPAR bias between CRDP-2 and MODIS C6.1 over LANDVAL sites for best quality pixels. 51
Figure 32: CRDP-2 fAPAR mean values over LANDVAL sites with percentage of BQ missing values lower than 10%. Different periods are highlighted: 2000-2007 (mono-sensor), 2008-2011 (SPOT/VGT & MetOp-A/AVHRR), 2012-2017 (SPOT/VGT or PROBA-V & MetOp-A/AVHRR & VIIRS), 2018-2020 (PROBA-V & Sentinel-3/OLCI & Metop-A or -C & VIIIRS). The number of observations per period and over time are also shown, along with mean, median and percentiles (5th, 95th) for each period. 52

Figure 33: Temporal evolution of the CRDP-2 fAPAR bias with MODIS over a subset of LANDVAL sites with percentage of BQ missing values lower than 10%. The number of observations over time are also shown. 53

LIST OF TABLES

Table 1: Validation metrics for product validation 19
Table 2: GCOS uncertainty and stability requirements for LAI and fAPAR. 20
Table 3: Summary of validation methodology for CRDP-2. 21
Table 4: Summary of quality flags used to remove pixels with suboptimal quality of each satellite product. LSB stands for least significant bit 22
Table 5: Characteristics of the existing LAI and fAPAR global satellite-based reference products. ANN and RTM stands for "Artificial Neural Network", and "Radiative Transfer Model", respectively. GSD stands for "Ground Sampling Distance" 24
Table 6: List of quality-controlled GBOV LPs V3.4 sites (GBOV V3.4_QC) used for validation. 29
Table 7: Median δ of different LAI and fAPAR products: CCI+ VP CRDP-2, C3S V3, CLMS V2 and NASA MODIS V6.1. Computation per biome type over LANDVAL sites for years 2004, 2012 and 2019. 49
Table 8: Summary of CCI+ VP CRDP-2 validation results 57

1 Introduction

1.1 Scope of this document

The purpose of this document is to present the validation results of Climate Change Initiative Vegetation Parameters (CCI+ VP) Leaf Area Index (LAI) and fraction of Absorbed Photosynthetically Active Radiation (fAPAR) products for the Climate Research Data Package cycle 2 (CRDP-2), derived from multi-sensor observations spanning the period from January 2000 to December 2020 (2000-2020). The CRDP-2 dataset has limited spatial coverage, encompassing a North-South latitudinal transect with extra tiles over Europe, and a selection of globally distributed sites (LAND VALidation sites, LANDVAL) along with additional sites where ground-based information is available.

The validation methods and datasets are described in Section 2. The validation results are presented in Section 3, and Section 4 provides the conclusions of this study. Supplementary material can be found in several annexes.

1.2 Related documents

Internal documents

Reference ID	Document
VP-CCI_D2.1_ATBD_V2.2	Algorithm Theoretical Basis Document: fAPAR and LAI, ESA CCI+ Vegetation Parameters http://climate.esa.int/media/documents/VP-CCI_D2.1_ATBD_V2.2.pdf
VP-CCI_D4.2_PUG_V2.2	Product User Guide: LAI and fAPAR, ESA CCI+ Vegetation Parameters CRDP-2 http://climate.esa.int/media/documents/VP-CCI_D4.2_PUG_V2.2.pdf
VP-CCI_D1.3_PVP_V2.0	CCI Vegetation. Product Validation Plan https://climate.esa.int/media/documents/VP-CCI_D1.3_PVP_V2.0.pdf

External documents

Reference ID	Document
GCOS-200, 2016	GCOS-200 (2016). The Global Observing System for Climate: Implementation Needs. WMO, Geneva, Switzerland https://library.wmo.int/idurl/4/55469
JCGM, 2014	JCGM, 2014. International Vocabulary of Metrology–Basic and General Concepts and Associated Terms, Chemistry International – News magazine for International Union of Pure and Applied Chemistry (IUPAC). Walter de Gruyter GmbH. https://doi.org/10.1515/ci.2008.30.6.21
GCOS-245, 2022	The 2022 GCOS ECVs Requirements. https://library.wmo.int/records/item/58111-the-2022-gcos-ecvs-requirements
ATBD-C3S_V3	Copernicus Climate Change Service. Algorithm Theoretical Basis Document – Multi-sensor CDR LAI and fAPAR v3.0. Ref: C3S_D312b_Lot5.1.4.4-v3.0_ATBD_CDR-ICDR_LAI_FAPAR_MULTI_SENSOR_v3.0_PRODUCTS_v1.0.1 https://dast.copernicus-climate.eu/documents/satellite-lai-fapar/D1.4.4-v3.0_ATBD_CDR_LAI_FAPAR_MULTI_SENSOR_v3.0_PRODUCTS_v1.0.1.pdf

ATBD_C3S_SA_V2	Copernicus Climate Change Service. Algorithm Theoretical Basis Document – Multi-sensor CDR Surface Albedo v2.0. Ref: D1.3.4-v2.0_ATBD_CDR_SA_MULTI_SENSOR_v2.0_PRODUCTS_v1.1 https://dast.copernicus-climate.eu/documents/satellite-albedo/D1.3.4-v2.0_ATBD_CDR_SA_MULTI_SENSOR_v2.0_PRODUCTS_v1.1.pdf
PQAR-C3S_V3	Copernicus Climate Change Service. Product Quality Assessment Report – Multi-sensor CDR LAI and fAPAR v3.0. Ref: D2.3.9-v3.0_PQAR_CDR_LAI_fAPAR_PROBAV_v3.0_PRODUCTS_v1.1 https://dast.copernicus-climate.eu/documents/satellite-lai-fapar/D2.3.9-v3.0_PQAR_CDR_LAI_FAPAR_MULTI_SENSOR_v3.0_PRODUCTS_v1.1.pdf
ATBD-CGLS_PBV_V2	Algorithm Theoretical Basis Document of LAI/fAPAR/FCOVER PROBA-V Collection 1km V2 in the Copernicus Global Land Service. https://land.copernicus.eu/global/sites/cgls.vito.be/files/products/CGLOPS1_ATBD_LAI1km-V2_I1.41.pdf
QAR-CGLS_PBV_V2	Quality Assessment Report of LAI/fAPAR/FCOVER PROBA-V Collection 1km V2 in the Copernicus Global Land Service. https://land.copernicus.eu/global/sites/cgls.vito.be/files/products/CGLOPS1_QAR_LAI1km-PROBAV-V2_I1.40.pdf
ATBD-MOD15	MODIS leaf area index (LAI) and fraction of photosynthetically active radiation absorbed by vegetation (FPAR) product (MOD15) – Algorithm Theoretical Basis Document, Version 4.0, 30th April 1999, NASA Goddard Space Flight Center, Greenbelt, MD, 20771. https://modis.gsfc.nasa.gov/data/atbd/atbd_mod15.pdf
ATBD-GBOV-LP3-LP4-LP5	Ground-Based Observations for Validation - Algorithm Theoretical Basis Document - Vegetation Products: LP3 (LAI), LP4 (FAPAR) and LP5 (FCOVER). https://gbov.acri.fr/public/docs/products/2021-09/GBOV-ATBD-LP3-LP4-LP5_v3.0-Vegetation.pdf
CAN_EYE_UG	CAN_EYE V6.4.91 USER MANUAL. Updated October, 10th 2017. https://www6.paca.inrae.fr/can-eye/content/download/3052/30819/version/4/file/CAN_EYE_User_Manual.pdf

1.3 General definitions

Leaf Area Index (LAI) is defined as the total one-sided area of all leaves in the canopy within a defined region, and is a non-dimensional quantity, although units of [m2/m2] are often quoted, as a reminder of its meaning [GCOS-200, 2016]. The selected algorithm in the CCI+ VP project uses a one dimensional (1-D) radiative transfer model, and LAI is uncorrected for potential effects of crown clumping. Its value can be considered as an effective LAI, notably the LAI-parameter of a turbid-medium model of the canopy that would let the model have similar optical properties as the true three dimensional (3-D) structured canopy with true LAI (Pinty et al., 2006). Additional information about the geometrical structure may be required for this correction to obtain true LAI (Nilson, 1971), which involves the estimation of the clumping index (CI), defined as the ratio between the true and effective LAI [see (Fang, 2021) for a review of methods to estimate CI].

Fraction of Absorbed Photosynthetically Active Radiation (fAPAR) is defined as the fraction of Photosynthetically Active Radiation (PAR; solar radiation reaching the surface in the 400-700 nm spectral region) that is absorbed by a vegetation canopy [GCOS-200, 2016]. In contrast to LAI, fAPAR is not only vegetation but also illumination dependent. In the CCI+ VP project we refer to fAPAR as the white-sky value (i.e. assuming that all the incoming radiation is in the form of isotropic diffuse

radiation). Total fAPAR is used and no differentiation is made between live leaves, dead foliage and wood.

Uncertainty is a measure to describe the statistically expected distribution of the deviation from the true value. Here, it is given as the physical value, which corresponds to the sigma-parameter of a gaussian distribution.

Accuracy is the degree of the "closeness of the agreement between the result of a measurement and a true value of the measurand" [JCGM, 2014]. Commonly, accuracy represents systematic errors and often is computed as the statistical mean bias, i.e., the difference between the short-term average measured value of a variable and the true value. The short-term average is the average of a sufficient number of successive measurements of the variable under identical conditions, such that the random error is negligible relative to the systematic error. The latter can be introduced by instrument biases or through the choice of remote sensing retrieval schemes [GCOS-200, 2016].

Precision or repeatability is the "closeness of the agreement between the results of successive measurements of the same measurand carried out under the same conditions of measurement" [JCGM, 2014].

Uncertainty is a "parameter, associated with the result of a measurement that characterizes the dispersion of the values that could reasonably be attributed to the measurand" [JCGM, 2014]. Uncertainty includes systematic and random errors.

2 Validation methodology

2.1 Overall validation procedure

The validation procedure, described in the product validation plan [VP-CCI_D1.3_PVP_V2.0], follows standardized validation protocols for satellite-based biogeophysical products (Camacho et al., 2025), fully compliant with the good practices guidelines for the validation of LAI satellites products defined by the Committee on Earth Observation Satellites (CEOS) Land Product Validation (LPV) subgroup (Fernandes et al., 2014). The standardized procedure was developed as a result of multiple validation studies of LAI and fAPAR (e.g., Camacho et al., 2013, 2024a; Fang et al., 2012; Garrigues et al., 2008; Weiss et al., 2007), and the former On Line Validation Exercise (OLIVE) tool (Weiss et al., 2014) hosted by the CEOS Calibration/Validation (Cal/Val) portal. The proposed methodology relies on comparisons with ground-based references (so-called direct validation) and comparisons with satellite-based references (i.e., product intercomparison).

- The direct validation is computed against the CEOS LPV DIRECT V2.1 dataset (Camacho et al., 2024b) up-scaled according with the CEOS LPV recommendations (Fernandes et al., 2014; Morisette et al., 2006), a quality-controlled (QC) subset of Copernicus Ground-Based Observations for Validation (GBOV) upscaled maps (Lerebourg et al., 2023), and in-situ data from *Analyse Multidisciplinaire de la Mousson Africaine* (AMMA) over grassland sites (Redelsperger et al., 2006) (see Section 2.3).
- Intercomparisons with similar remote sensing products can determine whether the products behave similarly in space and time on a global scale and help identify differences between products that should be examined in more detail to diagnose product anomalies and support algorithm refinements. The LAI and fAPAR products used as satellite-based references in this exercise are: the Copernicus Land Monitoring Service 1 km V2 (CLMS V2), the Copernicus Climate Change Service V3 (C3S V3), and the National Aeronautics and Space Administration (NASA) MODerate resoluition Imaging Spectrometer C6.1 (MODIS C6.1) (see details in Section 2.2.2). The LANDVAL network of sites (Fuster et al., 2020; Sánchez-Zapero et al., 2023, 2020) is used for sampling global conditions. LANDVAL is composed of 720 sites, of which 521 sites originate from the Surface Albedo Validation Sites (SAVS 1.0) database (Loew et al., 2016), and complemented with 20 desert calibration sites (Lacherade et al., 2013) and additional homogenous sites selected to cover under-sampled regions and biome types. These analyses are achieved by aggregating land cover classes of the C3S Land Cover v2.1[1] on 9 generic classes (biomes): Evergreen Broadleaf Forest (EBF, 9.2% of LANDVAL sites), Deciduous Broadleaf Forest (DBF, 8.2%), Needle-Leaf Forest (NLF, 11.5%), Other Forests (OF, 0.8%), Cultivated (CUL, 20.6%), Herbaceous (HER, 12.5%), Shrublands (SHR, 14.4%), Flooded vegetation (FLO, 3.2%) and Sparsely vegetated and Bare Areas (SBA, 19.6%).

The following criteria are analysed in the following sections: product completeness, spatial consistency, temporal consistency, error evaluation, which involves Accuracy, Precision and Uncertainty (APU) and stability. In addition, the conformity test to assess compliance with the Global Climate Observing System (GCOS) uncertainty requirements is also performed when possible.

2.1.1 Product Completeness

Completeness corresponds to the absence of spatial and temporal gaps in the data. Missing data are mainly due to cloud or snow contamination, poor atmospheric conditions or technical problems during the acquisition of the images and is generally considered by users as a severe limitation of a

[1] https://cds.climate.copernicus.eu/datasets/satellite-land-cover?tab=overview

given product. It is therefore mandatory to document the completeness of the product (i.e., the distribution in space and time of missing data). The following analysis are conducted:

- Maps of percentage of missing values (only over LANDVAL sites) during 2000-2020 considering all pixels and best quality pixels
- Temporal evolution of missing values for the whole period (all pixels and best quality).

2.1.2 Spatial consistency

Spatial consistency refers to the realism and repeatability of the spatial distribution of retrievals over the globe. A first qualitative check of the realism and repeatability of spatial distribution of retrievals and the absence of strange patterns or artefacts (e.g., missing values, stripes, unrealistic low values, etc.) can be achieved through systematic visual analysis of all global maps based on the expert knowledge of the scientist. The spatial consistency can be quantitatively assessed by comparing the spatial distribution of the product under study with that of a validated reference product. The following analyses are conducted:

- Visualization of zoom over selected tiles at full resolution, and the visualization of global maps (i.e., the transect) at a reduced (1/4 pixels) resolution.
- Maps (i.e., the transect) of differences, at a reduced (1/4 pixels) resolution, between the product under study and reference products to identify regions showing spatial inconsistencies for further analysis (e.g., temporal profiles).

2.1.3 Temporal consistency

Temporal consistency refers to the realism of seasonal and inter-annual variations. The realism of the temporal variations can be qualitatively analysed by displaying temporal trajectories of satellite products and ground measurements (when available). The following analyses are conducted:

- The realism of the temporal variations of the product under study are qualitatively assessed as compared to reference products and available ground measurements. Different periods are displayed (whole period, 4-years period, and periods with availability of ground measurements).

2.1.4 Error evaluation and conformity testing

Accuracy, precision and uncertainty are evaluated by several metrics (Table 1) reporting the goodness of fit between the products and the corresponding reference dataset.
Commonly, accuracy represents systematic errors and often is computed as the statistical mean bias (B). Precision represents the dispersion of product retrievals around their expected value and can be estimated by the standard deviation (STD) of the difference between retrieved satellite product and the corresponding reference estimates. Uncertainty includes systematic and random errors and can be assessed using the Root Mean Square Deviation (RMSD). In addition to these metrics, other statistics are useful to evaluate the goodness of fit between two datasets including linear model fits. For this purpose, Major Axis Regression (MAR) is computed instead Ordinary Least Squares (OLS) because it is specifically formulated to handle error in both of the x and y variables (Harper, 2014). It should be noted that strong and/or multiple outliers can affect the classical metrics described above (i.e. B and STD): in such cases, using the median deviation (MD) to estimate the systematic error, and the median absolute deviation (MAD) as a measure of precision, is recommended as good practice.

The following analyses are conducted for best quality pixels:

- Scatter plots and validation metrics (Table 3) versus references for LANDVAL and per biome.

- Histograms of product values per biome are evaluated over LANDVAL sites. The analysis is complemented with violin plots of bias with reference products per biome.

Note that two additional aspects of the product precision are also investigated: the inter-annual and the intra-annual precision (Fernandes et al., 2014).

- Intra-annual precision (smoothness) corresponds to temporal noise assumed to have no serial correlation within a season. In this case, the anomaly of a variable from the linear estimate based on its neighbours can be used as an indication of intra-annual precision. It can be characterized (Weiss et al., 2007) as follows: for each triplet of consecutive observations, the absolute value of the difference between the centre P(dn+1) and the corresponding linear interpolation between the two extremes P(dn) and P(dn+2) is computed: $\delta = \left| P(d_{n+1}) - P(d_n) - \frac{P(d_n)-P(d_{n+2})}{d_n-d_{n+2}}(d_n - d_{n+1}) \right|$ Eq. 1
  The distribution of the intra-annual precision is analysed, and the median δ value is used as a quantitative indicator of the inter-annual precision (Fernandes et al., 2014; Wang et al., 2019). Hence, the lower median of δ values, the higher the inter-annual precision.

- Median deviations of an upper (95^{th}) and lower percentile (5^{th}) of variable between consecutive years are indicators of inter-annual precision, i.e., dispersion of variable values from year to year (Fernandes et al., 2014). Note that cultivated sites are not considered in this analysis due to the non-natural variability in this land cover type due to agricultural practices (e.g., crop rotation).

Conformity testing is the process to determine whether an estimated quantity is within the range of tolerable values or not. Up to now, in most validation studies, satellite and references uncertainties have not been considered in the conformity testing. In those cases, the data points which are within the tolerance intervals (requirements) are considered conform and the others are non-conform. This decision rule is known in metrology as “shared risk” or “simple acceptance” conformity testing. The shared risk approach can provide a first assessment of the conformity with requirements. Nevertheless, if product and references uncertainties are known, the “guarded acceptance” testing is preferable for a better understanding of the compliance of requirements, considering the uncertainty of the apparent error (Camacho et al., 2024a). As our ground references and some satellite references do not have well-characterized uncertainties, the shared risk conformity test (conform / non-conform) has been evaluated against GCOS goal and threshold uncertainty requirements [GCOS-245, 2022] (see Table 2). The following analyses are conducted:

- Percentage of compliant retrievals with |bias| < GCOS requirements is computed for each reference dataset.

Table 1: Validation metrics for product validation

Statistics	Comment
N	Number of samples. Indicative of the power of the validation
B	Mean Bias. Difference between average values of x and y. Indicative of accuracy and offset.
MD	Median deviation between x and y. Best practice reporting the accuracy.
STD	Standard deviation of the pair differences. Indicates precision.
MAD	Median absolute deviation between x and y. Best practice reporting the precision.
RMSD	Root Mean Square Deviation. RMSD is the square root of the average of squared errors between x and y.
MAR	Slope and offset of the Major Axis Regression linear fit. Indicates some possible bias
R	Correlation coefficient. Indicates descriptive power of the linear accuracy test. Pearson coefficient is used.

Table 2: GCOS uncertainty and stability requirements for LAI and fAPAR.

Requirement	ECV	Goal	Threshold
Uncertainty	LAI	10% for LAI≥0.5 0.05 for LAI<0.5	20% for LAI≥0.5 0.1 for LAI<0.5
	fAPAR	5% for fAPAR≥0.05 0.0025 for fAPAR<0.05	10% for fAPAR≥0.05 0.005 for fAPAR<0.05
Stability (per decade)	LAI	<3%	<6%
	fAPAR	<1.5%	<3%

2.1.5 Stability

Stability is the property of an instrument to provide similar measurements when the measurand remains constant in time. Analysis of multidecadal long-term stability of satellite data records is a key requirement for the applicability of these products for climate observation. This is of particular importance in data records created from different satellite sensors, as the transition from one sensor to another may create artificial changes in the time series (Mota et al., 2021). While stability assessment has not been addressed in depth for biophysical variables, other EO community has defined stability as the change in bias (apparent error) over a time period (Merchant, 2013). As we do not have long-term ground reference to compare against the CRDP-2, we use satellite-based references instead. The following analyses are conducted:

- Hovmöller plots of the bias during the whole period between CRDP-2 and reference products over LANDVAL sites for best quality retrievals are computed to assess temporal changes in the bias. MODIS V6.1 is used as the main reference as it is a stable dataset.
- Mean values over a subset of LANDVAL sites, those with less than 10% missing values for best quality pixels over the entire period, along with the number of observations were computed to ensure that a very similar number of observations was used across the full time series. Mean, median and 5th-95th percentiles were computed for four different periods (using different input sensors). Bias with MODIS over this subset of sites was also computed for fAPAR.
- Mean values over LANDVAL sites (best quality pixels) per biomes were computed for the whole period. Mean, median and 5th-95th percentiles were computed for four different

periods (using different input sensors). Bias with MODIS per biome was also computed for fAPAR.

2.1.6 Summary of validation procedure

Table 3 summarizes the validation criteria used for the quality assessment of the products under study. It should be noted that several criteria are evaluated only using a combination of three years 2004, 2012 and 2019. This choice was made to represent the different combinations of sensor input data in the results (see Section 2.2.1): 2004 is based on mono-sensor (i.e., SPOT5/VGT2) observations, 2012 is based on multi-sensor observations (i.e., SPOT5/VGT2, MetOp-A/AVHRR-3, SuomiNPP/VIIIRS) and 2019 is also based on multi-sensor observations but incorporates a larger number of satellites (i.e., PROBA-V, Sentinel-3 (A+B)/OLCI, MetOp-C/AVHRR-3 and SuomiNPP/VIIRS). Then, the complete dataset period (2000–2020) is used to assess various criteria (e.g., completeness, temporal consistency, error evaluation, and stability), while a shorter window (2012–2015) is also analysed to better display temporal features.

Table 3: Summary of validation methodology for CRDP-2.

Quality Criteria	Reference	Coverage /period	Metrics Results
Product completeness	C3S V3 CLMS V2 (non-filled) MODIS V6.1	LANDVAL /2000-2020	- Distribution of gaps
Spatial consistency	Expert knowledge	TRANSECT /2004,2012,2019	-Visual inspection of maps
	C3S V3 CLMS V2 MODIS V6.1	TRANSECT /2004,2012,2019	-Maps of differences with references.
Temporal consistency	C3S V3 CLMS V2 MODIS V6.1	LANDVAL 2000-2020 (& 2012-2015)	-Qualitative inspection of the realism of the temporal variations.
	GBOV V3.4 + satellite products	GBOV sites /2013-2020	
	AMMA + satellite products	AMMA sites /2005-2016	
Error evaluation (vs ground-based reference)	DIRECT V2.1	DIRECT sites /2000-2020	-Scatter plots and validation metrics. Conformity testing. -Added C3S V3, CLMS V2 & MODIS V6.1 for benchmarking
	GBOV V3.4_QC	GBOV sites /2013-2020	
	AMMA	AMMA sites /2005-2016	
Error evaluation (vs satellite-based references)	C3S V3 CLMS V2 MODIS V6.1	LANDVAL /2004,2012,2019	- Overall scatter plots and validation metrics. Conformity vs. GCOS requirements. - Analysis per biome type: PDFs of retrievals, violin-plots of bias, scatter plots and validation metrics. -Intra-annual precision
		LANDVAL /2000-2020	-Inter-annual precision
Stability	C3S V3 CLMS V2 MODIS V6.1	LANDVAL /2000-2020	-Hovmöller plots of bias - Mean, median and 5th-95th percentiles for different periods over subset of LANDVAL sites

	and per biome - Evolution of Bias (t) and slope bias/year over a subset of LANDVAL sites and per biome

To compare different products, a similar spatial support area and temporal support period must be defined:

- Spatial support area:
  - The error and stability assessments were performed at 3 km x 3 km (i.e., average values of 3x3 pixels in case of CCI+VP, C3S V3 and CLMS V2, and 6x6 pixels in case of MODIS C6.1). Previously, MODIS was re-sampled over Plate Carrée projection, which is the CCI, C3S and CLMS common grid. The exception was the comparison with AMMA sites (with no upscaling) that was performed at 1 km x 1 km.
  - For product completeness, temporal consistency, intra- and inter-annual precision, the nominal spatial resolution of each product (i.e., 1km for C3S, CCI, CLMS and 500m for MODIS) was used to preserve its original values.

- Temporal support period:
  - The error evaluation and stability assessment against satellite products were performed at the 5-days temporal frequency of CCI products. The closest date of the reference products (8-days or 10-days) is the used for comparisons.
  - The error evaluation against ground-based products was performed on the date of the in-situ observation. Satellite product estimates were interpolated to the date of the in-situ observation by using the two adjacent dates, weighted according to their temporal distance (in days) from the in-situ measurement date.
  - For product completeness, temporal consistency, intra- and inter-annual precision, the nominal temporal resolution of each product (i.e., 5-days in case of CCI, 10-days for C3S and CLMS and 8-days for MODIS) was used to preserve its original values.

The validation is mainly conducted over best quality (BQ) retrievals to avoid the use of low quality or invalid retrievals. BQ pixels are selected according to the different quality flags of the CCI+ VP and reference products (described in the next section). Table 4 summarizes the quality flags used to select BQ retrievals.

Table 4: Summary of quality flags used to remove pixels with suboptimal quality of each satellite product. LSB stands for least significant bit

Product	Quality Flag (LSB = bit 0)
CCI+VP	Bit 8 (RETR_UNTRUSTED) and bit 9 (RETR_LOW_QUALITY) of invcode p_chisquare < 0.5
C3S V3	retrieval_flag: bit 0 (obs_is_fillvalue), bit 6 (tip_untrusted), bit 7 (obs_unusable)
CLMS 1km V2	Bit 0 (Land/Sea: Sea) Bit 5 (Input status: All reflectance data out of range or invalid) Bits 6,7,8 (LAI/FAPAR/FCover status: Out of range) (*) Bit 2 (Filled: filled) (*) Only used for product completeness criteria.
NASA MODIS C6.1	Bits 5,6,7 of FparLai_QC, which correspond to SCF_QC or five-level confidence score: -2 Main (RT) method failed due to bad geometry, empirical algorithm used. -3 Main (RT) method failed due to problems other than level 2. -4 Pixel not produced at all, value could not be retrieved).

2.2 Satellite products

This section provides an overview of the LAI and fAPAR satellite products used in this exercise.

2.2.1 Evaluated dataset: CCI+VP CRDP-2

CCI+VP Climate Research Data Package 2 (CRDP-2) are generated with OptiSAIL (Blessing et al., 2024) [VP-CCI_D2.1_ATBD_V2.2], which is a retrieval and error propagation framework using automatic differentiation for gradient, Jacobian and Hessian computations. It is built around the established components 4SAILH (Scattering of Arbitrarily Inclined Leaves, with 4-stream extension and hot-spot, Verhoef et al., (2007)), PROSPECT-D (simulation of leaf spectra, version D including senescence, Féret et al., (2017)), TARTES (Two-streAm Radiative Transfer in Snow Libois et al., (2013)), with the addition of an empirical soil reflectance model, a semi-empirical soil moisture model, the Ross-Thick-Li-Sparse Bidirectional Reflectance Distribution Function (BRDF) model, and a cloud contamination simulation. They directly simulate Top Of Canopy (TOC) reflectances for given sets of spectrally invariant parameters (e.g. LAI, leaf pigments etc.) and scene geometries at given bands. In order to retrieve these parameters for observed TOC reflectance data, an inversion is made for each pixel. During cycle-1 of this project repeatedly cloud-contaminated data was encountered, which was not flagged as such. Therefore, the cloud contamination model of OptiSAIL was activated, which simulates the effect of variable amounts of thin clouds per observation. This significantly reduces the number of outlier retrievals. The inversion in OptiSAIL minimises a cost function with data and prior term. It uses gradient information which is efficiently provided by adjoint code of the models. These adjoint codes are obtained by Automatic Differentiation (AD), which allows for quick adaptation of the whole system to changes in the models. The main outputs are canopy parameters, LAI (effective), fAPAR and their uncertainties, as well as additional parameters (e.g. leaf pigments) and albedo.

The validation is performed over the CRDP-2, a climate data record of 21 years (2000-2020) based on multi-sensor input-data (see Figure 1). The dataset was generated over a globally distributed selection of 1122 sites and a latitudinal transect (see Figure 2) distributed as 10^o x 10^o tiles (note that additional tiles covering the Mediterranean area were also processed). In this exercise, we are focusing on LAI (effective) and fAPAR and their uncertainties. More information about the output layers can be found in the user manual [VP-CCI_D4.2_PUG_V2.2].

Figure 2 illustrates the sampling strategy for the validation. It consists in two approaches:

- A selection of sites for product intercomparison (i.e., LANDVAL V1.1) and those sites used for direct validation of LAI and fAPAR (i.e., DIRECT V2.1, GBOV, AMMA).
- The latitudinal transect for the evaluation of the spatial consistency.

Figure 1: Sensor input data used to generate CCI+VP CRDP-2.

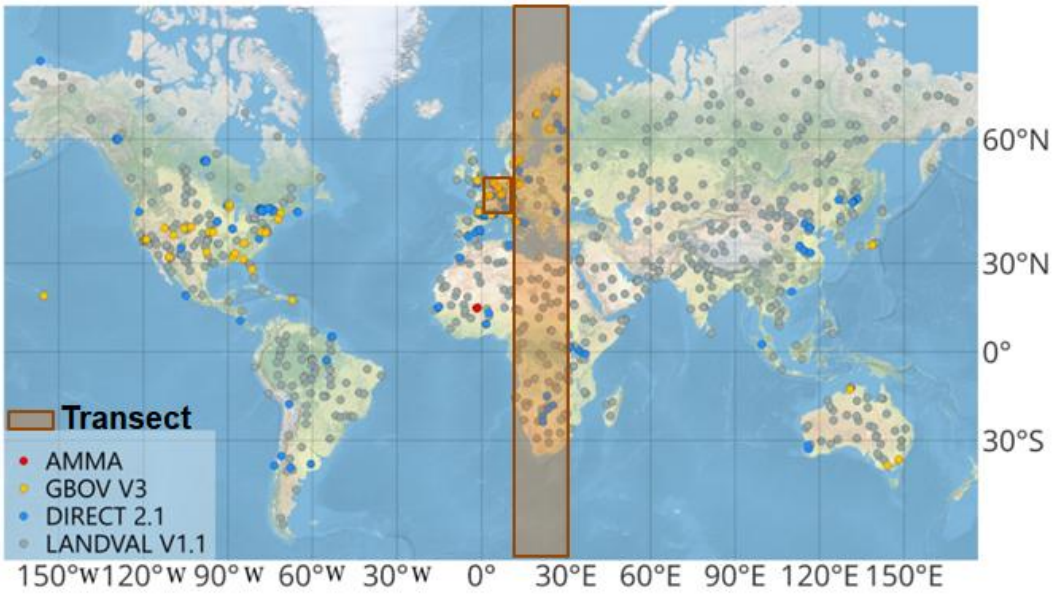

Figure 2: Sampling strategy: A) selected sites from LANDVAL, GBOV V3, DIRECT_2.1 and AMMA. B) Latitudinal Transect (see red rectangles)

2.2.2 Reference satellite products

Table 5 summarizes the main characteristics of LAI and fAPAR satellite products used in this evaluation.

Table 5: Characteristics of the existing LAI and fAPAR global satellite-based reference products. ANN and RTM stands for "Artificial Neural Network", and "Radiative Transfer Model", respectively. GSD stands for "Ground Sampling Distance"

LAI/fAPAR Product	Satellite /Sensor	GSD	Frequency /compositing	Temporal availability	Algorithm	Clumping	Reference
C3S multi-sensor V3	SPOT/VGT	1 km	10 days /20 days (recursive using BRDF SPOT/VGT climatology).	1999-2013	TIP applied to VIS and NIR broadband albedos	Non accounted	(Pinty et al., 2006) [ATBD-C3S_V3]
	PROBA/VGT			2014-2020			
CLMS Collection 1km V2	SPOT/VGT	1 km	10 days /variable	1999-2013	ANN trained with CYC and MOD + gap filling & smoothing	Weighted of CYC and MOD	(Verger et al., 2023) [ATBD-CGLS_PBV_V2]
	PROBA/VGT			2014-2020			
NASA MOD15A2H V6.1	TERRA /MODIS	500 m	8 days /8 days	2000-present	Inversion RTM 3D	Plant, canopy & landscape	(Knyazikhin et al., 1998) [ATBD-MOD15]

2.2.2.1 Copernicus Climate Change Service multi-sensor SPOT/VGT & PROBA-V V3 (C3S V3)

C3S LAI and fAPAR multi-sensor V3.0 products are generated using the Two-stream Inversion Package (TIP) algorithm (Pinty et al., 2006), which provides effective LAI and fAPAR along with their

uncertainties by applying the TIP to Visible (VIS) and Near Infra-Red (NIR) broadband albedos using Système Pour l'Observation de la Terre VEGETATION instrument onboard of SPOT4 & 5 (SPOT/VGT,1999-2013) and PRoject for On-Board Autonomy Vegetation instrument (PROBA-V,2014-2020) data. They can be found at the Climate data store of C3S (https://cds.climate.copernicus.eu/datasets/satellite-lai-fapar?tab=overview). More details on the retrieval procedure can be found in the Algorithm Theoretical Basis Document (ATBD) [ATBD-C3S_V3].

The input data is surface albedo version 2 (see ATBD [ATBD_C3S_SA_V2]), which incorporates harmonized measurements from the platforms National Oceanic and Atmospheric Administration (NOAA-[7…17]), SPOT-[4-5] and PROBA-V, which result in almost 40 years of satellite observations. Main characteristics related to the harmonization of the multi-sensor SA retrieval approach are:

- The pre-processing step provides harmonised pixel classification approach (cloud, snow and shadow pixels) and harmonized atmospheric correction scheme (including 148 aerosol models compared to SA v1.0 which is using only the continental model).
- A spectral harmonization module was created to provide TOC reflectance values as if they had been acquired with SPOT/VGT-2.
- The BRDF retrieval module uses BRDF climatology data from SPOT/VGT. The algorithm relies on a similar core as previous versions (Kalman filters and BRDF model fit) but with the addition of a reference BRDF (climatology derived from VGT BRDF) to (i) reduce the gaps in time series, and (ii) introduce multi-sensor information in each albedo estimation to increase homogeneity among the datasets derived from each sensor.

The validation report of C3S LAI & fAPAR V3 [PQAR-C3S_V3] showed good completeness and reliable values. Good temporal consistency was found when the products are derived from different sensors (Advance Very High Resolution Radiometer - AVHRR, VGT, PBV), providing a climate data record of more than 40 years of data, using harmonized input data from different sensors (AVHRR, PBV, VGT). The transition of AVHRR V3 to VGT V3 showed however negative bias (VGT < AVHRR). VGT V3 also provided slightly lower values than PBV V3. C3S V3 showed overall good spatial and temporal consistency with reference satellite products (C3S V2, CLMS 300 m, Visible/Infrared Imager Radiometer Suite VNP - VIIRS V1). It is important to note that a systematic negative bias in C3S fAPAR V3 values, ranging between -30% and -20%, was found when compared to all references (CLMS PBV V2, VIIRS and EUMETSAT Polar System (EPS) VEGetation Algorithm (VEGA) products). The comparison with ground data showed overall good results for fAPAR (but underestimation of highest values) and systematic negative bias for C3S LAI V3 products. Another limitation of the products is the high density of points with LAI and fAPAR V3 very close to 0 (mainly in winter at northern latitudes).

2.2.2.2 Copernicus Land Monitoring Service Collection 1km SPOT/VGT & PROBA-V V2 (CLMS V2)

The CLMS LAI & fAPAR Collection 1km version 2 products are globally provided from 1999 to 2020 at https://land.copernicus.eu/en/products/vegetation/leaf-area-index-v2-0-1km. The retrieval algorithm (Verger et al., 2023) [] was initially defined for the estimation of LAI, fAPAR (and fractional vegetation COVER, fCOVER) from the VEGETATION series of observations and was latter applied to daily top-of-canopy reflectance provided by the PROBA-V sensor. As the neural network (ANN) algorithm was trained with SPOT/VGT observations, two specific adaptations were applied to achieve good consistency when applied to PROBA-V data. First, a spectral conversion was applied on the actual PROBA-V TOC reflectances to get SPOT/VGT-like TOC reflectances values. Second, PROBA-V ANN outputs were rescaled with regard to SPOT/VGT ANN output using a polynomial function fitted over BELMANIP2.1 sites. The CLMS V2 algorithm aims providing improved products as compared to CLMS V1 (Baret et al., 2013), although derived from the same sensors observations, with smoother retrievals and no missing values. CLMS V2 products have 10 days frequency. Similarly to CLMS V1, CLMS V2 capitalizes on the development and validation of already existing products: Carbon cYcle and Change in Land Observational Products from an Ensemble of Satellites (CYCLOPES) version 3.1 and MODIS

collection 5, and the use of neural networks (Baret et al., 2013; Verger et al., 2008). The basic underlying assumption is that a strong link exists between VEGETATION observations and the fused product resulting from CYCLOPES and MODIS products. Products are associated with quality assessment flags as well as quantified uncertainties.
The algorithm starts from the daily PROBA-V top-of-canopy reflectance products. The output is the instantaneous first guess of the three variables. Then, a temporal smoothing and gap filling (TSGF) method is applied, using several techniques including the Savitzky-Golay filter, a climatology (Verger et al., 2013) or interpolation methods to smooth the time profile and fill the gaps.
The CLMS PROBA-V Collection 1 km V2 products were validated over the period October 2013–October 2014 [QAR-CGLS_PBV_V2], and the quality stability was systematically checked every year. The products displayed better spatial coverage (no gaps) and smoother profiles than CLMS V1 and MODIS C5 products. Specifically, over evergreen broadleaf forests, the CLMS V2 presented smooth trajectories (climatology based) with high values and very limited seasonality while CLMS V1 showed seasonality and noise due to permanent clouds. The accuracy assessment over a limited number of concomitant ground-based measurements (<15) showed RMSD values of 0.79 and 0.12 for LAI and fAPAR, respectively.
More recently, the quality of CLMS V2 was assessed with due attention to consistency and improvements with CLMS V1 (Verger et al., 2023). CLMS V2 showed a similar accuracy as V1 for LAI and slight improvements for fAPAR as evaluated over the limited ground measurements available (DIRECT V2). In addition, CLMS V2 highly improves V1 in terms of product completeness and does not show any missing data thanks to climatological gap filling. CLMS V2 and V1 time series showed high temporal consistency in most of the situations. V2 corrects the inconsistencies identified in V1 at very high Northern latitudes and for evergreen broadleaf forest (noise and discontinuities in V1). Additionally, V2 improves both the inter- and intra-annual precision as a result of the smoothing and gap filling.

2.2.2.3 National Aeronautics and Space Administration MODIS V6.1 (MODIS V6.1)

NASA Moderate-resolution Imaging Spectroradiometer (MODIS) aboard Terra C6.1 LAI and fAPAR products (MOD15A2H) are available at a spatial resolution of 500 m over a sinusoidal grid and a step of eight days since 2000 at https://ladsweb.modaps.eosdis.nasa.gov.
The algorithm retrieves LAI and FAPAR values given sun and view directions, Bidirectional Reflectance Factor (BRF) for each spectral band, uncertainties (i.e., relative stabilized precision, (Wang et al., 2001)) in input BRFs, and land cover classes based on an 8-biome classification map (Myneni et al., 2002; Yang et al., 2006). The operational LAI/fAPAR algorithm consists of a main algorithm that is based on 3D radiative transfer equation and a backup algorithm. By describing the photon transfer process, this algorithm links surface spectral BRFs to both structural and spectral parameters of the vegetation canopy and soil (Asrar and Myneni, 1991; Ross, 1981). Given atmosphere corrected BRFs and their uncertainties, the algorithm finds candidates of LAI and fAPAR by comparing observed and modeled BRFs that are stored in biome type specific Look-Up-Tables. All canopy/soil patterns for which observed and modeled BRFs differ within biome-specified thresholds of uncertainties (e.g., 30% and 15% for red and near-infrared bands, respectively, for forest biomes) are considered candidate solutions and the mean values of LAI and fAPAR from these solutions are reported as outputs. The mean and dispersion of LAI/fAPAR candidates are reported as retrieval and its reliability, respectively. The law of energy conservation (reflectance, transmittance and absorbance sum up to unity) and the theory of spectral invariance are two important features of this main algorithm [ATBD-MOD15]. MODIS does not provide retrievals over desert areas due to the biome dependency of the algorithm (Myneni et al., 2002; Yang et al., 2006).
The main algorithm may fail to localize a solution if uncertainties of input BRFs are larger than threshold values or due to deficiencies of the RT model that result in incorrect simulated BRFs. In such cases, a backup empirical method based on relations between Normalized Difference Vegetation Index (NDVI) and LAI/fAPAR (Knyazikhin et al., 1998; Myneni and Williams, 1994) is utilized to output

LAI/fAPAR with lower quality (called the backup algorithm). It should be noted that pixels computed by this backup solution are discarded from this analysis.
The consistency between of previous collections C5 and C6 was analysed (Nestola et al., 2017; Yan et al., 2016a) without finding spatial differences due to resolution changes with an RMSD between both versions of 0.091 for fAPAR (Yan et al., 2016a). The accuracy assessment performed over 45 fAPAR ground measurements showed an overestimation of both C5 and C6 fAPAR products over sparsely vegetated areas (Yan et al., 2016b). Comparisons with SPOT/VGT Collection 1km V1 products showed similar spatial distributions at a global scale (Yan et al., 2016b), and temporal comparisons for the 2001–2004 period showed that the products properly captured the seasonality of different biomes, except in evergreen broadleaf forests.
The improvements of C6.1 respect to C6 are:

- The Version 6.1 Level-1B products have been improved by undergoing various calibration changes that include: changes to the response-versus-scan angle approach that affects reflectance bands for Aqua and Terra MODIS, corrections to adjust for the optical crosstalk in Terra MODIS infrared bands, and corrections to the Terra MODIS forward look-up table update for the period 2012 - 2017.
- A polarization correction has been applied to the L1B Reflective Solar Bands.

2.3 Reference ground datasets

In this section, the reference ground datasets are described.

2.3.1 CEOS LPV DIRECT 2.1

Ground references of high quality are needed to validate satellite-based products. The DIRECT 2.1 database (Camacho et al., 2024b) constitutes a major effort of the international community to provide suitable ground reference for the validation of LAI, FAPAR and Fraction of Vegetation Cover (FVC) satellite products. DIRECT V2.1 is endorsed by CEOS and hosted on the CEOS Cal/Val portal (https://calvalportal.ceos.org/lpv-direct-v2.1). It compiles ground reference upscaled values over a 3 km x 3 km area, and we refer to it as CEOS LPV DIRECT 2.1.
The ground data collected over elementary sampling units was upscaled using high spatial resolution imagery following CEOS LPV guidelines to properly account for the spatial heterogeneity of the site. Ground measurements included in the first version (DIRECT) were resulting from several international activities including Validation of Land European Remote sensing Instruments (VALERI), BigFoot, Southern African Regional Science Initiative – 2000 (SAFARI-2000), Canada Centre for Remote Sensing (CCRS), Boston University and ESA campaigns compiled by S. Garrigues (Garrigues et al., 2008), and later ingested in the CEOS LPV OLIVE tool (Weiss et al., 2014) for accuracy assessment. DIRECT database was revised to remove those sites without understory measurements (Camacho et al., 2013) and after that it was expanded with the inclusion of Implementation of Multi-scale Agricultural Indicators Exploiting Sentinels (ImagineS) sites (Camacho et al., 2021). CEOS LPV DIRECT 2.1 is the last update including 44 new sites from China (Fang et al., 2019; Song et al., n.d.) and 2 sites from European Space Agency (ESA) Fiducial Reference Measurements For Vegetation (FRM4Veg) (Brown et al., 2021), with a total of 176 sites around the world (7 main biome types) and 189 effective LAI values, 280 LAI, 128 FAPAR and 122 FCOVER values covering the period from 2000 to 2021.
It should be noted that the uncertainty associated to LAI reference maps is expected to be around 1 LAI units for dense forest (Fernandes et al., 2003) or around 0.5 for croplands (Martínez et al., 2009), which is around 20%. Therefore, with the available ground truth reference data is difficult to achieve the strict optimal requirements on accuracy for LAI products. Further research on FAPAR and FCOVER should be conducted to evaluate the uncertainty attached to ground reference maps, which could be also slightly higher than goal requirements for satellite-based products.

2.3.2 The Ground-Based Observations for Validation V3 (GBOV V3)

The GBOV dataset [2] covers up to 53 sites from different networks, mainly National Ecological Observatory Network (NEON), instrumented GBOV sites and Integrated Carbon Observation System (ICOS). The validation focuses on Land products (LP) database version 3.4 for LAI (LP-3) and fAPAR (LP-4), the latest release which includes a reprocessing of the entire time series up to 2025. Note LAI (LP-3) is an actual (or true) LAI and not effective LAI, so we can only use it for correlation analysis with CRDP-2 dataset (effective LAI). LPs are ground-based maps based on the RTM-based retrievals which are calibrated with Reference Measurements (RM) (Lerebourg et al., 2023). The Sentinel-2 Simplified Level 2 Processor (SL2P) based on PROSAIL (Jacquemoud et al., 2009) and neuronal networks are used to retrieve high-spatial resolution maps of effective LAI (PROSAIL does not account for clumping) and fAPAR. Calibration function between RM and PROSAIL outputs are generated to correct the bias.
Three different generic calibration functions are established, two of them for forest sites (one for those sites coming from NEON and GBOV and one for additional sites, mostly from ICOS but also few Terrestrial Ecosystem Research Network (TERN) sites) and one for non-forest sites. Note that ICOS sites were not used as for those sites a constant understory value was considered in the RM, which is considered a large source of uncertainty. It should be also noted that the in GBOV v3.4 sparsely vegetated sites were not delivered yet (a new empirical transfer function is in development for these sites).

It is important to emphasize that the use of a generic transfer function approach in GBOV—as opposed to the site-dependent transfer functions recommended and widely used in the CEOS LPV (e.g., DIRECT 2.1 database (Camacho et al., 2024b))—raises significant concerns about potential biases at certain sites. Consequently, before using the GBOV dataset, we have performed quality control, which consists of assessing the consistency of RM with LPs over visually homogeneous forest sites, where direct comparison of each RM with LP at 300 m spatial resolution can be made without expecting large systematic deviations due to the spatial heterogeneity of the sites. The homogeneity of the sites was visually assessed using Google Earth.

The mean bias and MAD were estimated considering all concomitant measurements (within ±5 days) with the valid LPs estimates, over the full available period of each site. Only sites with B<20% and MAD<25% between LPs and RMs are considered for validation. Moreover, LP values where either the input or output is out of range or with less than 70% of the native spatial resolution pixels are valid are discarded for validation. Finally, a subset of GBOV V3.4 meeting our quality requirements (GBOV V3.4_QC) is selected for validation purposes. The final list of sites included in GBOV LPs V3.4_QC is listed in Table 6. All correspond to NEON forest sites except the GBOV FUJI site. ICOS LPs presented large bias with the RMs are not selected also because they do not resolve temporally the understory.

[2] https://land.copernicus.eu/en/products/GBOV (dataset access 02/10/2025)

Table 6: List of quality-controlled GBOV LPs V3.4 sites (GBOV V3.4_QC) used for validation.

#	Site ID	Lat (°N)/Lon (°E)	Land cover type	LP v3.4 function type	Network data provider
1	BART	44.0639/-71.2873	OF	A1	NEON
10	FUJI	35.4435/138.7649	NLF	A1	GBOV
14	HARV	42.5378/-72.1715	OF	A1	NEON
19	JERC	31.1948/-84.4688	NLF	A1	NEON
28	ORNL	35.9641/-84.2826	OF	A1	NEON
33	SCBI	38.8929/-78.1395	OF	A1	NEON
34	SERC	38.8902/-76.5601	OF	A1	NEON
40	STEI	45.5089/-89.5864	DBF	A1	NEON
43	TALL	32.9505/-87.3933	NLF	A1	NEON
47	UKFS	39.0404/-95.1922	DBF	A1	NEON
48	UNDE	46.2340/-89.5375	OF	A1	NEON

2.3.3 AMMA – Cycle Atmosphérique et Cycle Hydrologique (CATCH) system

AMMA – *Cycle Atmosphérique et Cycle Hydrologique* (CATCH) observing system has collected a data set composed of LAI, fAPAR and clumping index in the Sahelian rangelands of *Gourma* region in Mali over the 2005-2017 period. Currently, the dataset[3] is available only for the 2005-2016 period

The measures were carried out at the sites previously installed in 1984 and monitored till 1994 by the International Livestock Centre for Africa (ILCA) and by the *Institut d'Economie Rurale* (IER, Bamako) (Hiernaux et al., 2009a, 2009b), and reactivated by the AMMA–CATCH observing system during the AMMA project (Redelsperger et al., 2006). These 1 km x 1 km sites were chosen within large and relatively homogeneous areas to sample the main vegetation types and canopies encountered within the super-site.

The variables were derived from the acquisition and the processing of hemispherical photographs taken along 1 km linear sampling transects mainly for herbaceous canopies, even if there is also one inundated forest site with a limited sampling (0.5 km). Then, only herbaceous canopies were used in this analysis as measurements are representative over 1 km x 1 km area. At each sampling date, 100 or 50 hemispherical photographs were acquired. Generally, hemispherical photographs were taken approximately every 10 days during the growing seasons for the herbaceous canopies. The collected hemispherical pictures were analysed using the CAN-EYE [CAN_EYE_UG] software and the estimated mean vegetation variables at the 1 km scale were computed by averaging all the measurements acquired along the transect.

[3] https://www.amma-catch.org/ (accessed on 22/10/2025)

3 Results

3.1 Product completeness

Figure 3 shows the spatial distribution of the percentage of missing values over LANDVAL sites for the entire 2000–2020 period of CRDP-2 fAPAR (same for LAI). It should be noted that MODIS V6.1 products are not included in this section as they do not provide data over desert regions due to their biome dependency (Myneni et al., 2002; Yang et al., 2006). The results are displayed considering all pixels and 'best quality' pixels according to quality flags (Table 4).

All pixels	'best quality' pixels
CCI+ VP	
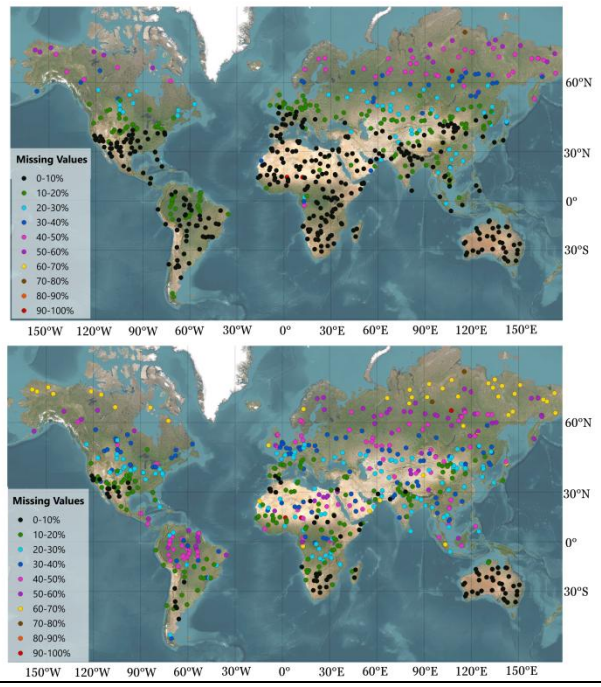	
C3S V3	
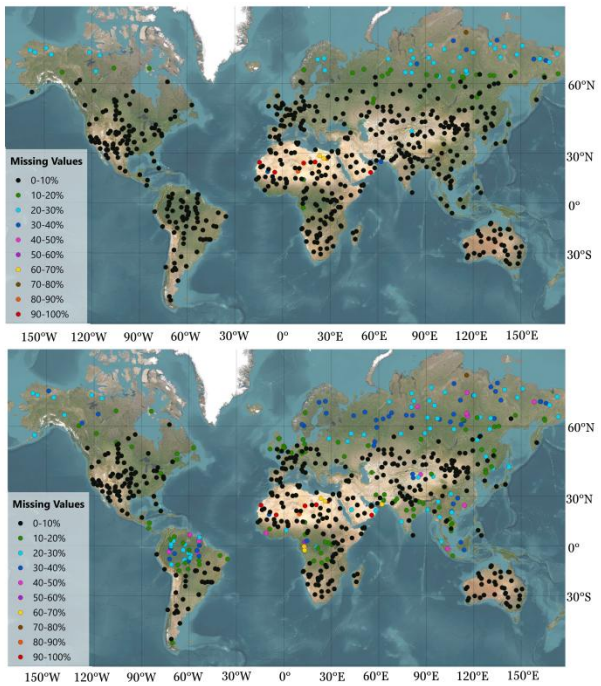	

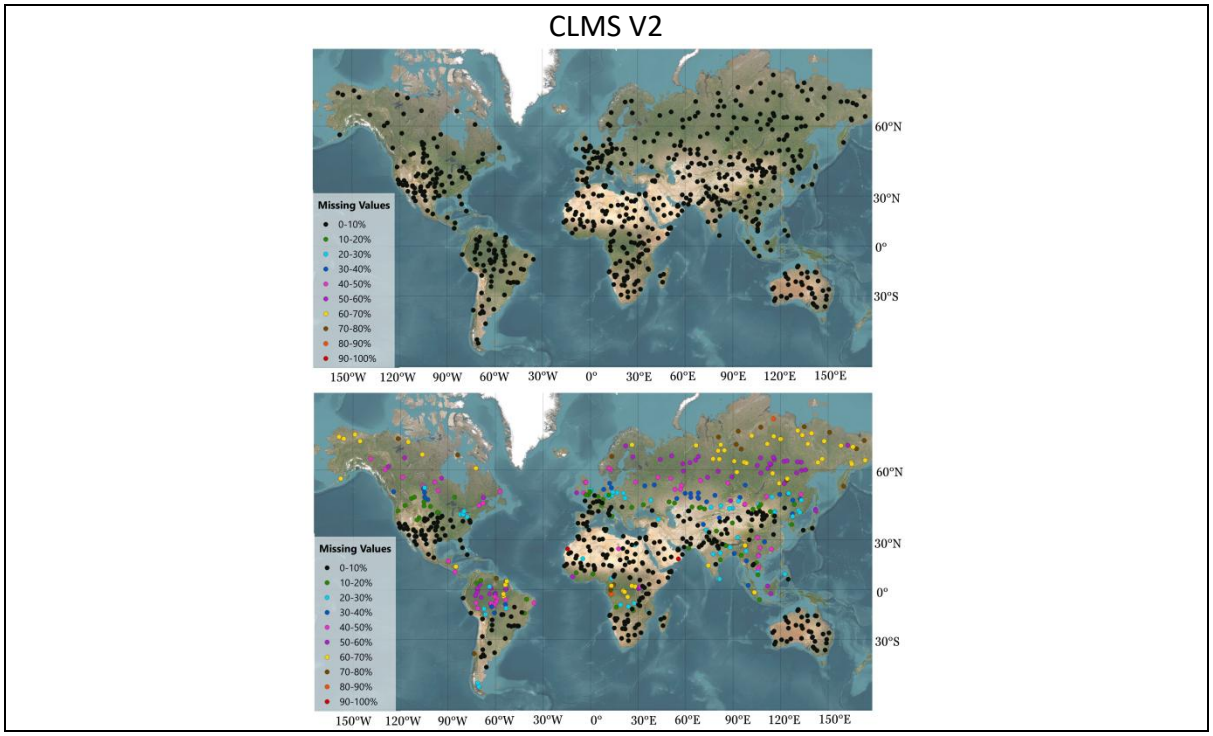

Figure 3: Maps of missing values (computed over LANDVAL sites) during 2000-2020 considering all (left) and best quality (right) pixels. From top to bottom: CCI+ VP, C3S V3 and CLMS V2 fAPAR products.

The main findings are:

- The CCI product (i.e., considering all pixels) provides good completeness across most regions globally, including equatorial areas, except for northern latitudes, like C3S product. However, the application of CCI quality flags discards a substantial number of retrievals, not only over areas typically affected by cloud cover (e.g., the equatorial belt) or snow-covered region, but also over other regions such as desert sites and southern Europe. As expected, CLMS V2 non-filled products exhibit missing data over regions typically affected by cloud cover and/or snow, such as the equatorial belt and northern latitudes.

Figure 4 illustrates the temporal evolution of missing values in CCI+ VP over LANDVAL sites for the whole 2000–2020 period, highlighting here the effect of different quality flags. Each flag corresponds to a specific retrieval condition: bit 8 (RETR_UNTRUSTED), bit 9 (RETR_LOW_QUALITY) and pixels with $\chi^2 < 0.5$. The figure also shows the fraction of pixels excluded when all quality flags are applied (BQ), providing insight into the overall data completeness and the impact of the quality control scheme over time.

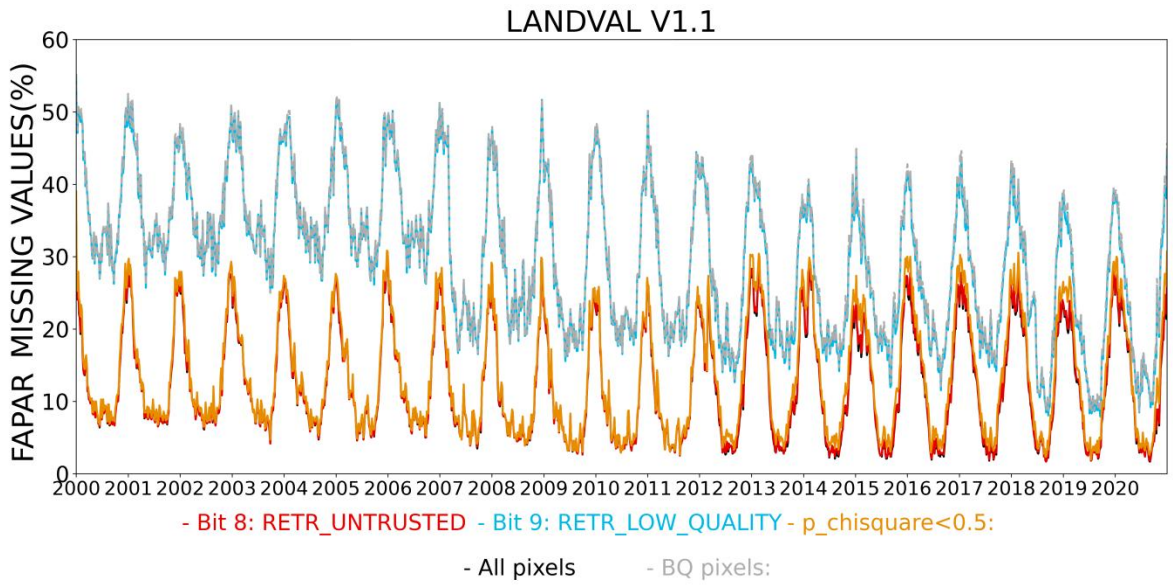

Figure 4: Temporal variation of the percentage of missing values over LANDVAL sites for CCI+VP CRDP-2 (2000–2020), considering different quality flags: bit 8 (RETR_UNTRUSTED, red), bit 9 (RETR_LOW_QUALITY, blue), and pixels with $\chi^2 < 0.5$ (yellow). Pixels excluded by all flags (BQ) are shown in grey.

Main conclusions from Figure 4 are:

- CRDP-2 exhibits the expected seasonal pattern of missing data with higher fractions of missing values during winter in the Northern Hemisphere, as previously observed for references datasets. This can be well explained by the increase of the cloud cover and snow-covered areas in high latitudes in winter.
- A temporal trend of completeness is observed: as additional sensors are incorporated from 2007 onwards, the increased number of available observations results in better completeness, mainly considering 'best quality' pixels and at the end of the period.
- The application of bit 8 (RETR_UNTRUSTED) and the χ^2 filter (pixels with $\chi^2 < 0.5$) has a low impact on product completeness, as the temporal fraction of missing data remains almost identical to that obtained without applying these flags. Only the χ^2 filter shows a minor effect, adding approximately 2–4% more missing data in the later years of CRDP-2, corresponding to periods when additional sensors were used in the CCI+ VP retrieval.
- Bit 9 (RETR_LOW_QUALITY) is the most restrictive flag. In particular, during the mono-sensor period (2000–2006), the application of this bit introduces a large fraction of missing values, especially during the Northern Hemisphere summer. Since 2007 (i.e., the first year with multiple sensors: VGT + AVHRR), and after 2018 (including OLCI sensors), a lower fraction of missing data is observed.

3.2 Spatial consistency

3.2.1 Visual inspection of maps

The spatial consistency CRDP-2 LAI and fAPAR layers were visually checked along with animations over the whole transect for the two variables. Figure 5 and Figure 6 show examples of the global

distributions of CCI+ VP LAI around mid-February and mid-July, respectively, for the years 2004, 2012, and 2019. Figure 7 and Figure 8 show the same date for fAPAR product.

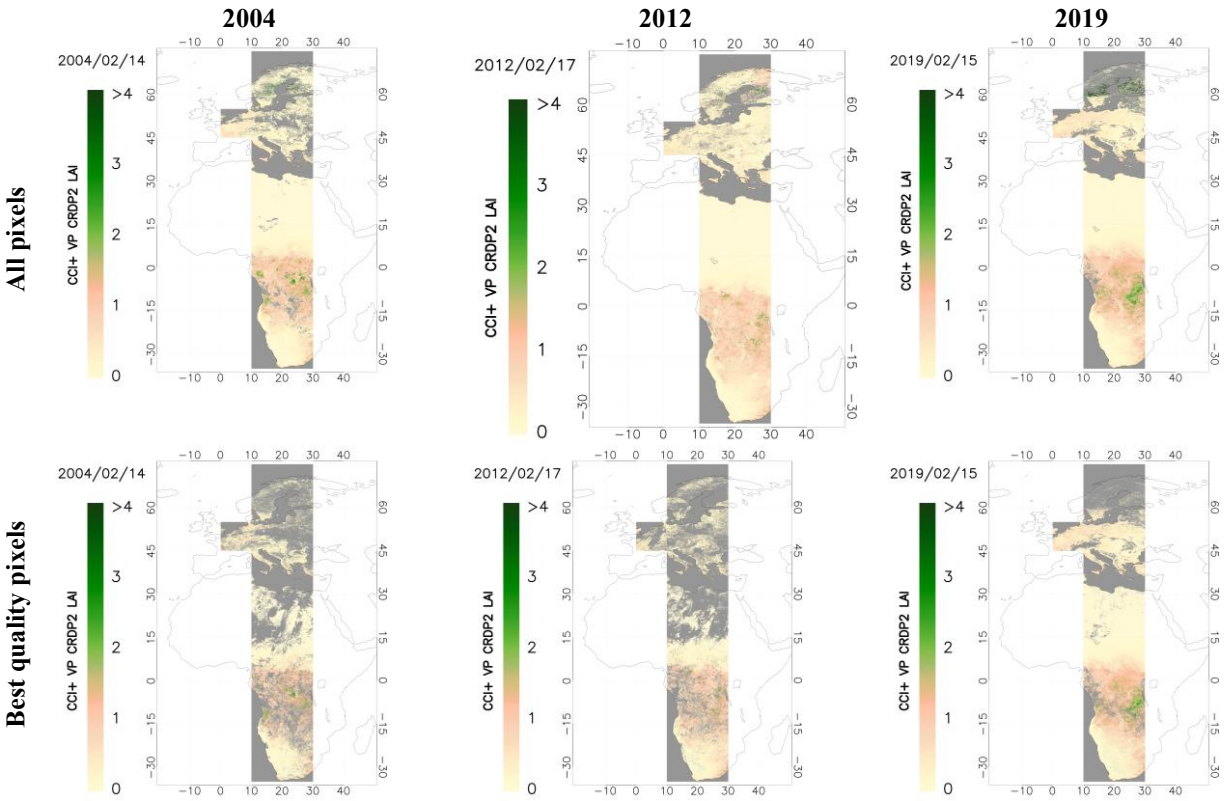

Figure 5: Maps CCI+ VP CRDP-2 LAI over the whole transect for all pixels (top) and best quality pixels (bottom) in mid-February for 2004 (left), 2012 (middle) and 2019 (right). Grey values correspond to missing or low-quality pixels.

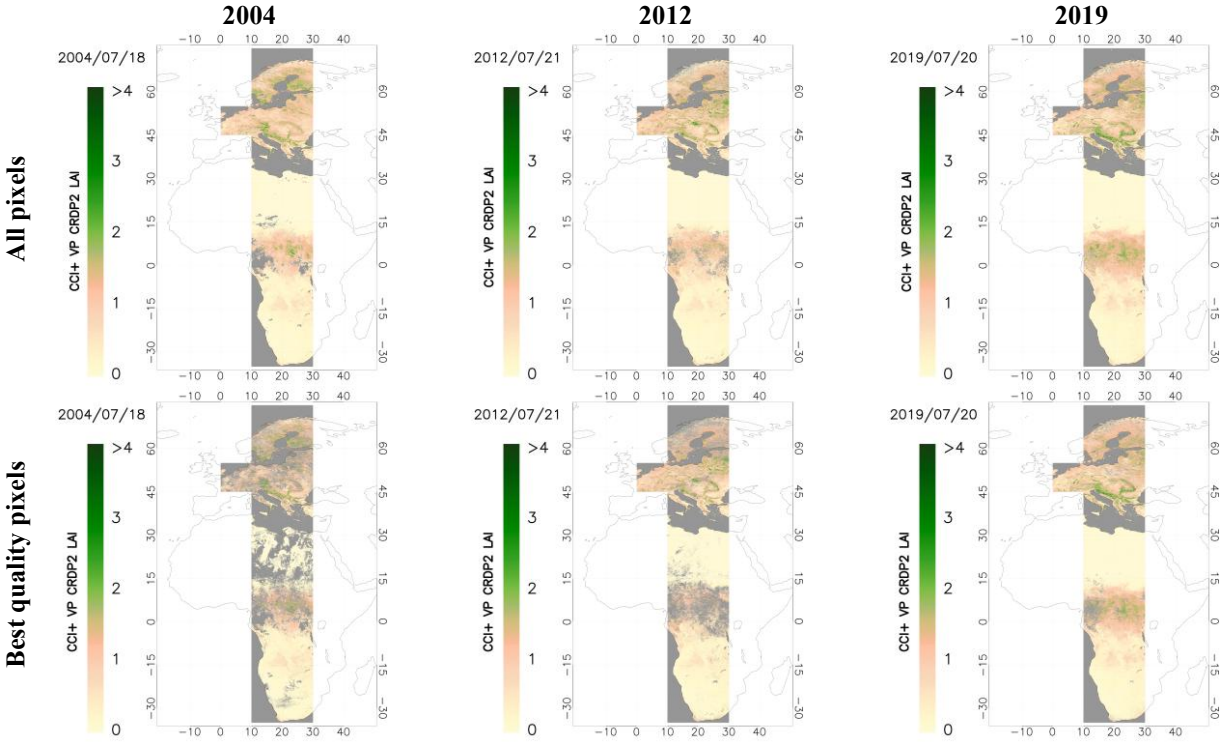

Figure 6: Maps CCI+ VP CRDP-2 LAI over the whole transect for all pixels (top) and best quality pixels (bottom) in mid-July for 2004 (left), 2012 (middle) and 2019 (right). Grey values correspond to missing or low-quality pixels.

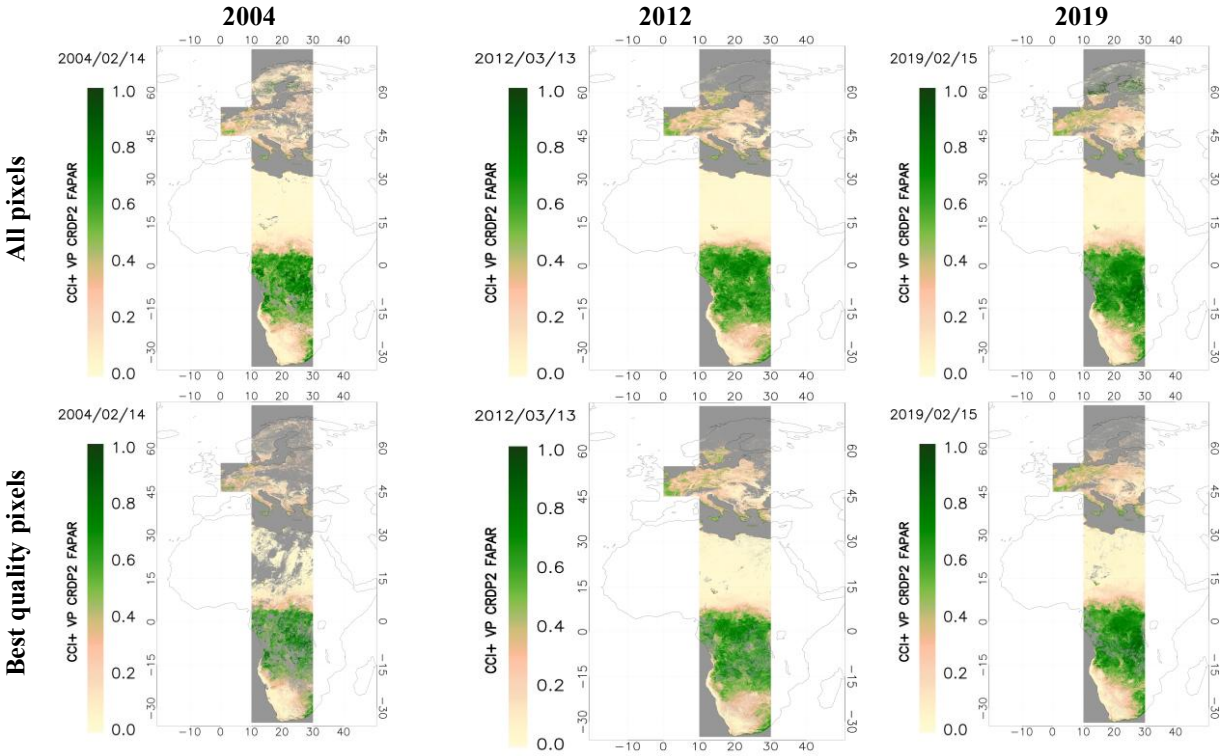

Figure 7: Maps CCI+ VP CRDP-2 fAPAR over the whole transect for all pixels (top) and best quality pixels (bottom) in mid-February for 2004 (left), 2012 (middle) and 2019 (right). Grey values correspond to missing or low-quality pixels.

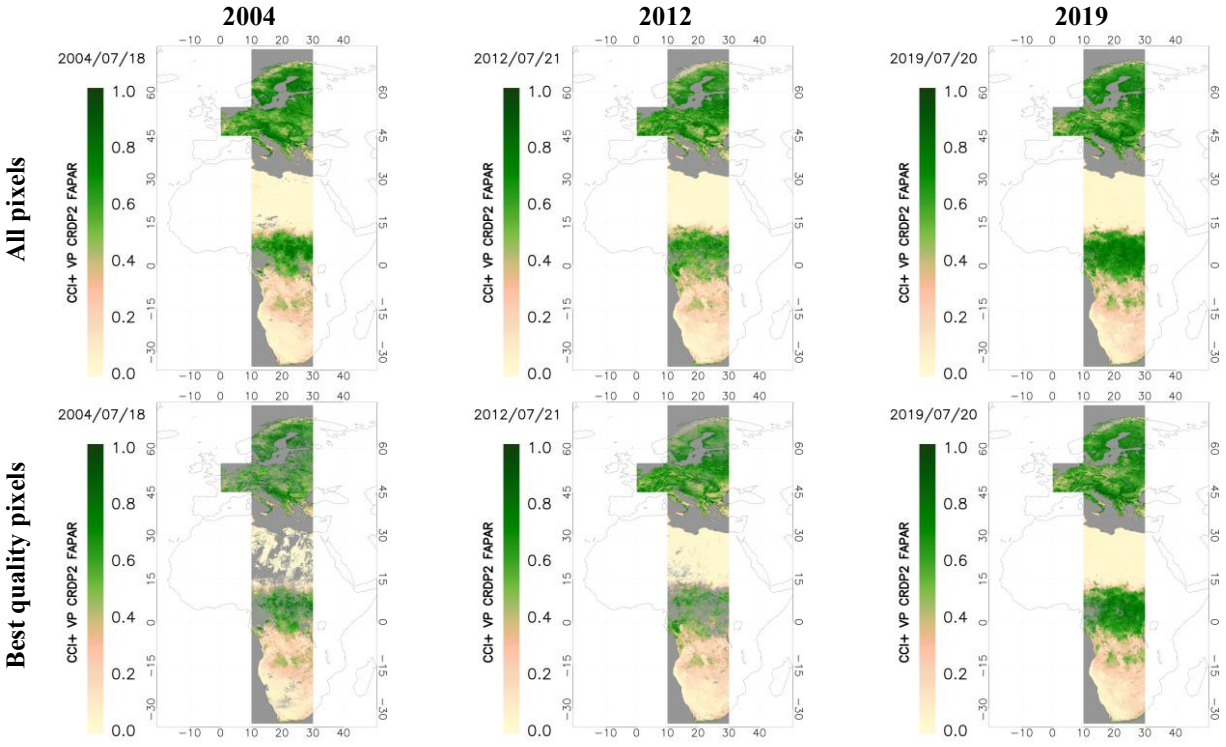

Figure 8: Maps CCI+ VP CRDP-2 FAPAR over the whole transect for all pixels (top) and best quality pixels (bottom) in mid-July for 2004 (left), 2012 (middle) and 2019 (right). Grey values correspond to missing or low-quality pixels.

The main findings for the visual inspection of the CRDP-2 maps over the transect are:

- Reliable spatial distributions are found over most areas for LAI and fAPAR products.
- Some unrealistic high values are found over high latitudes, typically during winter. Most of them are effectively removed when the quality flags are applied.
- Unexpected low LAI values are observed over dense vegetation areas, such as equatorial forests.
- The use of quality flags removes large areas with realistic values, mainly in northern hemispheric wintertime. The effect is greater in 2004 (mono-sensor period) and lower in 2018 (availability of many sensors). This is mainly related to the bit 9_LOW QUALITY. Therefore, the application of this "LOW_QUALITY" flag needs to be done with caution, mainly during the first years of the dataset.

3.2.2 Analysis of differences

The spatial distributions of differences between CCI+ VP and the reference satellite products are evaluated in this section. Figure 9 presents the difference map between CRDP-2 and C3S V3 LAI products for mid-June 2012 (similar spatial distributions of differences were found for the other evaluated years). Similarly, Figure 10 displays the difference maps between CCI+ VP CRDP-2 and the C3S V3, CLMS V2, and NASA MODIS V6.1 fAPAR products for mid-July 2012 (similar difference maps were obtained for other years).

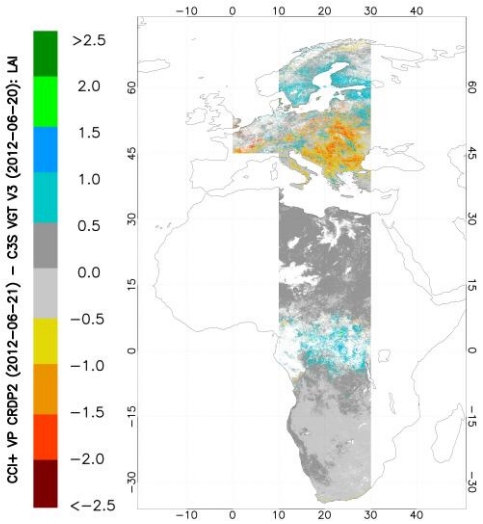

Figure 9: Map of differences between CCI+ VP CRDP-2 and C3S V3 LAI products (best quality pixels) over the whole transect in mid-June 2012.

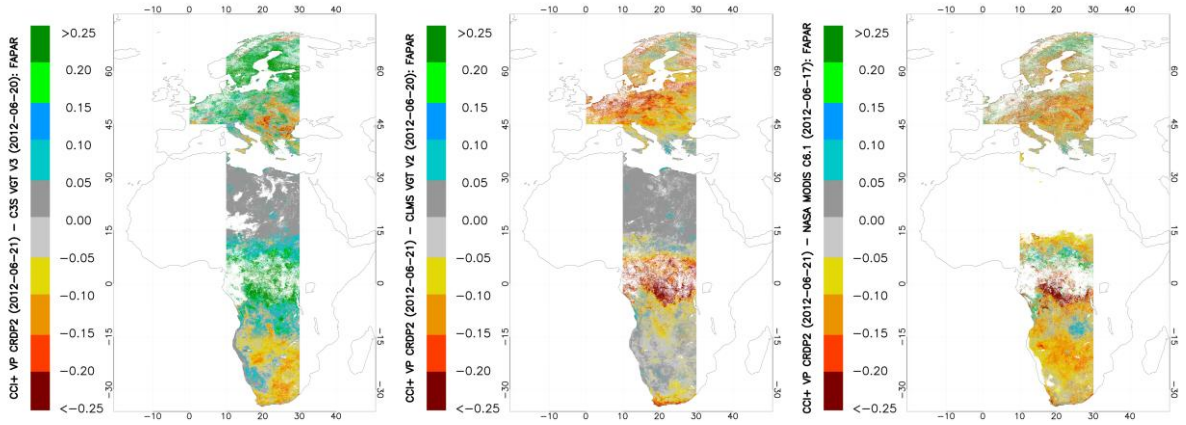

Figure 10: Maps of differences between CCI+ VP CRDP-2 and C3S V3, CLMS V2 and MODIS V6.1 fAPAR products (best quality pixels) over the whole transect in mid-June 2012.

Main results of the spatial analysis of differences between CCI+ VP CRDP-2 and reference products are:

- For LAI, the largest discrepancies with C3S V3 occur over northern latitudes and equatorial regions, where CCI+VP provides higher LAI values (around 0.5 – 1). Conversely, CCI+VP provides lower values than C3S over mid latitudes in Europe.
- For fAPAR:
    - CRDP-2 shows large discrepancies as compared to C3S, showing higher values across northern and equatorial regions (differences up to 0.25), but lower values over southern Africa.
    - CRDP-2 tends to provide systematically lower values than both CLMS and MODIS products over most regions, in particular tropical areas and some regions in central Europe.

3.3 Temporal consistency

This section evaluates the consistency of the multi-sensor CRDP-2 temporal variations in comparison with the reference products (C3S VGT+PBV V3**,** CLMS VGT+PBV V2, and NASA MODIS V6.1) and multi-temporal ground-based data from GBOV V3.4 and AMMA (when available), best quality retrievals are displayed. From Figure 11 to Figure 17, two examples for each main biome type (EBF, DBF, NLF, croplands, herbaceous, shrublands and SBA) are displayed. For better inspection of the temporal variations, the 2012-2015 period is shown when no ground data are available, otherwise, the period with available ground data is displayed. Annex I shows additional temporal profiles for the whole time series.

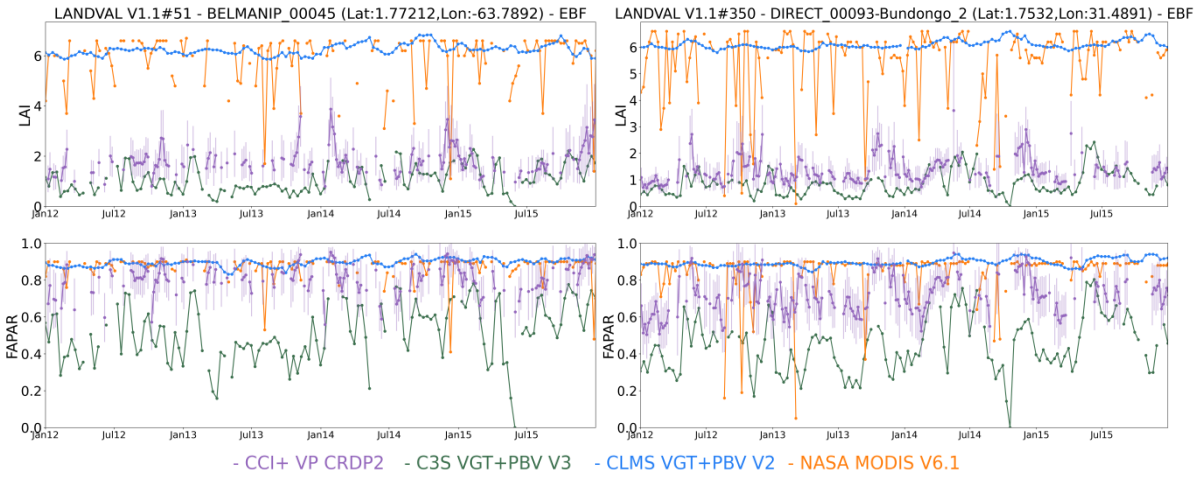

Figure 11: Temporal profiles of BQ retrievals over two selected LANDVAL evergreen broadleaved forest (EBF) sites of CCI+ VP (purple), C3S V3 (green), CLMS V2 (blue) and MODIS V6.1 (orange). Note: CCI+ VP and C3S provide effective LAI values.

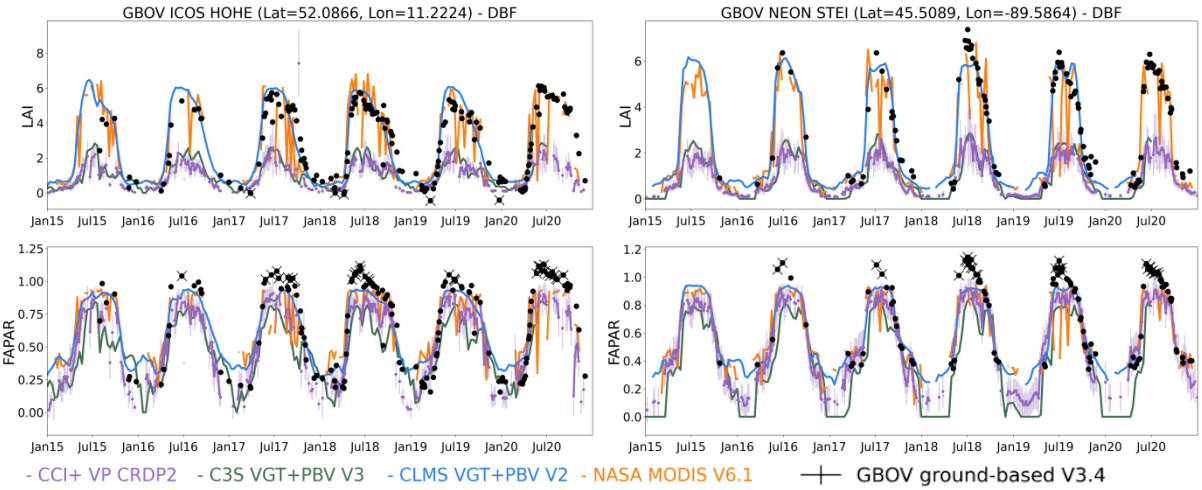

Figure 12: Same as in Figure 11 but over two selected GBOV deciduous broadleaved forests (DBF). Crosses in GBOV data indicates out-of-range estimates.

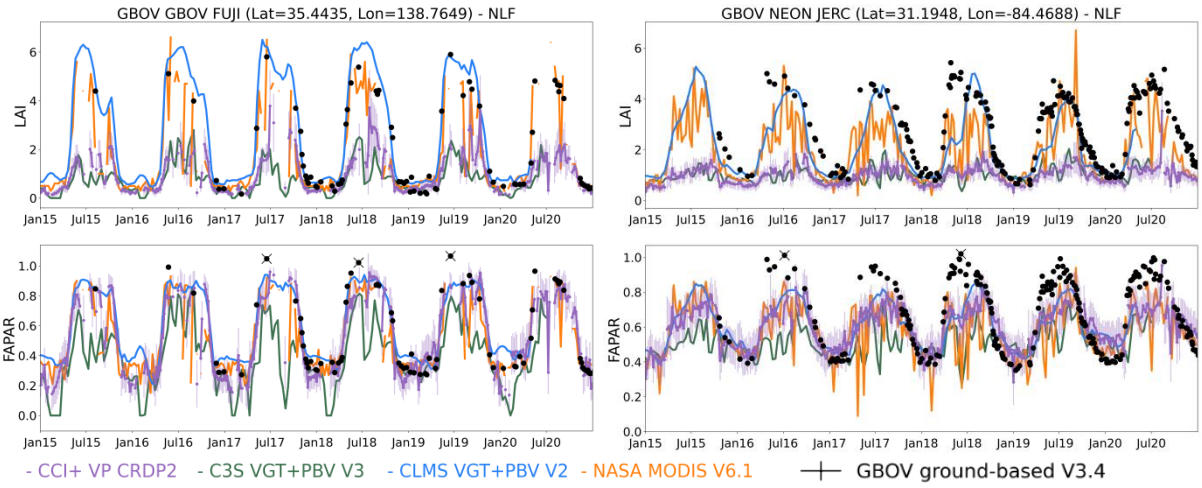

Figure 13: Same as in Figure 11 but over two selected GBOV needle-leaf forests (NLF).

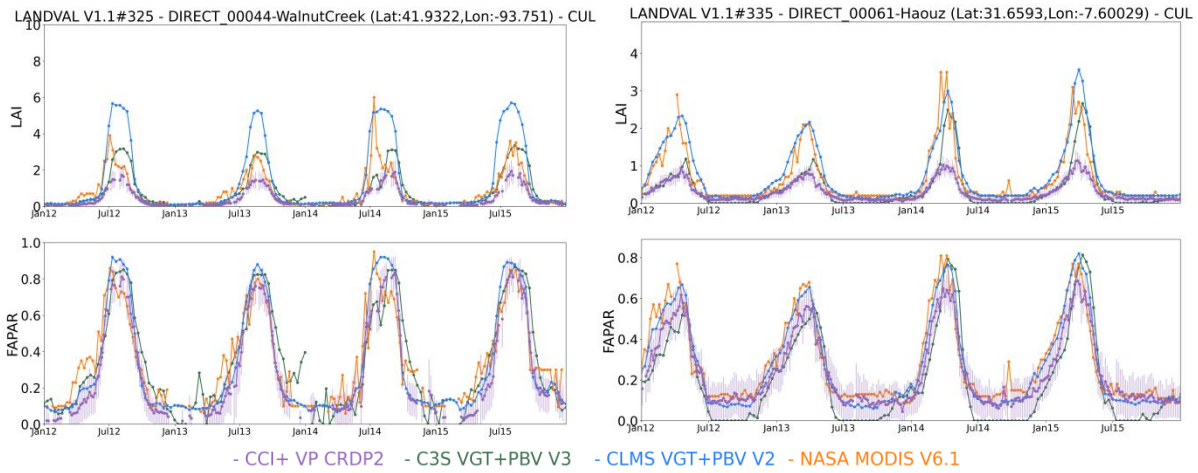

Figure 14: Same as in Figure 11 but over two selected LANDVAL cultivated sites.

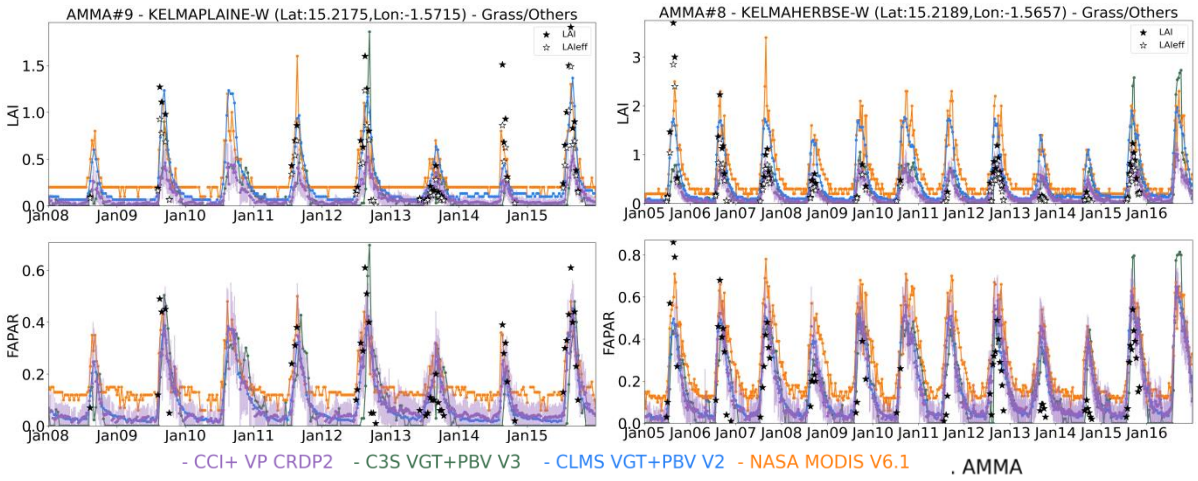

Figure 15: Same as in Figure 11 but over two selected AMMA herbaceous sites.

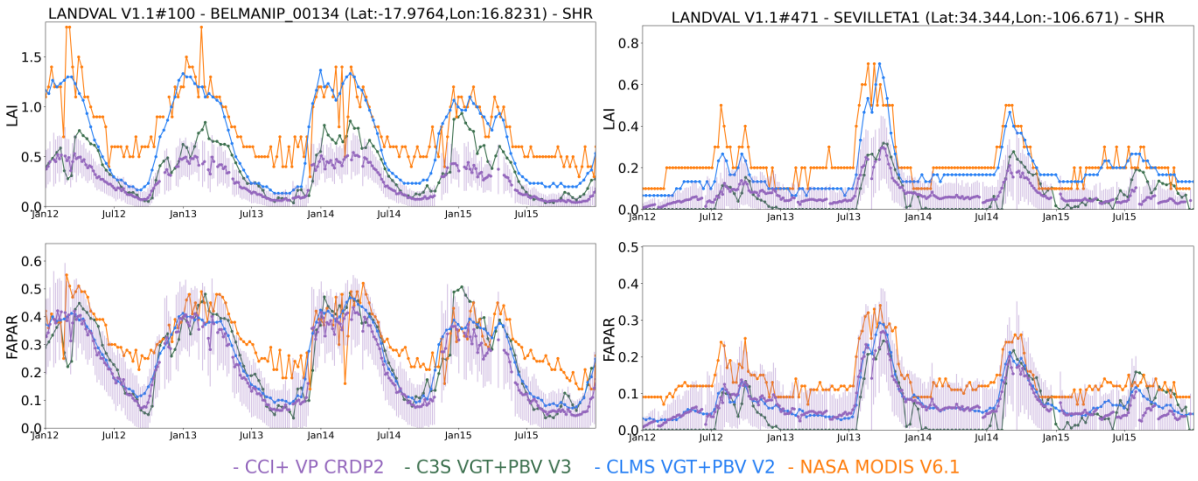

Figure 16: Same as in Figure 11 but over two selected LANDVAL shrublands sites.

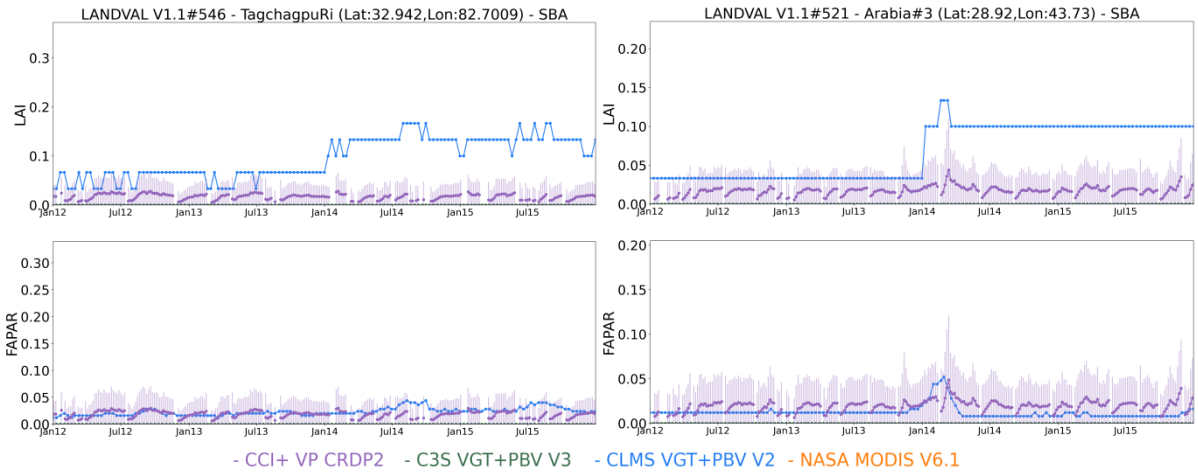

Figure 17: Same as in Figure 11 but over two selected LANDVAL sparse and bare areas.

Main results from the visual inspection of CCI+ VP CRDP-2 temporal trajectories are:

- For EBF biome type (Figure 11), CCI+ VP exhibits noisy temporal trajectories, as expected due to the persistent clouds over this biome. However, the level of noise is lower than in C3S and MODIS products. In contrast, CLMS V2 trajectories are very smooth with minimal seasonality, consistent with the smoothing techniques applied in the temporal composites (Verger et al., 2023). Regarding the magnitude of values, CCI provides higher LAI estimates than C3S, as previously observed over the transect. The large discrepancy with other references is due to the product definition (effective vs true LAI). For fAPAR, CCI provides values comparable to those of CLMS and MODIS, improving notably the C3S estimates (systematically lower than other satellite products).
- For DBF (Figure 12) and NLF (Figure 13), remarkably good seasonal and inter-annual variations were found, similar to that of satellite-based and ground-based products. For LAI, CCI (and C3S) shows lower magnitude of values than CLMS and MODIS references due to different definitions (LAIeff vs LAI). For fAPAR, remarkably good agreement is also found in terms of magnitude of values.
- Similarly for cultivated (Figure 14), herbaceous (Figure 15) and shrublands (Figure 16) biomes, CRDP-2 product captures the same seasonality and temporal dynamics as the reference satellite products and ground data when available (e.g., AMMA sites in Figure 15). For LAI, CCI provides systematically lower values than C3S at the maximum peak of vegetation development. For fAPAR, CCI values are similar to other references such as CLMS. This is remarkable for low values where CRDP-2 displays reliable temporal variations, and notably improves C3S with a high occurrence of unrealistic zero values (e.g., AMMA sites in Figure 15 or LANDVAL V1.1#471 in Figure 16).
- CCI provides very low or near-zero values over sparsely vegetated (Figure 17, left) and bare areas (Figure 17, right). Minor variations can be observed, but they remain well within the uncertainty budget. The transition from SPOT/VGT to PROBA-V in 2014 does not introduce any apparent bias, in contrast to the discontinuities (positive bias) observed in the CLMS products. Therefore, the CRDP-2 demonstrates remarkably good continuity across the transition in sensor input data.

3.4 Error evaluation (direct validation)

3.4.1 Comparison with DIRECT 2.1

This section presents the comparison of CCI+ VP multi-sensor CRDP-2**,** C3S VGT+PBV V3, CLMS VGT+PBV V2, and NASA MODIS V6.1 against the DIRECT 2.1 ground-based reference maps over 3 km x 3 km. Figure 18 illustrates the comparison of CCI and C3S with DIRECT 2.1 effective LAI, while Figure 19 shows the comparison of the four products with DIRECT 2.1 fAPAR. Only concomitant samples flagged as 'best quality' across all satellite products under evaluation were considered.

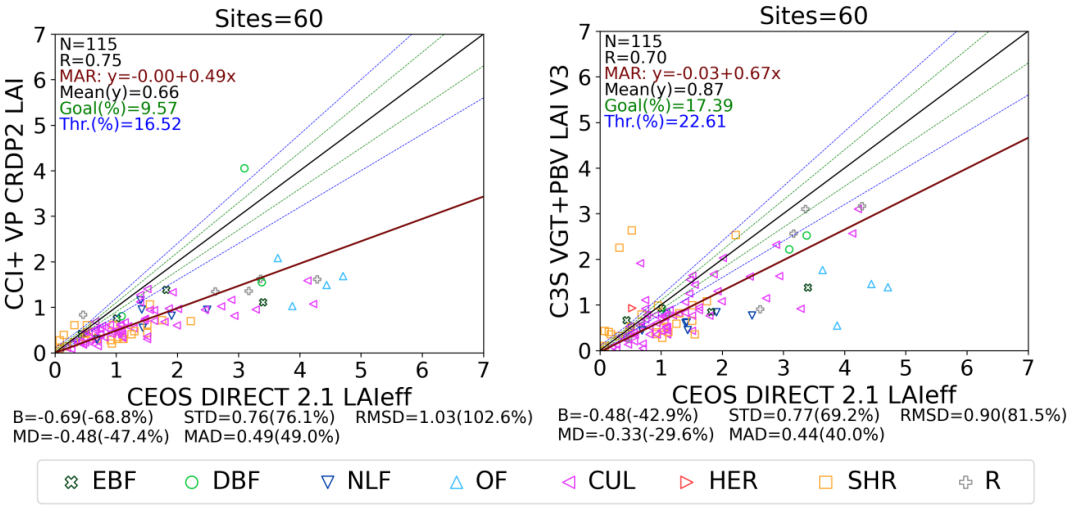

Figure 18: Scatter plots between CCI+ VP CRDP-2 (left) and C3S V3 (right) LAI products versus DIRECT 2.1 LAIeff ground-based maps. 'EBF' stands for evergreen broadleaved forests, 'DBF' for deciduous broadleaved forests, 'NLF' for needle-leaf, 'OF' for other forests, 'CUL' for cultivated, 'HER' for herbaceous, 'SHR' for shrublands and 'R' for rice. Green and blue lines stand for goal and threshold levels, respectively. The brown line represents the MAR fit, while the green and blue lines indicate the goal and threshold levels, respectively.

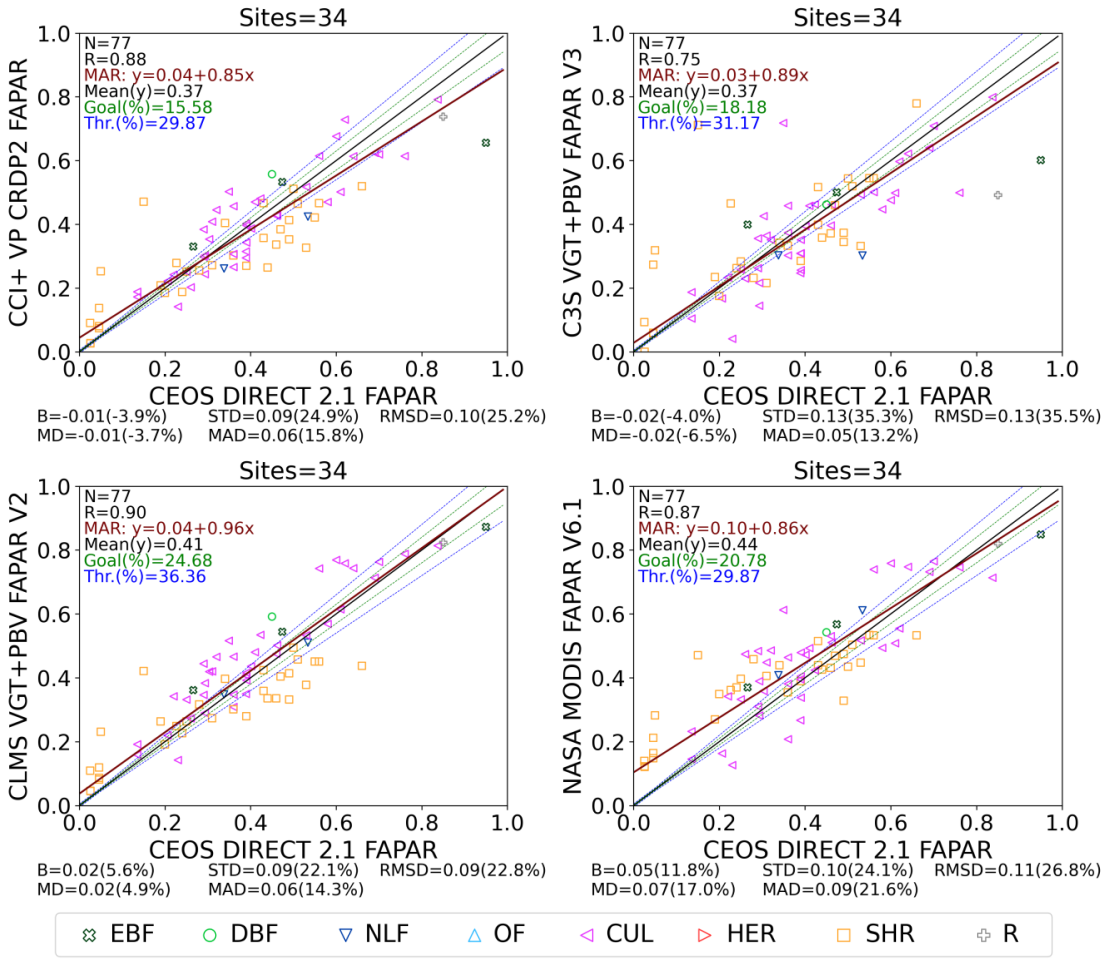

Figure 19: Scatter plots between CCI+VP CRDP-2 (top left), C3S V3 (top right), CLMS V2 (bottom left) and MODIS V6.1 (bottom right) fAPAR products versus DIRECT 2.1 fAPAR ground-based maps. 'EBF' stands for evergreen broadleaved forests, 'DBF' for deciduous broadleaved forests, 'NLF' for needle-leaf, 'OF' for other forests, 'CUL' for cultivated, 'HER' for herbaceous, 'SHR' for shrublands and 'R' for rice. The brown line represents the MAR fit, while the green and blue lines indicate the goal and threshold levels, respectively.

Main findings for LAIeff (Figure 18) are:

- CRDP-2 shows good correlation (R = 0.75), slightly better than C3S, and RMSD of 1.03 which is slightly worse than C3S.
- CRDP-2 underestimates effective LAI ground references with biases of -68.8%, primarily over forest areas. This systematic tendency is also reflected in the slopes of the MAR relationships (0.49 for CCI). CRDP-2 shows larger underestimation than C3S (bias around -43%).
- Only 9.6% and 16.5% of CCI retrievals fall within the GCOS goal and threshold uncertainty requirements, respectively.

Main findings for fAPAR (Figure 19) are:

- CRDP-2 provides noteworthy results, showing high correlation (R = 0.88), very low negative bias (B = -0.01 (-3.9%), MD = -0.01 (-3.7%)) and an overall uncertainty (RMSD) of 0.10.
- CCI performs similarly to CLMS V2 (RMSD = 0.09), although the latter exhibits a positive bias of 5.6%. Both CCI and CLMS show the best agreement with DIRECT 2.1.
- CCI outperforms C3S and MODIS products, with RMSD of 0.13 and 0.11 for C3S and MODIS, respectively. Note that MODIS shows a clear tendency to overestimate low fAPAR values in sparsely vegetated areas as previously reported (e.g., D'Odorico et al., 2014).

- Despite the good overall validation metrics, CRDP-2 shows low fraction of retrievals compliant with the GCOS goal (15.6%) and threshold (29.9%) uncertainty requirements, which is indicative of the very demanding GCOS requirements.

3.4.2 Comparison with GBOV V3.4

This section reports the comparison of CCI+ VP CRDP-2**,** C3S VGT+PBV V3**,** CLMS VGT+PBV V2, and NASA MODIS V6.1 against a subset of quality controlled GBOV V3.4 ground-based reference maps (GBOV V3.4_QC) at 3 km x 3 km. Figure 20 presents the comparison with GBOV V3.4 LAI. Note that, due to differences in definition (i.e., effective LAI in CCI and C3S versus actual LAI in GBOV), the validation metrics are expressed exclusively in terms of correlation. Figure 21 shows the comparison with GBOV V3.4_QC fAPAR. Only concomitant BQ samples across all satellite products were used.

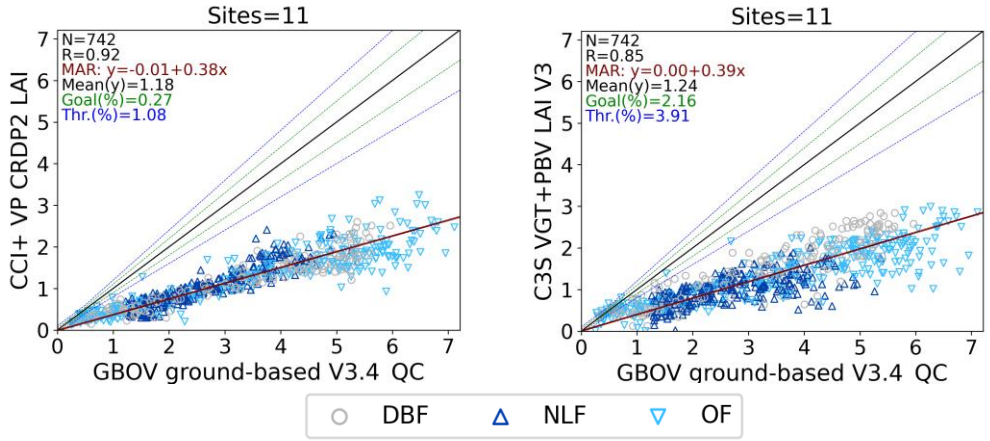

Figure 20: Scatter plots between CCI+ VP CRDP-2 (left) and C3S V3 (right)LAI products versus GBOV ground-based V3.4_QC LAI. 'DBF' stands for deciduous broadleaved forests, 'NLF' for needle-leaf and 'OF' for other forests. The brown line represents the MAR fit, while the green and blue lines indicate the goal and threshold levels, respectively.

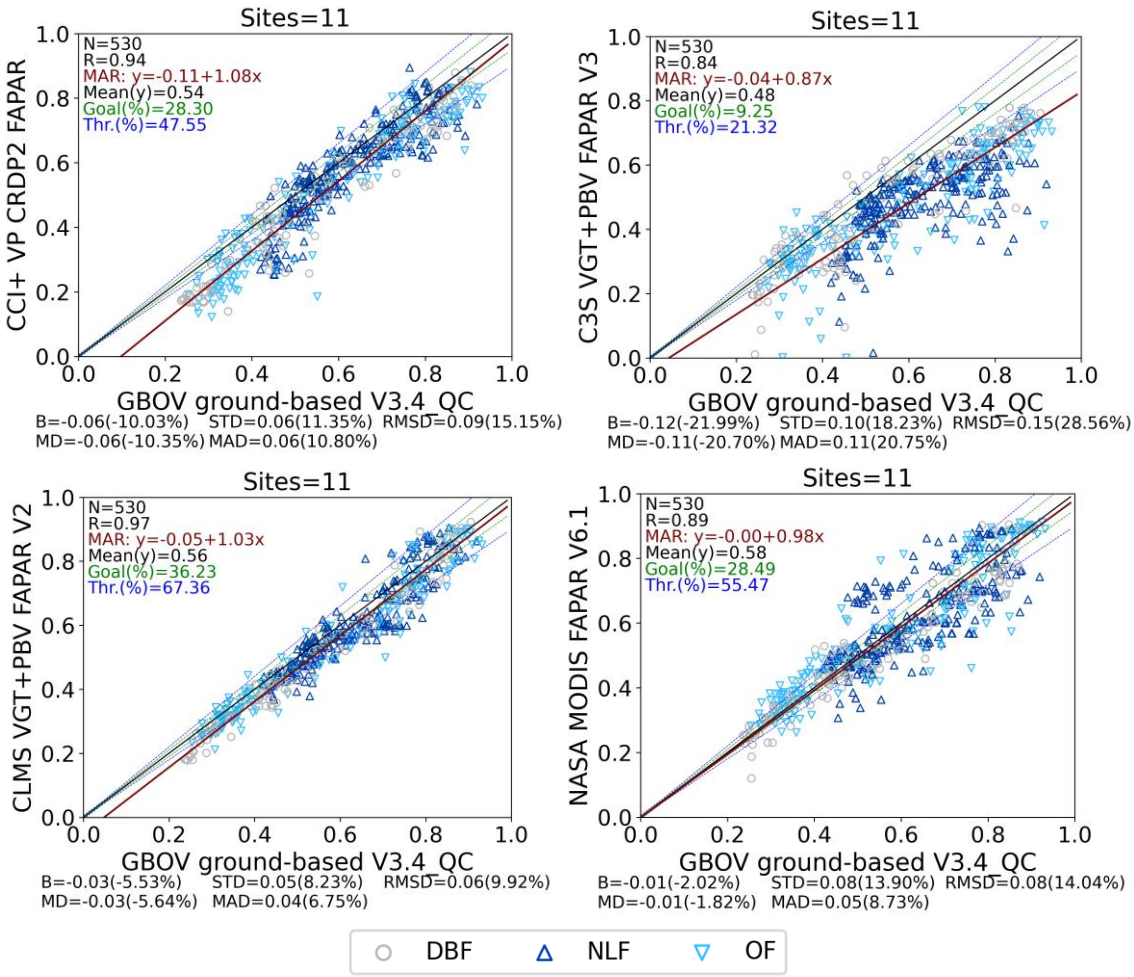

Figure 21: Scatter plots between CCI+VP CRDP-2 (top left), C3S V3 (top right), CLMS V2 (bottom left) and MODIS V6.1 (bottom right) fAPAR products versus GBOV ground-based V3.4_QC fAPAR. 'DBF' stands for deciduous broadleaved forests, 'NLF' for needle-leaf and 'OF' for other forests. The brown line represents the MAR fit, while the green and blue lines indicate the goal and threshold levels, respectively.

Main findings for LAI (Figure 20) are:

- CRDP-2 LAI (effective) is highly correlated with GBOV V3.4_QC LAI, with R = 0.92, outperforming the results of C3S.
- Large systematic differences are observed due to the different product definition (as expected). It should be noted that the clumping index over forests typically ranges between 0.6 and 0.8 (Chen et al., 2005); therefore, the observed systematic differences can only be partially corrected if the clumping index factor is accounted for.

Main findings for fAPAR (Figure 21) are:

- CRDP-2 tends to slightly underestimate GBOV V3.4_QC values, with a mean bias of -0.06 (-10%) and an overall uncertainty (RMSD) of 0.09. Note that GBOV measures fIPAR instead fAPAR (with fIPAR slightly higher that fAPAR in most conditions, (Wojnowski et al., 2021)).
- CRDP-2 outperforms the C3S in terms of accuracy (B = -0.12, -22%) and is overall similar to MODIS (RMSD = 0.08, although with lower correlation). CLMS is the best performing product with optimal validation metrics (R= 0.97, B=-0.03, RMSD= 0.06).

- In terms of GCOS uncertainty requirements, CRDP-2 meets goal and threshold requirements in 28.3% and 47.6% of cases, respectively. This is similar to MODIS and shows better compliance than C3S V3.

3.4.3 Comparison with AMMA

This section presents the comparison of CRDP-2**,** C3S V3**,** CLMS V2, and MODIS V6.1 against the AMMA ground measurements over grassland sites. Figure 22 shows the comparison with AMMA effective LAI, while Figure 23 shows the comparison with AMMA fAPAR measurements. Only concomitant samples flagged as 'best quality' across the satellite products under evaluation were considered. In this case, the comparison was performed at a spatial support of 1 km², consistent with the AMMA ground measurements collected over transects of approximately 1 km.

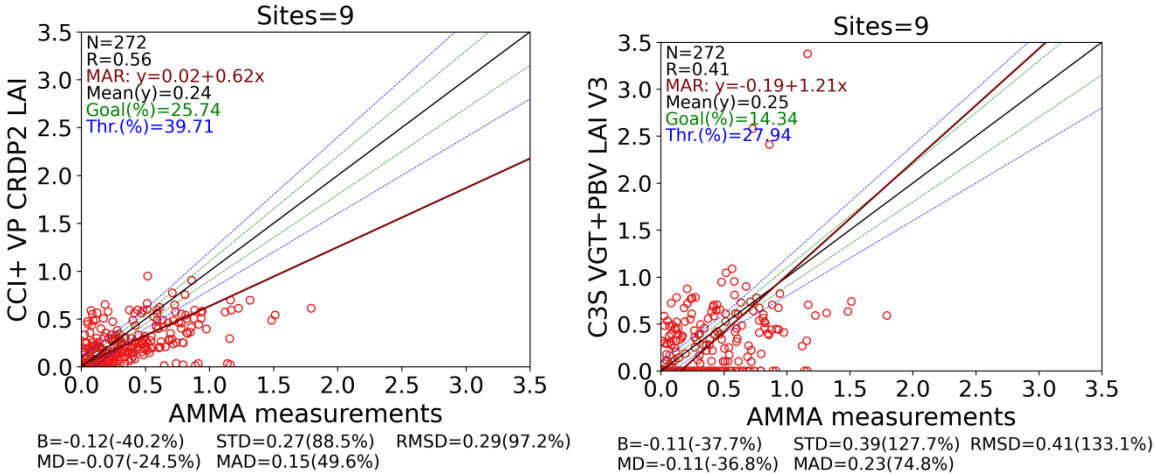

Figure 22: Scatter plots between CCI+ VP CRDP-2 (left) and C3S V3 (right) LAI products versus AMMA LAIeff ground data. The brown line represents the MAR fit, while the green and blue lines indicate the goal and threshold levels, respectively.

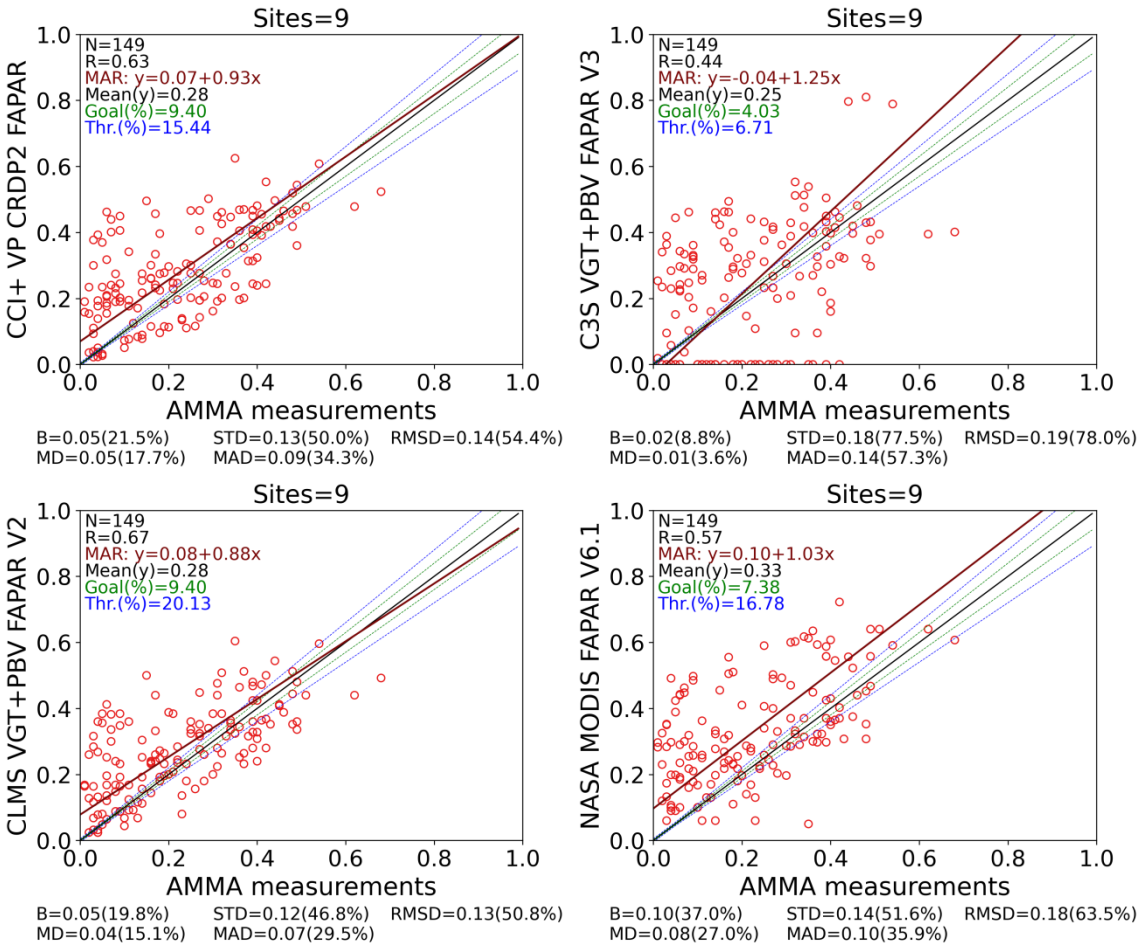

Figure 23: Scatter plots between CCI+VP CRDP-2 (top left), C3S V3 (top right), CLMS V2 (bottom left) and MODIS V6.1 (bottom right) fAPAR products against AMMA fAPAR ground data. The brown line represents the MAR fit, while the green and blue lines indicate the goal and threshold levels, respectively.

Main findings for LAI products (see Figure 22) are:

- CRDP-2 underestimates AMMA LAIeff measurements, with a bias of -0.12 (-40.2%) and slope of 0.62. Correlation of R = 0.56 and overall uncertainty (RMSD) of 0.29 are found.
- CRDP-2 improves the C3S retrievals in terms of RMSD (0.41) and correlation (0.41). Note that a high proportion of C3S LAI values are zero, a well-known limitation of the C3S V3 product [PQAR-C3S_V3].
- For CCI, 25.7% and 39.7% of cases fall within the optimal and threshold GCOS uncertainty levels, respectively, outperforming C3S.

Main findings for fAPAR products (Figure 23) are:

- CRDP-2 tends to overestimate AMMA measurements over grasslands, with a mean bias of 0.05 (21.5%) and an overall uncertainty (RMSD) of 0.14, similar to CLMS V2 performance (B = 0.05, 19.8%; RMSD = 0.13).
- CRDP-2 improves validation results of C3S V3 (RMSD = 0.19) and MODIS (RMSD = 0.18). Note, again, the large proportion of C3S fAPAR values equal to zero, a known limitation of the C3S product [PQAR-C3S_V3].

- In terms of GCOS requirements, 9.4% and 15.4% of cases comply with the goal and threshold uncertainty requirements, respectively. These results are comparable to those of CLMS (9.4% and 20.1%) and MODIS (7.4% and 16.8%), and superior to C3S (4.0% and 6.7%).

3.5 Error evaluation (product intercomparison)

3.5.1 Overall analysis

The overall consistency between CCI+ VP CRDP-2 and other satellite products (C3S VGT+PBV V3**,** CLMS VGT+PBV V2, and NASA MODIS V6.1) was assessed for the years 2004, 2012 and 2019. The three years (2004, 2012, and 2019) were aggregated into a single figure, where all corresponding 'best quality' retrievals over LANDVAL sites are jointly displayed to provide an overall consistency assessment of different single-sensor (2004) and multi-sensor (2012, 2019) periods. Figure 24 show the scatter plots between pair of products providing effective LAI (i.e., CCI vs. C3S) whilst Figure 25 shows the scatter plots of CCI versus C3S, CLMS and MODIS fAPAR products. The comparison of multi-sensor CRDP-2 with the mono-sensor CRDP-1 dataset can be found in Annex VI.

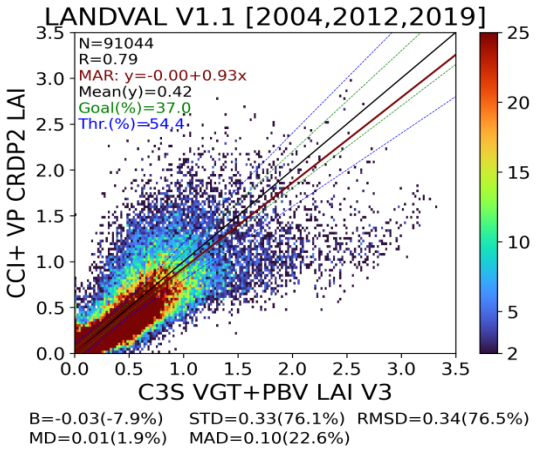

Figure 24: Scatter plot between CCI+VP CRDP-2 and C3S V3 satellite LAI products (colorbar represents density of points). Computation over best quality retrievals over LANDVAL sites for years 2004, 2012 and 2019. The brown line represents the MAR fit, while the green and blue lines indicate the goal and threshold levels, respectively.

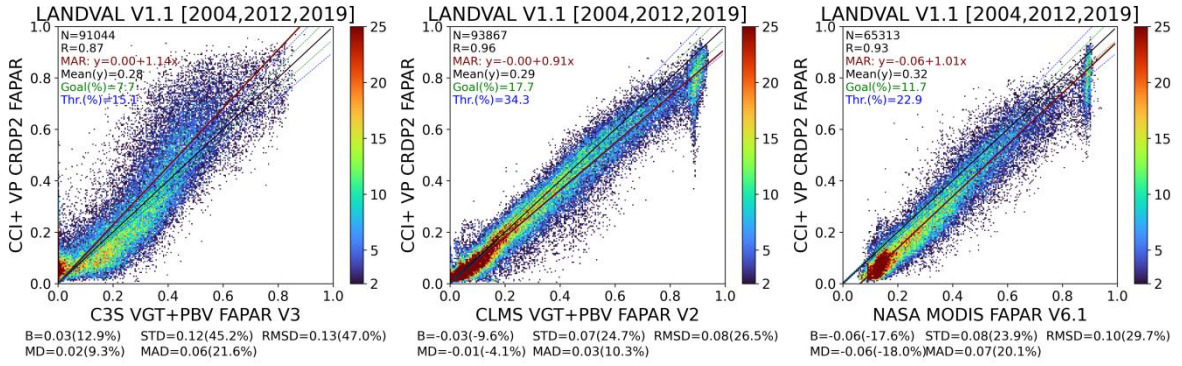

Figure 25: Scatter plots between CCI+VP CRDP-2 and reference satellite C3S V3, CLMS V2 and NASA V6.1 fAPAR products (colorbar represents density of points). Computation over best quality retrievals over LANDVAL sites for years 2004, 2012 and 2019. The brown line represents the MAR fit, while the green and blue lines indicate the goal and threshold levels, respectively.

The comparison of CCI +VP CRDP-2 and C3S V3 LAI products (Figure 24) shows:

- CRDP-2 provides slightly lower values than C3S V3, with a mean bias of -0.03 (-7.9%), primarily observed at higher LAI values (MAR slope of 0.93). Note that CRDP-2 LAI provides lower values than CRDP-1 values (bias=-0.1 (-20.6%), see Annex VI)
- The overall uncertainty (RMSD) is 0.34, with 37.0% and 54.4% of samples within the GCOS goal and threshold uncertainty requirements, respectively.

For fAPAR (Figure 25), the main results are:

- The comparison of CRDP-2 with CLMS V2 shows the best agreement (RMSD = 0.08, R = 0.96). CRDP-2 generally provides slightly lower values than CLMS, with a mean bias of -0.03 (-9.6%), mainly observed at the lower (fAPAR < 0.2) and higher (fAPAR > 0.8) ranges, the latter typically associated with EBF cases where CLMS V2 applies gap-filling techniques based on climatology values.
- The comparison of CRDP-2 with MODIS shows also good overall agreement (RMSD = 0.10, R = 0.93). CRDP-2 tends to provide lower values than MODIS (B = -0.06, -17.6%), mainly at low fAPAR ranges, consistent with the well-documented tendency of NASA MODIS products to overestimate fAPAR at the lowest value ranges (D'Odorico et al., 2014; Fuster et al., 2020).
- The weakest overall agreement is observed with C3S fAPAR products (RMSD = 0.13, R = 0.87), with a clear tendency of CRDP-2 to provide higher fAPAR values (B = 0.03, 12.9%) in line with other satellite products.
- Note that CRDP-2 fAPAR shows good agreement with CRDP-1 fAPAR, showing a slight negative bias of -0.02 (-5.3%) and RMSD of 0.08 (Annex VI).

3.5.2 Analysis per biome type

This section presents the overall spatio-temporal consistency per biome. Figure 26 and Figure 27 show the histograms of effective LAI and fAPAR retrievals, respectively, and the violin-plots of the bias of CCI+ VP with references per main biome type. Additionally, the scatterplots (with their associated statistics) per biome type are also available in Annex II.

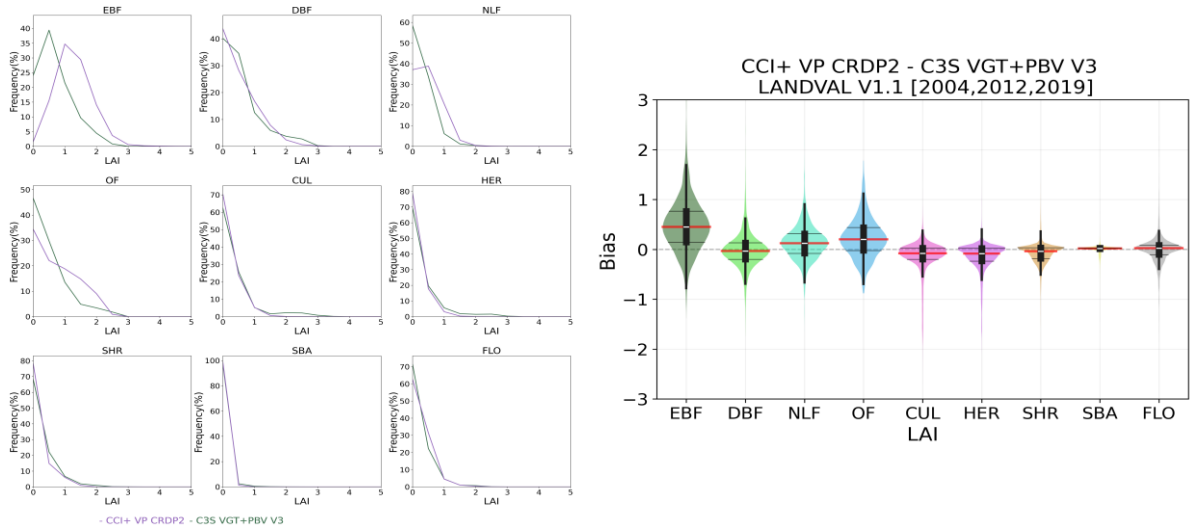

Figure 26: Left: Distribution of LAI values for CCI+ VP CRDP-2 and C3S V3 products per main biome type for years 2004, 2012 and 2019. Right: Violin-plots of the bias between CCI+ VP and C3S V3 products per biome type. In the violin-plots, red horizontal bars indicate median values, horizontal dashed black lines stretch from first and third quartile of the data, and vertical black lines stretch from the lower and upper adjacent value.

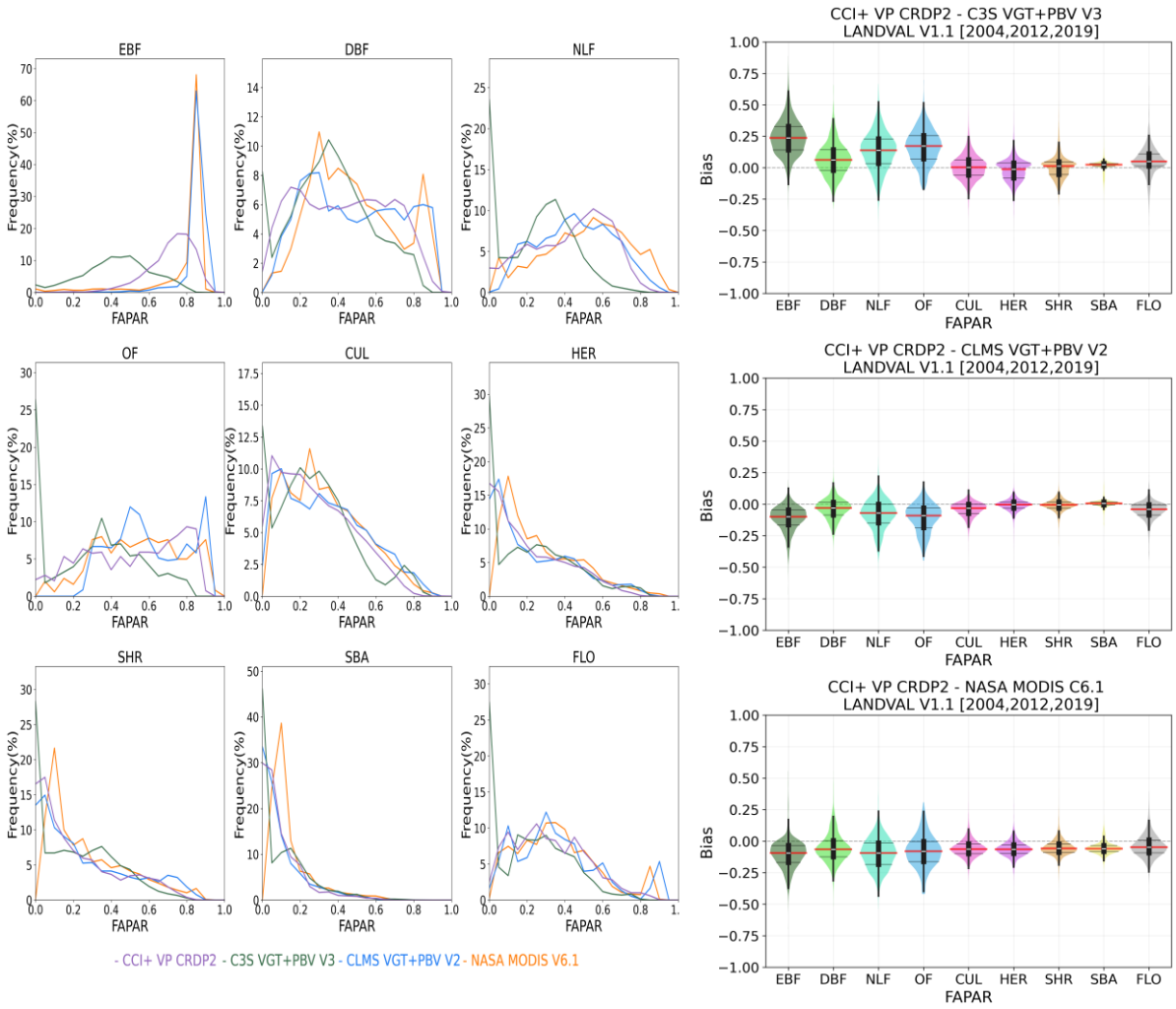

Figure 27: Left: Distribution of fAPAR values for CCI+ VP CRDP-2, C3S V3, CLMS V2 and NASA MODIS V6.1 products per main biome type for years 2004, 2012 and 2019. Right: Violin-plots of the bias between CCI+ VP CRDP-2 and rest of products per biome type. In the violin-plots, red horizontal bars indicate median values, horizontal dashed black lines stretch from first and third quartile of the data, and vertical black lines stretch from the lower and upper adjacent value.

For LAI (Figure 26):

- CCI CRDP-2 generally provides higher values than C3S over forest sites, mainly for EBF.
- Similar LAI retrieval distributions are observed between CCI and C3S over non-forest sites; however, CCI tends to underestimate C3S retrievals for cultivated and herbaceous areas.

For fAPAR (Figure 27):

- CCI fAPAR values agree better with CLMS V2 and NASA MODIS than with C3S.
- CCI shows a similar distribution of retrievals to the reference datasets for most biome types, except for EBF where large discrepancies are found (C3S < CCI < CLMS and NASA). A similar bias pattern is found for the other forest cases, with CCI providing more similar values to CLMS and MODIS (slight negative bias) than to C3S (positive bias).
- For non-forest sites, CCI agrees well with CLMS V2 with bias close to zero. In the comparison with MODIS, the well-known tendency of MODIS LAI and fAPAR to overestimate sparsely vegetated sites or biomes with lower vegetation density (HER, SHR, SBA) is observed in the

histograms (D'Odorico et al., 2014; Fuster et al., 2020), which partly explain the negative biases in the comparison with CRDP-2 retrievals for these biomes

- C3S also exhibits the previously reported [PQAR-C3S_V3] tendency to produce a high frequency of fAPAR values equal to zero across all biomes (except EBF), which result in elongated violin plots of the bias distribution.

3.5.3 Intra-annual precision

The histograms of the intra-annual precision (δ, the so-called smoothness) for CCI+ VP CRDP-2 and reference products are shown Figure 28 for LAI (left side) and fAPAR (right side). It should be noted that, for LAI, only products providing effective LAI values were included (i.e., CCI and C3S). The analysis was performed over LANDVAL sites for years 2004, 2012 and 2019, and median δ values are reported as indicators of the intra-annual precision of the products. Only concomitant sites providing data are included in the analysis. Table 7 shows the summary of median δ values per main biome type.

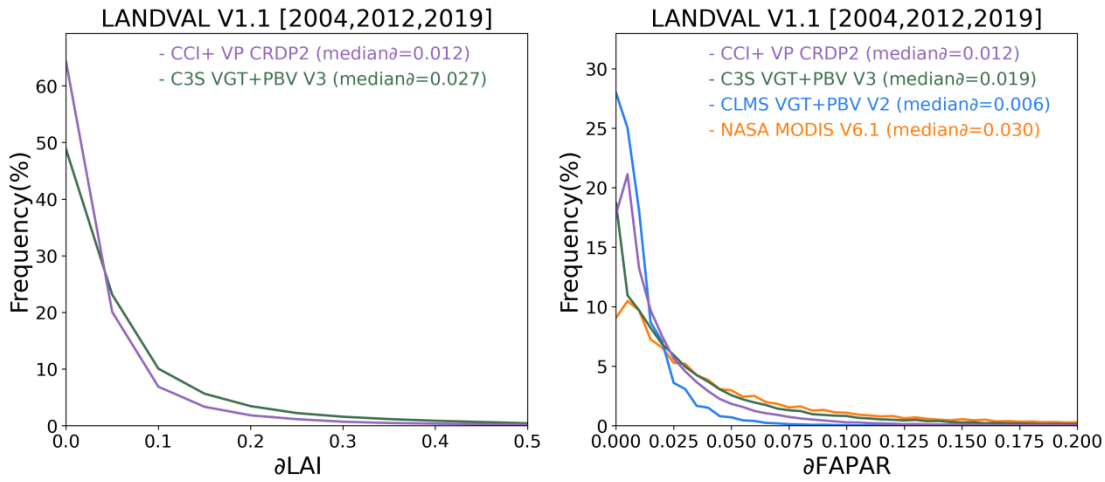

Figure 28: Histograms of delta function (smoothness) of different LAI and fAPAR products: CCI+ VP CRDP-2 (purple), C3S V3 (green), CLMS V2 (blue) and NASA MODIS V6.1 (orange) products over LANDVAL sites for years 2004, 2012 and 2019. In case of LAI, only products providing LAIeff values are displayed.

Table 7: Median δ of different LAI and fAPAR products: CCI+ VP CRDP-2, C3S V3, CLMS V2 and NASA MODIS V6.1. Computation per biome type over LANDVAL sites for years 2004, 2012 and 2019.

Median δ – LANDVAL 2004, 2012 and 2019						
Biome	**LAI**		**fAPAR**			
	CCI+ VP	**C3S V3**	**CCI+ VP**	**C3S V3**	**CLMS V2**	**MODIS V6.1**
All	0.012	0.027	0.012	0.019	0.006	0.030
EBF	0.130	0.123	0.028	0.043	0.002	0.015
DBF	0.038	0.064	0.019	0.026	0.010	0.040
NLF	0.055	0.047	0.026	0.023	0.010	0.055
OF	0.069	0.046	0.029	0.025	0.008	0.080
CUL	0.018	0.043	0.013	0.022	0.010	0.035
HER	0.010	0.025	0.008	0.015	0.006	0.025
SHR	0.008	0.019	0.007	0.012	0.006	0.020
SBA	0.001	0.000	0.004	0.007	0.004	0.015

FLO	0.019	0.030	0.016	0.020	0.007	0.045

The main findings are:

- For LAI, CRDP-2 shows overall much lower δ values than C3S, indicating higher precision at short time scale. This is observed for most biomes, except for EBF, NLF and OF.
- For fAPAR, CRDP-2 provides overall higher precision (i.e., lower δ values) than C3S and MODIS. As expected, CLMS V2 shows the lowest δ values, since this product applies smoothing techniques within its algorithm, an evident feature in the previous temporal consistency analysis.

3.5.4 Inter-annual precision

To investigate the inter-annual precision of the products, median absolute anomalies (MAD) of the upper 95th and lower 5th percentiles between consecutive years were computed over LANDVAL sites excluding croplands. Figure 29 and Figure 30 show the inter-annual precision between pairs of consecutive years for the evaluated LAI (effective) and fAPAR products over the 01/2000-12/2019 period (since 2020 year is not complete in CLMS and C3S datasets). The median value across the entire period is considered as indicator of inter-annual precision.

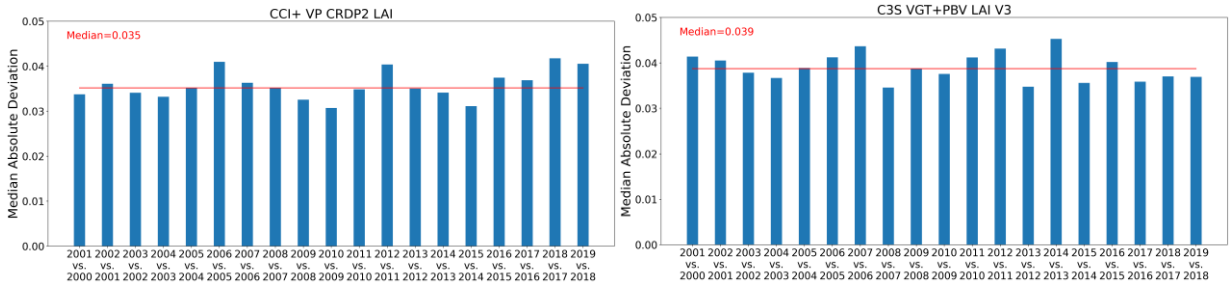

Figure 29: Median absolute deviation (MAD) of the 5th and 95th percentiles between consecutive years (2000-2019 period) over LANDVAL sites for CCI+ VP CRDP-2 (left), C3S V3 (right).

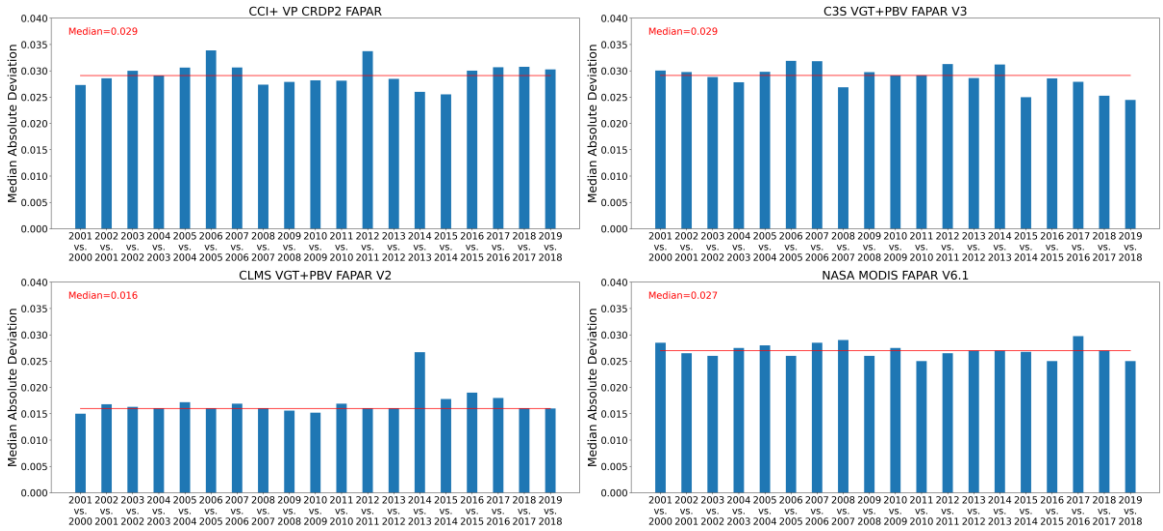

Figure 30: Median absolute deviation (MAD) of the 5th and 95th percentiles between consecutive years (2000-2019 period) over LANDVAL sites for CCI+ VP CRDP-2 (top left), C3S V3 (top right), CLMS V2 (bottom left) and NASA V6.1 (bottom right) fAPAR products.

Main findings of the inter-annual precision analysis are:

For LAI:

- CRDP-2 provides slightly better inter-annual precision (MAD = 0.035) than C3S (MAD = 0.039).
- The use of different sensors does not appear to affect inter-annual precision, as similar MAD values are obtained for different pairs of consecutive years.

For fAPAR:

- CRDP-2 provides overall inter-annual precision identical to C3S (MAD = 0.029) and similar (slightly worse) than MODIS (MAD = 0.027).
- CLMS V2 exhibits, as expected for a smoothed product, the best overall inter-annual precision (MAD = 0.016). However, the MAD is much larger (almost twice as high) for 2014 compared to 2013, clearly indicating that the transition from SPOT/VGT (2013) to PROBA-V (2014) has a significant impact on the CLMS V2 product. On the contrary, for CRDP-2, the use of different sensor input data does not have any major effect on the inter-annual precision along the period.

3.6 Stability

To investigate the stability of the CRDP-2 data record, Hovmöller plot of the fAPAR bias between CRDP-2 and MODIS data over LANDVAL for BQ retrievals is shown (Figure 31). MODIS product is selected as it is a stable reference, where CLMS and C3S are somehow impacted by the transition from SPOT/VGT to PROBA-V in the time series (e.g., Mota et al., 2021). Nevertheless, Hovmöller plots with other references are shown in Annex III for comparison.

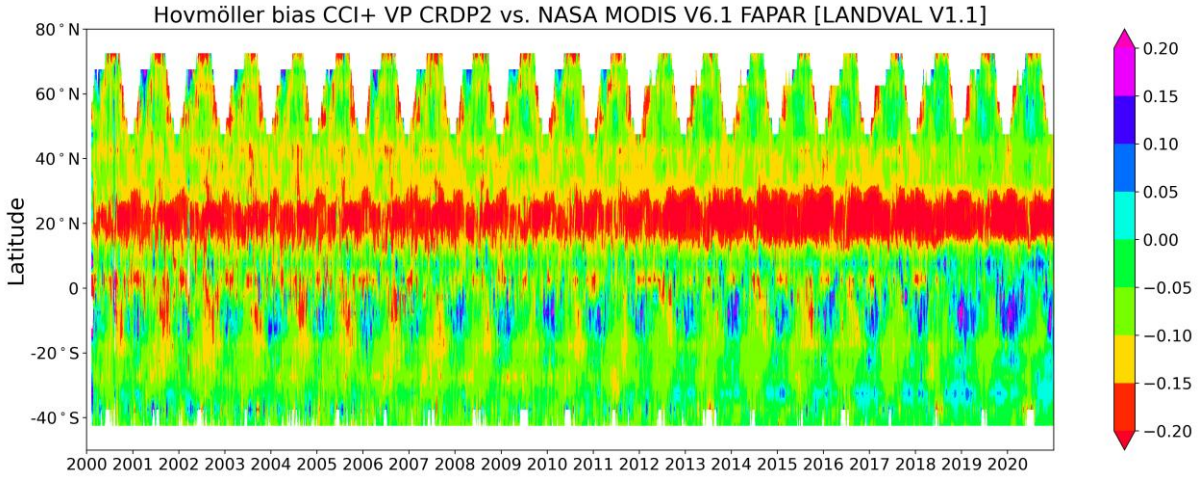

Figure 31: Hovmöller plots of the fAPAR bias between CRDP-2 and MODIS C6.1 over LANDVAL sites for best quality pixels.

The Hovmöller plot of the fAPAR bias with MODIS product shows a trend in the bias with the time. The bias (negative in sign) is higher in the first years (mono-sensor) and tends to decrease with time over both hemispheres for the multi-sensor period. In particular, the bias is lower or even change from negative to positive in some latitudes for the last three years where multiple sensors are used. Similar results are found in the comparison with other satellite references (see Annex III). However, it should be noted that the number of best-quality retrievals changes significantly over time (as discussed in Section 3.1), which can have an impact in the analysis.

To better investigate if there is a change in the bias with time, we have selected only LANDVAL sites where the total percentage of missing values is lower than 10%, which excludes northern latitudes and equatorial regions (see spatial distribution of sites in Figure 3). Figure 32 shows the evolution of

the fAPAR mean values for BQ pixels, highlighting different periods as a function of the input sensor. The number of observations is also shown. Figure 33 shows the evolution of the FAPAR bias with MODIS for the same selection of sites.

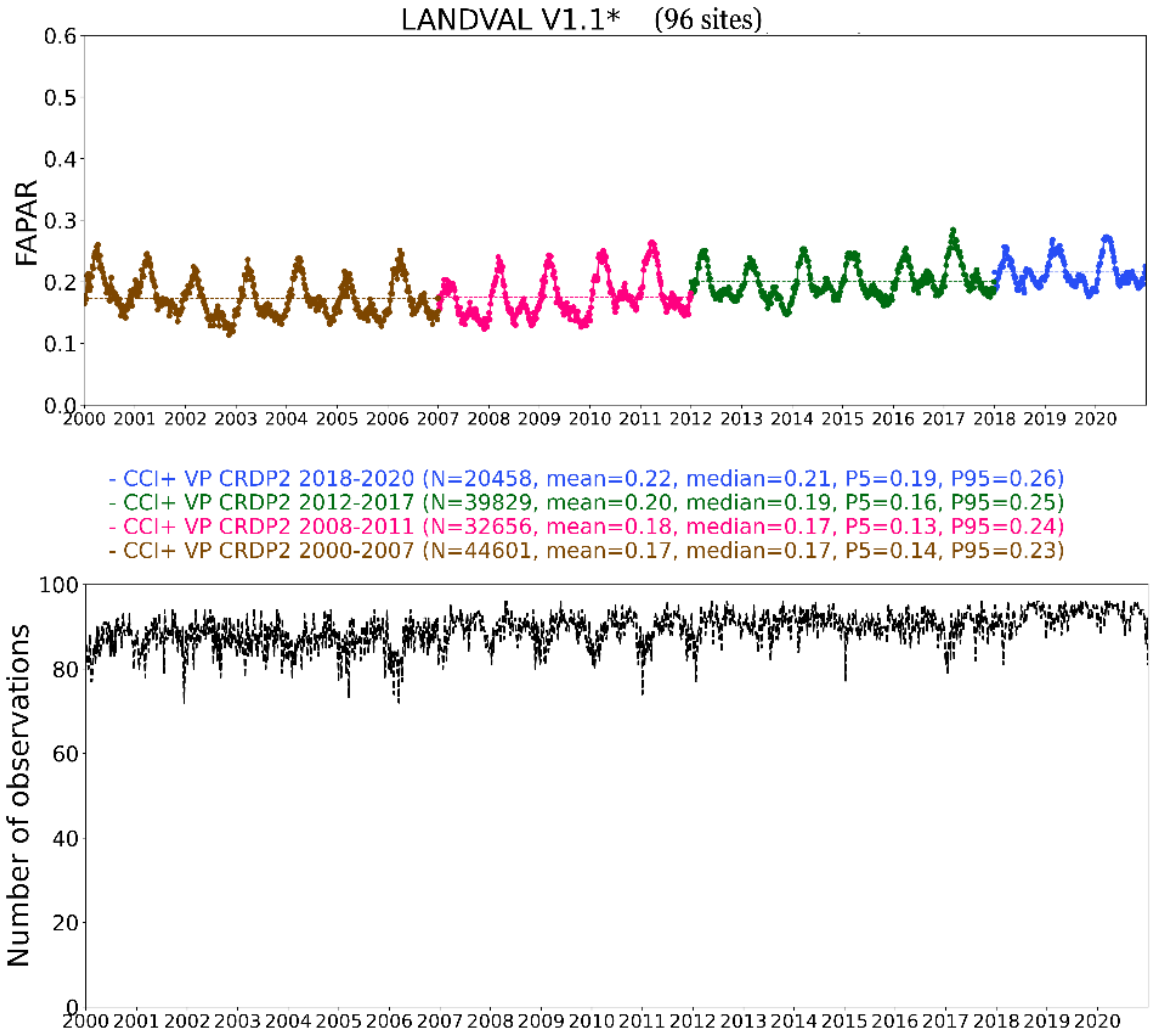

Figure 32: CRDP-2 fAPAR mean values over LANDVAL sites with percentage of BQ missing values lower than 10%. Different periods are highlighted: 2000-2007 (mono-sensor), 2008-2011 (SPOT/VGT & MetOp-A/AVHRR), 2012-2017 (SPOT/VGT or PROBA-V & MetOp-A/AVHRR & VIIRS), 2018-2020 (PROBA-V & Sentinel-3/OLCI & Metop-A or -C & VIIIRS). The number of observations per period and over time are also shown, along with mean, median and percentiles (5th, 95th) for each period.

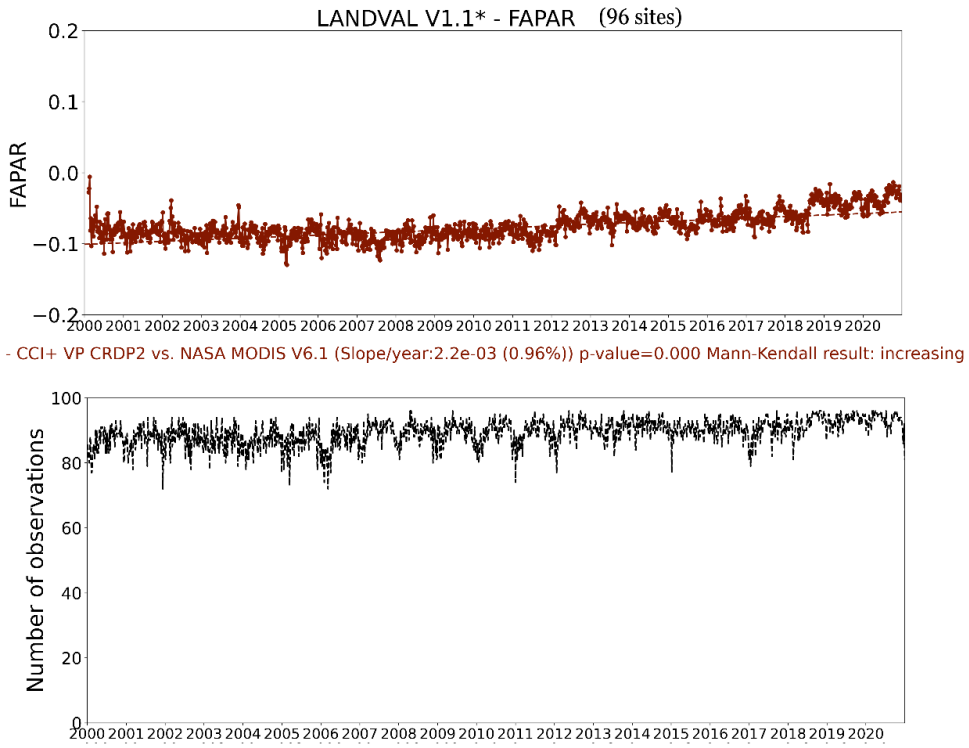

Figure 33: Temporal evolution of the CRDP-2 fAPAR bias with MODIS over a subset of LANDVAL sites with percentage of BQ missing values lower than 10%. The number of observations over time are also shown.

The main findings of the analysis over a subset of LANDVAL sites with low percentage of missing values are:

- CRDP-2 provides very similar mean, median and percentile fAPAR values for the first two periods (2000-2007, 2008-2011). However, the mean, median and percentiles increases in the last two periods (2012-2017 and 2018-2020). The increase is noticeable in the last period where Sentinel-3 is introduced as input together with MetOp-C, but there is also an orbital drift in PROBA-V to take in consideration.
- This trend in the mean values is also observed in the bias with respect to MODIS, even if the number of observations remains very similar over time. The reduction in bias over time is positive in terms of a gain in accuracy when more sensors are used. However, it introduces a stability issue as the change of bias per decade (9.6 % over these sites) is much larger than the GCOS threshold requirement on stability (3%). Therefore, users should use the CRDP-2 with caution for trend analysis, particularly the last years of the CRDP-2 time series. At the time of writing this report, additional analysis is being carried out to identify the role of each sensor of the stability of the time series.
- Note that the observed trends are also found for both LAI and fAPAR over most biomes (except flooded vegetation and SBA) when all LANDVAL sites are considered (see Annex IV & Annex V for further information).
- A deeper look into the temporal profiles over the whole time series at site level reveals also the observed trends (see Annex I).

4 Conclusions

This report presents the quality assessment of CCI+ VP LAI and fAPAR CRDP-2 (2000-2020) products, the estimates are based on OptiSAIL model and multi-sensor input data. CRDP-2 is generated over a latitudinal North-South transect and over a selection of global sites allowing both product intercomparison (LANDVAL) and direct validation (DIRECT 2.1, GBOV, AMMA) purposes. The methodology is described in the product validation plan [VP-CCI_D1.3_PVP_V2.0], in agreement with standardized validation procedures for satellite-based biogeophysical products (Camacho et al., 2025) compliant with the CEOS LPV LAI best practices validation protocol (Fernandes et al., 2014). Two main validation approaches are defined: comparison with ground-based measurements (i.e., direct validation) and comparison with satellite products (i.e., product intercomparison) using C3S VGT+PBV V3, CLMS VGT+PBV V2, and NASA MODIS V6.1 as reference datasets. Several criteria of performance are evaluated, including completeness, spatial consistency, temporal consistency, error evaluation (accuracy, precision and uncertainty), conformity testing with regard to GCOS uncertainty requirements and stability.

The summary of the validation results is provided in Table 8. Main conclusions for each quality criteria are:

Product completeness

- CRDP-2 shows the expected temporal pattern of missing data, showing higher fractions during Northern Hemisphere winters.
- Spatial maps indicate that CCI provides good spatial coverage, though quality flags reduce usable pixels in cloud-affected regions but also over deserts.
- Among CCI quality flags, bit 9 (RETR_LOW_QUALITY) has the largest impact on completeness, while bit 8 (RETR_UNTRUSTED) and the χ^2 filter minimally affect the overall data availability. Bit 9 (RETR_LOW_QUALITY) removes large amount of apparently good observations particularly during the mono-sensor period (2000-2007), and users should use this flag with caution these years.
- Incorporation of additional sensors over time improves product completeness mainly for 'best quality' pixels, particularly in later years.

Spatial consistency

- LAI and fAPAR spatial distributions are generally reliable across most regions.
- Some unrealistic high values occur in northern regions during winter; most are removed when applying quality layers, though a few remain.
- Unexpected low LAI values (LAI < 2) are observed over equatorial forest areas.
- Comparison with reference products show the largest inconsistencies with C3S LAI and fAPAR (for both dense and sparsely vegetated areas), whereas with MODIS and CLMS fAPAR consistent lower values are typically found

Temporal consistency

- Realistic temporal dynamics across all main biomes when compared with ground and satellite-based references.
- Improves the realism of temporal dynamics compared to C3S and MODIS datasets for low vegetation values, showing similar temporal variations to CLMS.

Error evaluation (direct validation)

- Comparison with DIRECT 2.1
  - Large underestimation of effective LAI (B=-0.69, ~69%) worse than C3S, even if it shows better correlation (R = 0.75) than C3S (R = 0.70).
  - Good agreement for fAPAR (B=-0.01, RMSD = 0.10), very similar to CLMS V2 (B = -0.02, RMSD = 0.09), while outperforming both C3S and NASA MODIS products.
  - Low percentage of compliance with GCOS goal/threshold requirements, 15.6 and 29.9%, respectively.
- Comparison with GBOV V3.4_QC:
  - CRDP-2 effective LAI shows strong correlation with GBOV (R = 0.92), outperforming C3S (R = 0.85), but with large systematic discrepancies partly explained by the different definition (effective vs. actual LAI).
  - For fAPAR, good agreement, with slightly underestimation and low uncertainty (B = -0.06, -10%, RMSD = 0.09), outperforming MODIS and C3S products. CLMS shows optimal accuracy (B=-0.03, RMSD= 0.06) with this QC selection of GBOV references.
  - GCOS compliance: 28.3% and 47.6% within goal and threshold limits, comparable to MODIS.
- Comparison with AMMA
  - Underestimation of LAIeff over grasslands (B = -0.12 (-40.2%), RMSD = 0.29), outperforming C3S in correlation and GCOS compliance.
  - For fAPAR, slightly overestimates (B = 0.05 (21.5%), RMSD = 0.14), performing comparably to CLMS, and better than C3S and MODIS products.
  - C3S shows a known limitation: high frequency of zero values for both LAI and fAPAR, even when ground measurements are non-zero.

Error evaluation (product intercomparison)

- Overall analysis
  - CRDP-2 generally shows slightly lower LAI than C3S (bias -7.9%), with moderate overall uncertainty (RMSD = 0.34) and ≈ 37–54% of samples within GCOS goal/threshold requirements.
  - For fAPAR, CRDP-2 agrees best with CLMS (RMSD 0.08, R = 0.96), shows good agreement with MODIS products, and has weaker agreement with C3S. CRDP-2 is closer to CLMS and MODIS than to C3S retrievals.
- Analysis per biome type
  - For LAI, CRDP-2 provides higher values than C3S in forests (especially EBF), while for non-forest areas shows similar distributions, but with CCI lower at the upper range for cultivated/herbaceous biomes.
  - For fAPAR, discrepancies occur mainly in forests (CCI slightly lower values than CLMS and MODIS, larger than C3S). MODIS overestimates sparsely vegetated biomes, and C3S shows frequent zero values, both are known limitation of existing datasets which are not present in CRDP-2.
- Intra-annual precision
  - CCI exhibits higher short-term precision across most biomes than C3S (for both LAI and fAPAR) and MODIS for fAPAR. CLMS, being a smoothed product, naturally provides the best results.

- Inter-annual precision
  - For LAI, CCI provides slightly better precision (MAD = 0.035) than C3S (0.039). The inter-annual precision remains unaffected by sensor changes.

- For fAPAR, CCI shows the same results than C3S (MAD = 0.029) and similar to MODIS (MAD = 0.027). CLMS shows much better overall inter-annual precision (MAD = 0.016) but is clearly impacted by sensor transition in 2014 (from SPOT/VGT to PROBA-V).

Stability

- Howmöller plot of the bias with reference products shows a temporal pattern. The investigation over sites with low fraction of missing values shows a reduction of bias with MODIS over time. While this can be interpreted as a gain of accuracy, the change per decade was found to exceed to the GCOS requirements on stability.
- CRDP-2 exhibits a gradual increase in LAI and fAPAR values over time after 2012, and particularly after 2018, likely linked to the inclusion of new sensors (Sentinel-3, MetOp-C) and/or PROBA-V orbital drift. This is observed across almost for all biomes (except SBA and Flooded vegetation).
- This suggests a potential stability issue that users should consider when performing long-term trend analyses. The impact of each sensor on the stability is currently under investigation.

Concluding remarks

The quality assessment of the CCI+ VP multi-sensor LAI and fAPAR products (CRDP-2, 2000–2020) demonstrates overall high consistency, accuracy, and robustness across multiple validation criteria and reference datasets. The products show reliable spatial and temporal behaviour, with effective removal of some spurious anomalies in northern latitudes through quality flags with no major inconsistencies related to sensor transitions. During the first years of the period, the use of quality flags (LOW_QUALITY) can also remove useful retrievals and the use of this flag should be used with caution in this period. Comparisons with ground-based and satellite-based references confirm that CRDP-2 achieves good performance, similar to CLMS V2 and superior to C3S V3 and MODIS V6.1 in several aspects, particularly for fAPAR. While LAI remains underestimated mainly over dense canopies, correlation with ground references is strong. Both LAI and fAPAR exhibit stable inter-annual precision and improved intra-annual smoothness relative to C3S or MODIS, confirming the overall robustness of the multi-sensor retrieval framework. However, since 2012 CRDP-2 exhibits a gradual increase in LAI and fAPAR values, as well as a reduction of bias with MODIS over time, highlighting an improvement of accuracy but a potential stability issue linked to sensor transitions. Users are therefore advised to exercise caution when using the dataset for trend analysis, particularly for the most recent years of the dataset**.**

Table 8: Summary of CCI+ VP CRDP-2 validation results. Symbols stand for: (+) good, (±) medium, (–) limited.

Criteria	performance	Comments
Product completeness	+	- Gaps located in northern latitudes (winter) and equatorial areas. - Adding new sensors over time improves completeness for 'best quality' pixels, particularly over the last years. - bit 9 (RETR_LOW_QUALITY) has the largest impact on completeness. It should be use with caution, as it also removes large number of valid retrievals.
Spatial consistency	±	- Reliable spatial distributions, except for unexpected low LAI (<2) over equatorial areas. - Overall similar spatial distributions than reference products, with main discrepancies over northern latitudes and equatorial areas.
Temporal consistency	+	- Reliable seasonal and inter-annual variations. Good temporal consistency with satellite-based and ground-based references.
Error evaluation: Direct validation vs DIRECT V2.1	±	- LAI: B=-0.69, RMSD=1.03, goal/threshold=9.6%/16.5%. CRDP-2<DIRECT 2.1 mainly for high values (forests). ▪ C3S V3 shows similar results. - fAPAR: B=-0.01, RMSD=0.1, goal/threshold=15.6%/29.9%. ▪ CLMS V2 shows similar results. C3S V3 and MODIS V6.1 show worse performance.
Error evaluation: Direct validation vs GBOV V3.4_QC (quality-controlled forest sites)	±	- LAI: R = 0.92 (vs. true LAI), better than C3S V3 (R =0.85). - fAPAR: B=-0.06, RMSD=0.09, goal/threshold=28.3%/47.6%. ▪ Similar performance to MODIS, and better than C3S. CLMS V2 shows optimal performances (RMSD=0.06).
Error evaluation: Direct validation vs AMMA	±	- LAI: B=-0.12, RMSD=0.29, goal/threshold=25.7%/39.7%. ▪ Improves C3S V3 performance. - fAPAR: B=0.05, RMSD=0.14, goal/threshold=9.4%/15.4%. ▪ Similar to CLMS V2 performance, better than MODIS V6.1 and C3S V3.
Error evaluation: Product intercomparison	±	LAI: - Vs. C3S V3: B=-0.03, RMSD=0.34, goal/threshold=37.0%/54.4%. - CCI > C3S in forests (especially EBF), CCI < C3S for cultivated/herbaceous biomes. fAPAR: - Vs. C3S V3: B=0.03, RMSD=0.13, goal/threshold=7.7%/15.1%. - Vs. CLMS V2: B=-0.03, RMSD=0.08, goal/threshold=17.7%/34.3%. - VS. MODIS: B=-0.06, RMSD=0.10, goal/threshold=11.7%/22.9%. - CCI agrees better with CLMS and MODIS than with C3S. Discrepancies in forests (CCI > C3S and slightly lower than CLMS or MODIS).
Intra-annual precision	+	- Better than C3S V3 and MODIS V6.1, and worse than CLMS V2 (as expected, smoothing techniques applied).
Inter-annual precision	+	- MAD of 0.035 and 0.029 for LAI and fAPAR. This indicator shows no impact from the transition between different input sensors during the period. - Similar than C3S V3 and MODIS V6.1, and worse than CLMS V2 (as expected, smoothing techniques applied)
Stability	-	- Change of mean, median, percentile values after 2012, and particularly after 2018 likely related to the different input data. - Change of bias over time (improved accuracy) particularly after 2012, introduce stability (change per decade) beyond GCOS requirements. Dataset should be used with caution for trend analysis. Bias trend under investigation.

5 References

Asrar, G., Myneni, R.B., 1991. Applications of Radiative Transfer Models for Remote Sensing of Vegetation Conditions and States, in: Photon-Vegetation Interactions. Springer Berlin Heidelberg, pp. 537–558. https://doi.org/10.1007/978-3-642-75389-3_17

Baret, F., Weiss, M., Lacaze, R., Camacho, F., Makhmara, H., Pacholcyzk, P., Smets, B., 2013. GEOV1: LAI and FAPAR essential climate variables and FCOVER global time series capitalizing over existing products. Part1: Principles of development and production. Remote Sens. Environ. 137, 299–309. https://doi.org/10.1016/j.rse.2012.12.027

Blessing, S., Giering, R., van der Tol, C., 2024. OptiSAIL: a system for the simultaneous retrieval of soil, leaf, and canopy parameters and its application to Sentinel-3 Synergy (OLCI+SLSTR) top-of-canopy reflectances. Sci. Remote Sens. 100148. https://doi.org/10.1016/J.SRS.2024.100148

Brown, L.A., Camacho, F., García-Santos, V., Origo, N., Fuster, B., Morris, H., Pastor-Guzman, J., Sánchez-Zapero, J., Morrone, R., Ryder, J., Nightingale, J., Boccia, V., Dash, J., 2021. Fiducial Reference Measurements for Vegetation Bio-Geophysical Variables: An End-to-End Uncertainty Evaluation Framework. Remote Sens. 2021, Vol. 13, Page 3194 13, 3194. https://doi.org/10.3390/RS13163194

Camacho, F., Cernicharo, J., Lacaze, R., Baret, F., Weiss, M., 2013. GEOV1: LAI, FAPAR essential climate variables and FCOVER global time series capitalizing over existing products. Part 2: Validation and intercomparison with reference products. Remote Sens. Environ. 137, 310–329. https://doi.org/10.1016/j.rse.2013.02.030

Camacho, F., Fuster, B., Li, W., Weiss, M., Ganguly, S., Lacaze, R., Baret, F., 2021. Crop specific algorithms trained over ground measurements provide the best performance for GAI and fAPAR estimates from Landsat-8 observations. Remote Sens. Environ. 260, 112453. https://doi.org/10.1016/J.RSE.2021.112453

Camacho, F., Martínez-Sánchez, E., Brown, L.A., Morris, H., Morrone, R., Williams, O., Dash, J., Origo, N., Sánchez-Zapero, J., Boccia, V., 2024a. Validation and Conformity Testing of Sentinel-3 Green Instantaneous FAPAR and Canopy Chlorophyll Content Products. Remote Sens. 2024, Vol. 16, Page 2698 16, 2698. https://doi.org/10.3390/RS16152698

Camacho, F., Sánchez-Zapero, J., Fang, H., Weiss, M., Brown, L.A., 2024b. CEOS LPV DIRECT V2.1: A database of upscaled LAI, FAPAR and Fcover values for satellite biophysical product validation. [Data set]. Zenodo. https://doi.org/10.5281/ZENODO.11235157

Camacho, F., Sánchez-Zapero, J., Martínez-Sanchez, E., 2025. Standardized validation of satellite-based biogeophysical products. Carbon Fluxes Biophys. Var. from Earth Obs. 153–205. https://doi.org/10.1016/B978-0-443-29991-9.00004-5

Chen, J.M., Menges, C.H., Leblanc, S.G., 2005. Global mapping of foliage clumping index using multi-angular satellite data. Remote Sens. Environ. 97, 447–457. https://doi.org/10.1016/J.RSE.2005.05.003

D'Odorico, P., Gonsamo, A., Pinty, B., Gobron, N., Coops, N., Mendez, E., Schaepman, M.E., 2014. Intercomparison of fraction of absorbed photosynthetically active radiation products derived from satellite data over Europe. Remote Sens. Environ. 142, 141–154. https://doi.org/10.1016/j.rse.2013.12.005

Fang, H., 2021. Canopy clumping index (CI): A review of methods, characteristics, and applications. Agric. For. Meteorol. 303, 108374. https://doi.org/10.1016/J.AGRFORMET.2021.108374

Fang, H., Wei, S., Liang, S., 2012. Validation of MODIS and CYCLOPES LAI products using global field measurement data. Remote Sens. Environ. 119, 43–54. https://doi.org/10.1016/j.rse.2011.12.006

Fang, H., Zhang, Y., Wei, S., Li, W., Ye, Y., Sun, T., Liu, W., 2019. Validation of global moderate resolution leaf area index (LAI) products over croplands in northeastern China. Remote Sens. Environ. 233, 111377. https://doi.org/10.1016/J.RSE.2019.111377

Féret, J.B., Gitelson, A.A., Noble, S.D., Jacquemoud, S., 2017. PROSPECT-D: Towards modeling leaf optical properties through a complete lifecycle. Remote Sens. Environ. 193, 204–215. https://doi.org/10.1016/J.RSE.2017.03.004

Fernandes, R., Butson, C., Leblanc, S., Latifovic, R., 2003. Landsat-5 TM and Landsat-7 ETM+ based accuracy assessment of leaf area index products for Canada derived from SPOT-4 VEGETATION data. Can. J. Remote Sens. 29, 241–258. https://doi.org/10.5589/m02-092

Fernandes, R., Plummer, S.E., Nightingale, J., Baret, F., Camacho, F., Fang, H., Garrigues, S., Gobron, N., Lang, M., Lacaze, R., Leblanc, S.G., Meroni, M., Martinez, B., Nilson, T., Pinty, B., Pisek, J., Sonnentag, O., Verger, A., Welles, J.M., Weiss, M., Widlowski, J.-L., Schaepman-Strub, G., Román, M.O., Nicheson, J., 2014. Global Leaf Area Index Product Validation Good Practices. Version 2.0. In G. Schaepman-Strub, M. Román, & J. Nickeson (Eds.), Best Practice for Satellite-Derived Land Product Validation (p. 76): Land Product Validation Subgroup (WGCV/CEOS), doi:10.5067/do [WWW Document]. https://doi.org/10.5067/doc/ceoswgcv/lpv/lai.002

Fuster, B., Sánchez-Zapero, J., Camacho, F., García-Santos, V., Verger, A., Lacaze, R., Weiss, M., Baret, F., Smets, B., 2020. Quality Assessment of PROBA-V LAI, fAPAR and fCOVER Collection 300 m Products of Copernicus Global Land Service. Remote Sens. 12, 1017. https://doi.org/10.3390/rs12061017

Garrigues, S., Lacaze, R., Baret, F., Morisette, J.T., Weiss, M., Nickeson, J.E., Fernandes, R., Plummer, S., Shabanov, N. V., Myneni, R.B., Knyazikhin, Y., Yang, W., 2008. Validation and intercomparison of global Leaf Area Index products derived from remote sensing data. J. Geophys. Res. Biogeosciences 113. https://doi.org/10.1029/2007JG000635

Harper, W. V., 2014. Reduced Major Axis regression: teaching alternatives to Least Squares. Proc. Ninth Int. Conf. Teach. Stat. 1–4. https://doi.org/10.1016/B978-0-12-420228-3.00013-0

Hiernaux, P., Diarra, L., Trichon, V., Mougin, E., Soumaguel, N., Baup, F., 2009a. Woody plant population dynamics in response to climate changes from 1984 to 2006 in Sahel (Gourma, Mali). J. Hydrol. 375, 103–113. https://doi.org/10.1016/J.JHYDROL.2009.01.043

Hiernaux, P., Mougin, E., Diarra, L., Soumaguel, N., Lavenu, F., Tracol, Y., Diawara, M., 2009b. Sahelian rangeland response to changes in rainfall over two decades in the Gourma region, Mali. J. Hydrol. 375, 114–127. https://doi.org/10.1016/J.JHYDROL.2008.11.005

Jacquemoud, S., Verhoef, W., Baret, F., Bacour, C., Zarco-Tejada, P.J., Asner, G.P., François, C., Ustin, S.L., 2009. PROSPECT + SAIL models: A review of use for vegetation characterization, Remote Sensing of Environment. Elsevier Inc. https://doi.org/10.1016/j.rse.2008.01.026

Knyazikhin, Y., Martonchik, J. V., Myneni, R.B., Diner, D.J., Running, S.W., 1998. Synergistic algorithm for estimating vegetation canopy leaf area index and fraction of absorbed photosynthetically active radiation from MODIS and MISR data. J. Geophys. Res. 103, 32257. https://doi.org/10.1029/98JD02462

Lacherade, S., Fougnie, B., Henry, P., Gamet, P., 2013. Cross calibration over desert sites: Description, methodology, and operational implementation. IEEE Trans. Geosci. Remote Sens. 51, 1098–1113. https://doi.org/10.1109/TGRS.2012.2227061

Lerebourg, C., Brown, L.A.., Morris, H., Dash, J., Bruniquel, V., 2023. Ground-Based Observations for Validation (GBOV) of Copernicus Global Land Products. Algorithm Theoretical Basis Document-Vegetation Products LP3 (LAI), LP4 (FAPAR) and LP5 (FCOVER) (LAI) and FCOVER. [WWW Document]. URL https://land.copernicus.eu/en/technical-library/algorithm-theoretical-basis-document-for-vegetation-products-lp-3-lai-lp-4-fapar-and-lp-5-fcover/@@download/file (accessed 6.27.25).

Libois, Q., Picard, G., France, J.L., Arnaud, L., Dumont, M., Carmagnola, C.M., King, M.D., 2013. Influence of grain shape on light penetration in snow. Cryosphere 7, 1803–1818. https://doi.org/10.5194/TC-7-1803-2013

Loew, A., Bennartz, R., Fell, F., Lattanzio, A., Doutriaux-Boucher, M., Schulz, J., 2016. A database of global reference sites to support validation of satellite surface albedo datasets (SAVS 1.0). Earth Syst. Sci. Data 8, 425–438. https://doi.org/10.5194/essd-8-425-2016

Martínez, B., García-Haro, F.J., Camacho, F., 2009. Derivation of high-resolution leaf area index maps in support of validation activities: Application to the cropland Barrax site. Agric. For. Meteorol. https://doi.org/10.1016/j.agrformet.2008.07.014

Merchant, C.J., 2013. Thermal remote sensing of sea surface temperature. Remote Sens. Digit. Image Process. 17, 287–313. https://doi.org/10.1007/978-94-007-6639-6_15/COVER

Morisette, J.T., Baret, F., Privette, J.L., Myneni, R.B., Nickeson, J.E., Garrigues, S., Shabanov, N. V., Weiss, M., Fernandes, R.A., Leblanc, S.G., Kalacska, M., Sánchez-Azofeifa, G.A., Chubey, M., Rivard, B., Stenberg, P., Rautiainen, M., Voipio, P., Manninen, T., Pilant, A.N., Lewis, T.E., Iiames, J.S., Colombo, R., Meroni, M., Busetto, L., Cohen, W.B., Turner, D.P., Warner, E.D., Petersen, G.W., Seufert, G., Cook, R., 2006. Validation of global moderate-resolution LAI products: A framework proposed within the CEOS land product validation subgroup. IEEE Trans. Geosci. Remote Sens. 44, 1804–1814. https://doi.org/10.1109/TGRS.2006.872529

Mota, B., Gobron, N., Morgan, O., Cappucci, F., Lanconelli, C., Robustelli, M., 2021. Cross-ECV consistency at global scale: LAI and FAPAR changes. Remote Sens. Environ. 263, 112561. https://doi.org/10.1016/j.rse.2021.112561

Myneni, R.B., Hoffman, S., Knyazikhin, Y., Privette, J.L., Glassy, J., Tian, Y., Wang, Y., Song, X., Zhang, Y., Smith, G.R., Lotsch, A., Friedl, M., Morisette, J.T., Votava, P., Nemani, R.R., Running, S.W., 2002. Global products of vegetation leaf area and fraction absorbed PAR from year one of MODIS data. Remote Sens. Environ. 83, 214–231. https://doi.org/10.1016/S0034-4257(02)00074-3

Myneni, R.B., Williams, D.L., 1994. On the relationship between FAPAR and NDVI. Remote Sens. Environ. 49, 200–211. https://doi.org/10.1016/0034-4257(94)90016-7

Nestola, E., Sánchez-Zapero, J., Latorre, C., Mazzenga, F., Matteucci, G., Calfapietra, C., Camacho, F., 2017. Validation of PROBA-V GEOV1 and MODIS C5 & C6 fAPAR Products in a Deciduous Beech Forest Site in Italy. Remote Sens. 9, 126. https://doi.org/10.3390/rs9020126

Nilson, T., 1971. A theoretical analysis of the frequency of gaps in plant stands. Agric. Meteorol. 8, 25–38. https://doi.org/10.1016/0002-1571(71)90092-6

Pinty, B., Lavergne, T., Dickinson, R.E., Widlowski, J.-L., Gobron, N., Verstraete, M.M., 2006. Simplifying the interaction of land surfaces with radiation for relating remote sensing products to climate models. J. Geophys. Res. 111, D02116. https://doi.org/10.1029/2005JD005952

Redelsperger, J.L., Thorncroft, C.D., Diedhiou, A., Lebel, T., Parker, D.J., Polcher, J., 2006. African Monsoon Multidisciplinary Analysis: An International Research Project and Field Campaign. Bull. Am. Meteorol. Soc. 87, 1739–1746. https://doi.org/10.1175/BAMS-87-12-1739

Ross, J., 1981. The radiation regime and architecture of plant stands, The radiation regime and architecture of plant stands. Springer Netherlands. https://doi.org/10.1007/978-94-009-8647-3

Sánchez-Zapero, J., Camacho, F., Martínez-Sánchez, E., Lacaze, R., Carrer, D., Pinault, F., Benhadj, I., Muñoz-Sabater, J., 2020. Quality Assessment of PROBA-V Surface Albedo V1 for the Continuity of the Copernicus Climate Change Service. Remote Sens. 2020, Vol. 12, Page 2596 12, 2596. https://doi.org/10.3390/rs12162596

Sánchez-Zapero, J., Martínez-Sánchez, E., Camacho, F., Wang, Z., Carrer, D., Schaaf, C., García-Haro, F.J., Nickeson, J., Cosh, M., 2023. Surface ALbedo VALidation (SALVAL) Platform: Towards CEOS LPV Validation Stage — Application to Three Global Albedo Climate Data Records. Remote Sens. 2023, Vol. 15, Page 1081 15, 1081. https://doi.org/10.3390/RS15041081

Song, B., Liu, L., Du, S., Zhang, X., Chen, X., Zhang, H., n.d. ValLaI_Crop, a validation dataset for coarse-resolution satellite LaI products over Chinese cropland. https://doi.org/10.1038/s41597-021-01024-4

Verger, A., Baret, F., Weiss, M., 2008. Performances of neural networks for deriving LAI estimates from existing CYCLOPES and MODIS products. Remote Sens. Environ. 112, 2789–2803. https://doi.org/10.1016/j.rse.2008.01.006

Verger, A., Baret, F., Weiss, M., Kandasamy, S., Vermote, E., 2013. The CACAO method for smoothing, gap filling, and characterizing seasonal anomalies in satellite time series. IEEE Trans. Geosci. Remote Sens. 51, 1963–1972. https://doi.org/10.1109/TGRS.2012.2228653

Verger, A., Sánchez-Zapero, J., Weiss, M., Descals, A., Camacho, F., Lacaze, R., Baret, F., 2023. GEOV2: Improved smoothed and gap filled time series of LAI, FAPAR and FCover 1 km Copernicus Global Land products. Int. J. Appl. Earth Obs. Geoinf. 123, 103479. https://doi.org/10.1016/J.JAG.2023.103479

Verhoef, W., Jia, L., Xiao, Q., Su, Z., 2007. Unified optical-thermal four-stream radiative transfer theory for homogeneous vegetation canopies. IEEE Trans. Geosci. Remote Sens. 45, 1808–1822. https://doi.org/10.1109/TGRS.2007.895844

Wang, Y., Tian, Y., Zhang, Y., El-Saleous, N., Knyazikhin, Y., Vermote, E., Myneni, R.B., 2001. Investigation of product accuracy as a function of input and model uncertainties: Case study with SeaWiFs and MODIS LAI/FPAR algorithm. Remote Sens. Environ. 78, 299–313. https://doi.org/10.1016/S0034-4257(01)00225-5

Wang, Z., Schaaf, C., Lattanzio, A., Carrer, D., Grant, I., Roman, M., Camacho, F., Yang, Y., Sánchez-Zapero, J., 2019. Global Surface Albedo Product Validation Best Practices Protocol. Version 1.0. In Z. Wang, J. Nickeson & M. Román (Eds.), Good Practices for Satellite-Derived Land Product Validation (p. 45): Land Product Validation Subgroup (WGCV/CEOS). [WWW Document]. https://doi.org/doi: 10.5067/DOC/CEOSWGCV/LPV/ALBEDO.001

Weiss, M., Baret, F., Block, T., Koetz, B., Burini, A., Scholze, B., Lecharpentier, P., Brockmann, C., Fernandes, R., Plummer, S., Myneni, R., Gobron, N., Nightingale, J., Schaepman-Strub, G., Camacho, F., Sanchez-Azofeifa, A., 2014. On line validation exercise (OLIVE): A web based service for the validation of medium resolution land products. application to FAPAR products. Remote Sens. 6, 4190–4216. https://doi.org/10.3390/rs6054190

Weiss, M., Baret, F., Garrigues, S., Lacaze, R., 2007. LAI and fAPAR CYCLOPES global products derived from VEGETATION. Part 2: validation and comparison with MODIS collection 4 products. Remote Sens. Environ. 110, 317–331. https://doi.org/10.1016/j.rse.2007.03.001

Wojnowski, W., Wei, S., Li, W., Yin, T., Li, X.X., Ow, G.L.F., Yusof, M.L.M., Whittle, A.J., 2021. Comparison of Absorbed and Intercepted Fractions of PAR for Individual Trees Based on Radiative Transfer Model Simulations. Remote Sens. 2021, Vol. 13, Page 1069 13, 1069. https://doi.org/10.3390/RS13061069

Yan, K., Park, T., Yan, G., Chen, C., Yang, B., Liu, Z., Nemani, R., Knyazikhin, Y., Myneni, R., 2016a. Evaluation of MODIS LAI/FPAR Product Collection 6. Part 1: Consistency and Improvements. Remote Sens. 8, 359. https://doi.org/10.3390/rs8050359

Yan, K., Park, T., Yan, G., Liu, Z., Yang, B., Chen, C., Nemani, R., Knyazikhin, Y., Myneni, R., 2016b. Evaluation of MODIS LAI/FPAR Product Collection 6. Part 2: Validation and Intercomparison. Remote Sens. 8, 460. https://doi.org/10.3390/rs8060460

Yang, W., Huang, D., Tan, B., Stroeve, J.C., Shabanov, N. V., Knyazikhin, Y., Nemani, R.R., Myneni, R.B., 2006. Analysis of leaf area index and fraction of PAR absorbed by vegetation products from the terra MODIS sensor: 2000-2005. IEEE Trans. Geosci. Remote Sens. 44, 1829–1841. https://doi.org/10.1109/TGRS.2006.871214

Annex I: Additional temporal profiles over the whole period

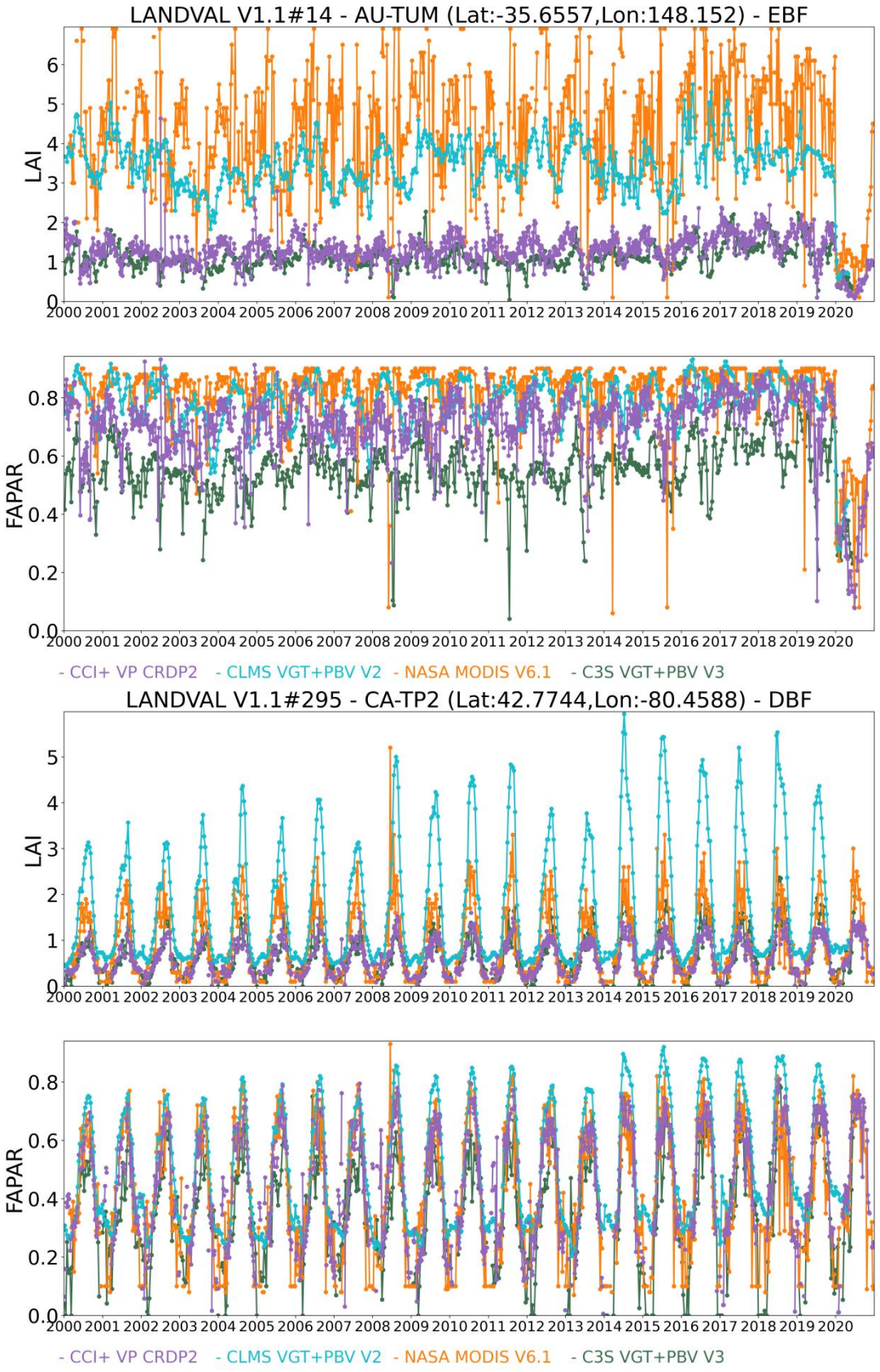

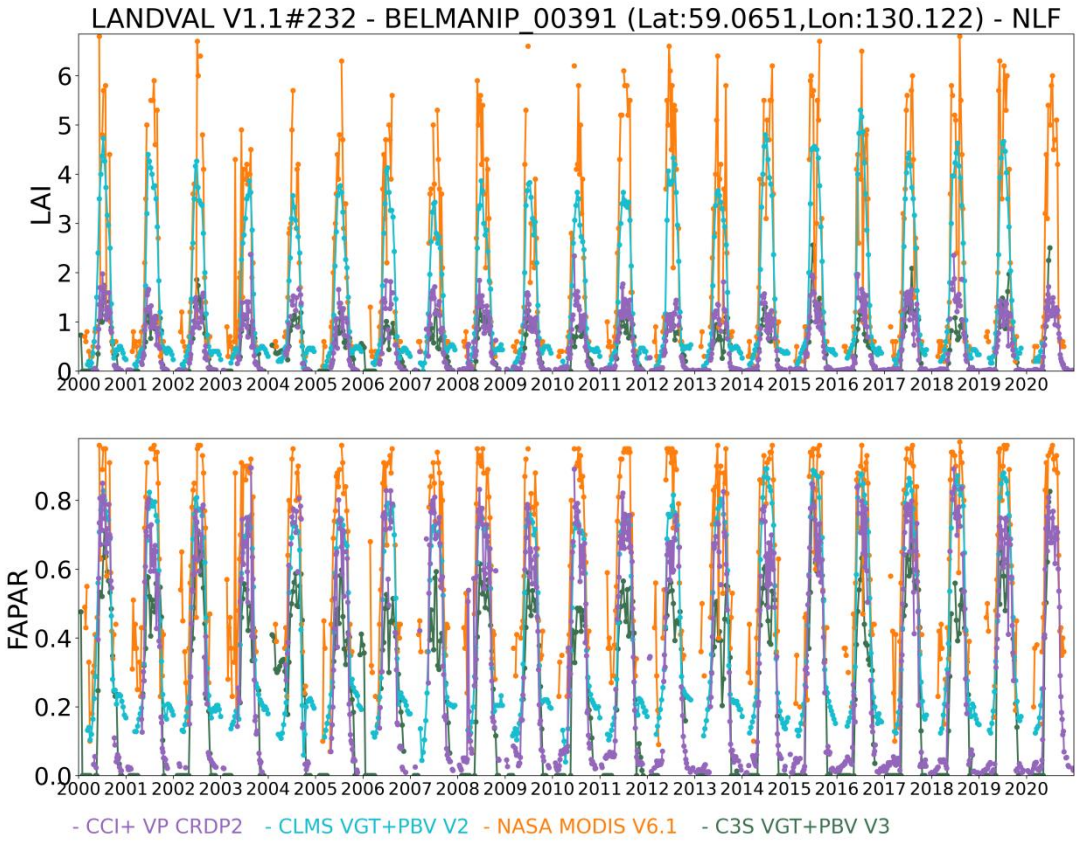
LANDVAL V1.1#232 - BELMANIP_00391 (Lat:59.0651,Lon:130.122) - NLF
LAI
FAPAR
2000 2001 2002 2003 2004 2005 2006 2007 2008 2009 2010 2011 2012 2013 2014 2015 2016 2017 2018 2019 2020
- CCI+ VP CRDP2 - CLMS VGT+PBV V2 - NASA MODIS V6.1 - C3S VGT+PBV V3

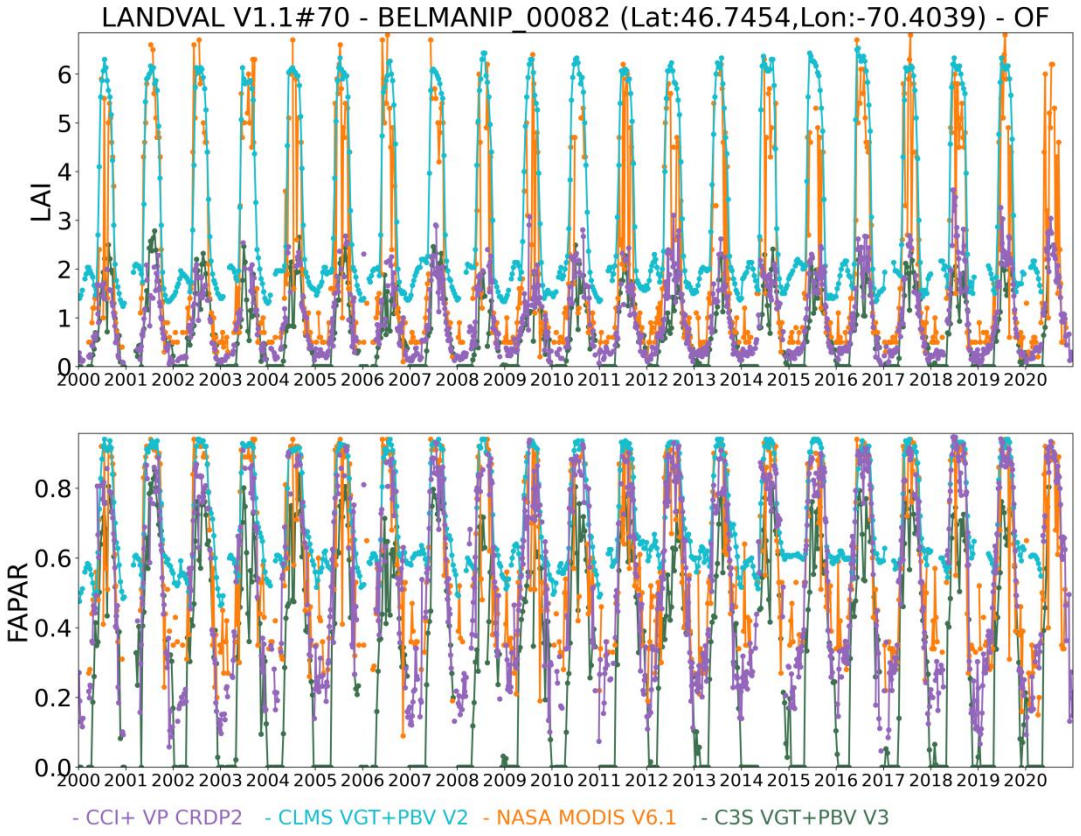
LANDVAL V1.1#70 - BELMANIP_00082 (Lat:46.7454,Lon:-70.4039) - OF
LAI
FAPAR
2000 2001 2002 2003 2004 2005 2006 2007 2008 2009 2010 2011 2012 2013 2014 2015 2016 2017 2018 2019 2020
- CCI+ VP CRDP2 - CLMS VGT+PBV V2 - NASA MODIS V6.1 - C3S VGT+PBV V3

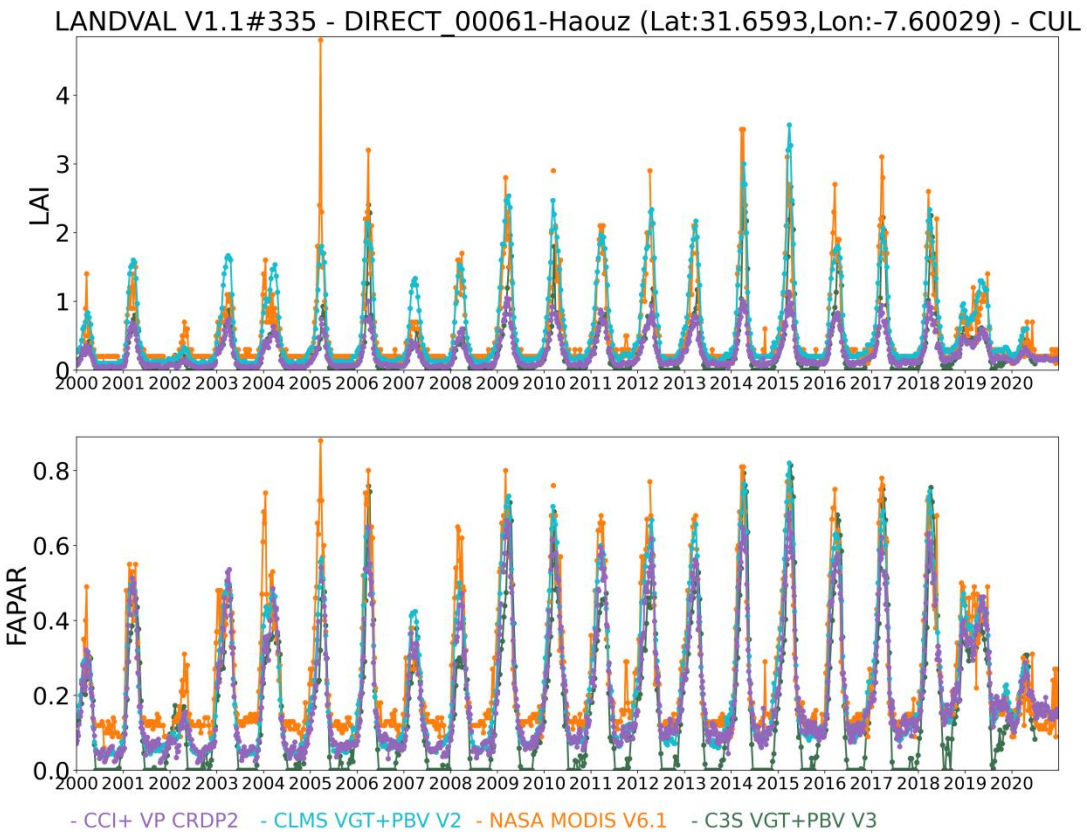
LANDVAL V1.1#335 - DIRECT_00061-Haouz (Lat:31.6593,Lon:-7.60029) - CUL
LAI
FAPAR
2000 2001 2002 2003 2004 2005 2006 2007 2008 2009 2010 2011 2012 2013 2014 2015 2016 2017 2018 2019 2020
- CCI+ VP CRDP2
- CLMS VGT+PBV V2
- NASA MODIS V6.1
- C3S VGT+PBV V3

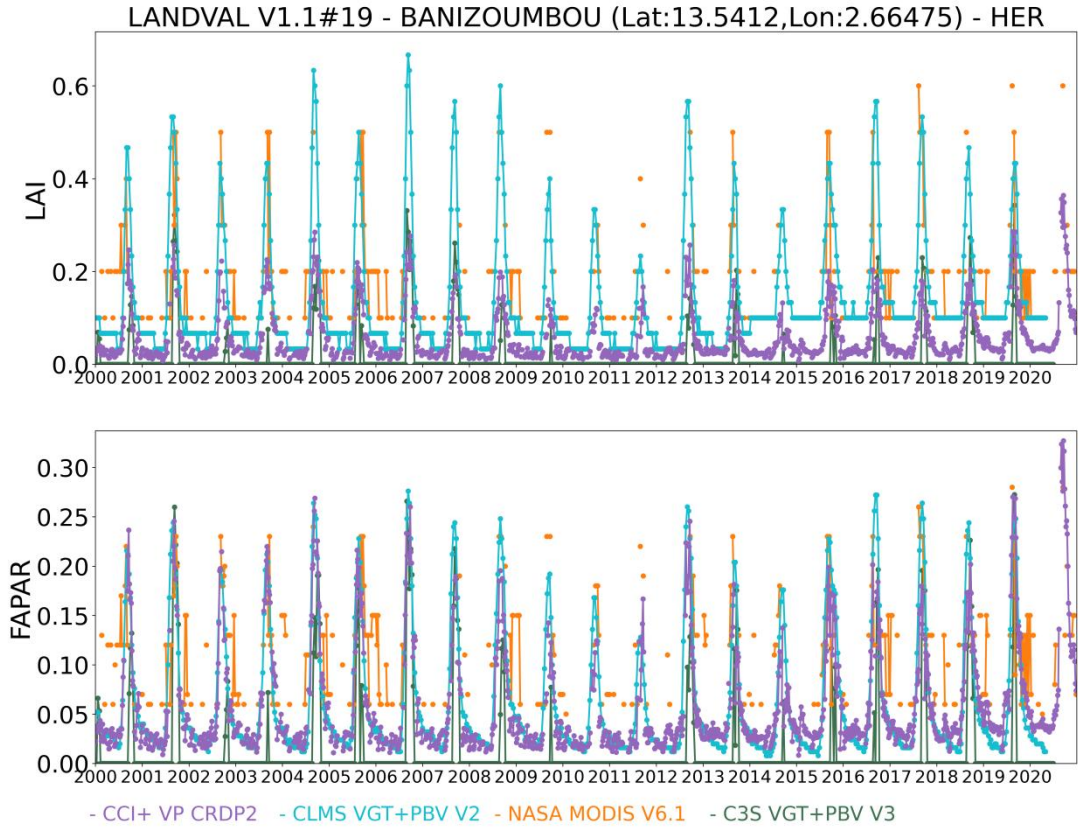
LANDVAL V1.1#19 - BANIZOUMBOU (Lat:13.5412,Lon:2.66475) - HER
LAI
FAPAR
2000 2001 2002 2003 2004 2005 2006 2007 2008 2009 2010 2011 2012 2013 2014 2015 2016 2017 2018 2019 2020
- CCI+ VP CRDP2
- CLMS VGT+PBV V2
- NASA MODIS V6.1
- C3S VGT+PBV V3

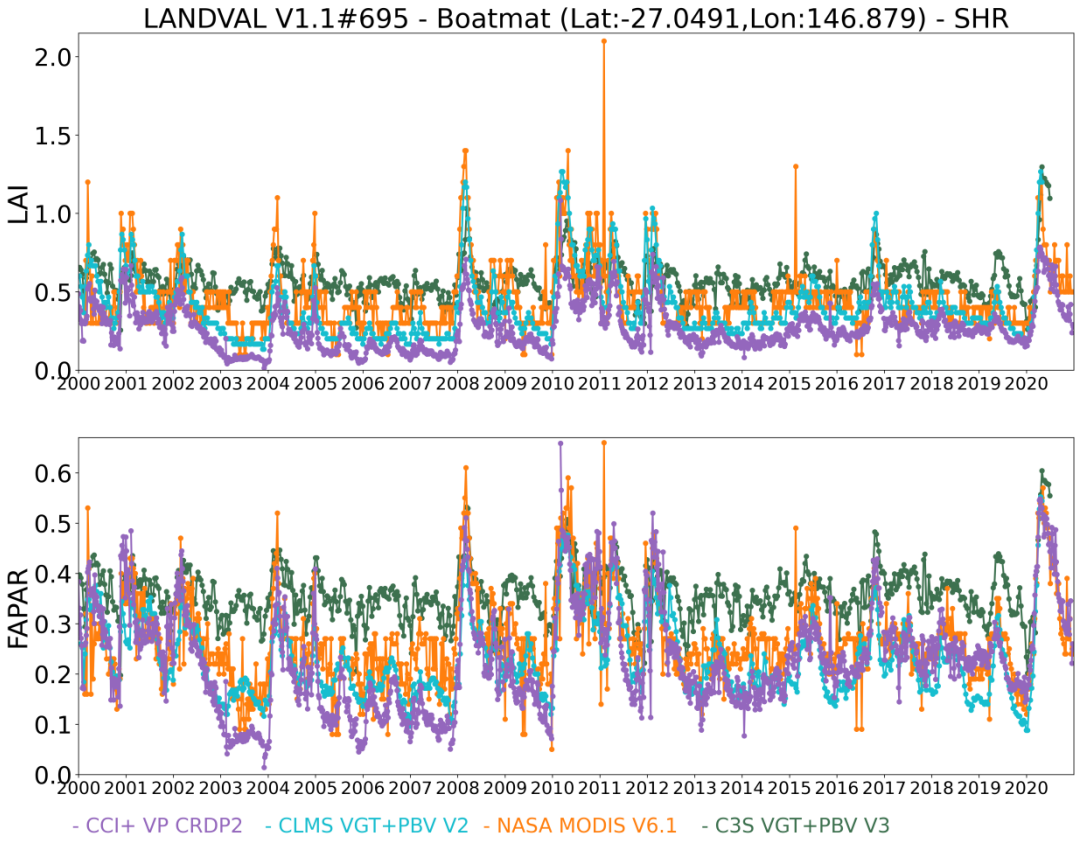
LANDVAL V1.1#695 - Boatmat (Lat:-27.0491,Lon:146.879) - SHR
LAI
FAPAR
2000 2001 2002 2003 2004 2005 2006 2007 2008 2009 2010 2011 2012 2013 2014 2015 2016 2017 2018 2019 2020
- CCI+ VP CRDP2
- CLMS VGT+PBV V2
- NASA MODIS V6.1
- C3S VGT+PBV V3

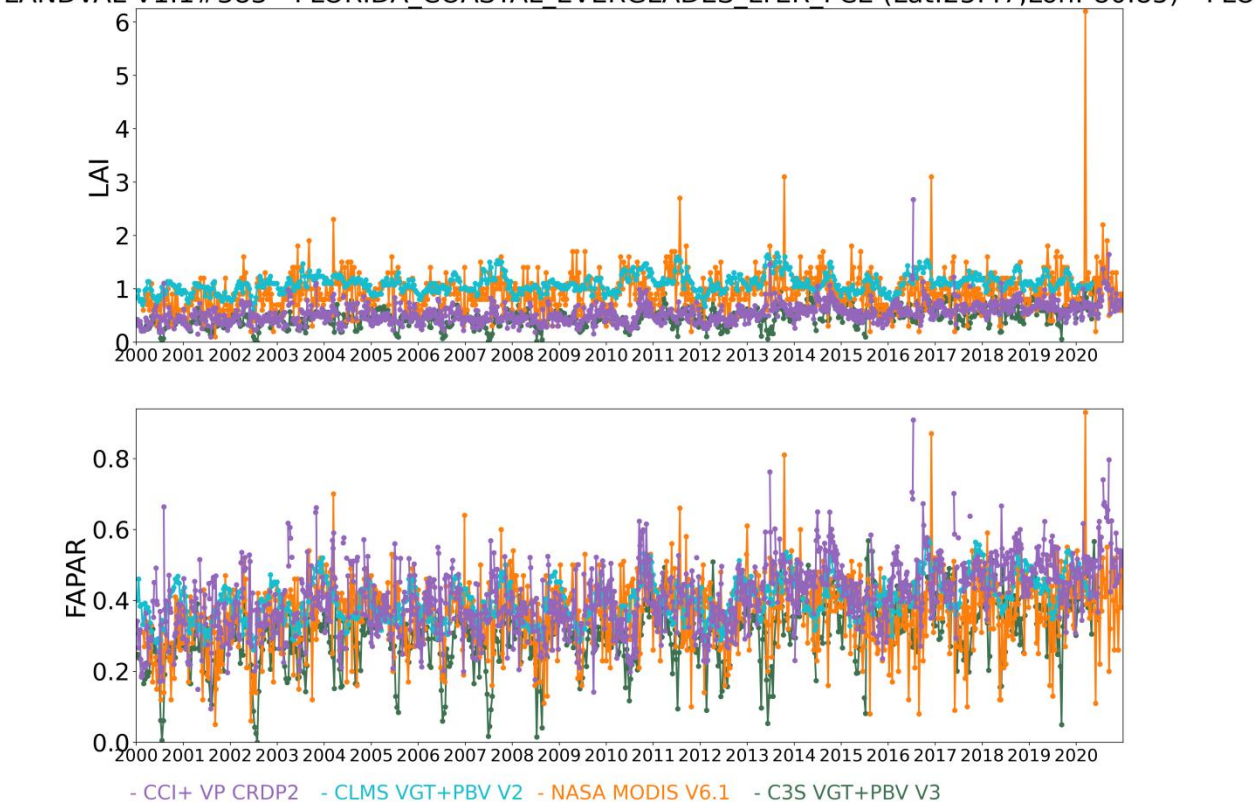
LANDVAL V1.1#383 - FLORIDA_COASTAL_EVERGLADES_LTER_FCE (Lat:25.47,Lon:-80.85) - FLO
LAI
FAPAR
2000 2001 2002 2003 2004 2005 2006 2007 2008 2009 2010 2011 2012 2013 2014 2015 2016 2017 2018 2019 2020
- CCI+ VP CRDP2
- CLMS VGT+PBV V2
- NASA MODIS V6.1
- C3S VGT+PBV V3

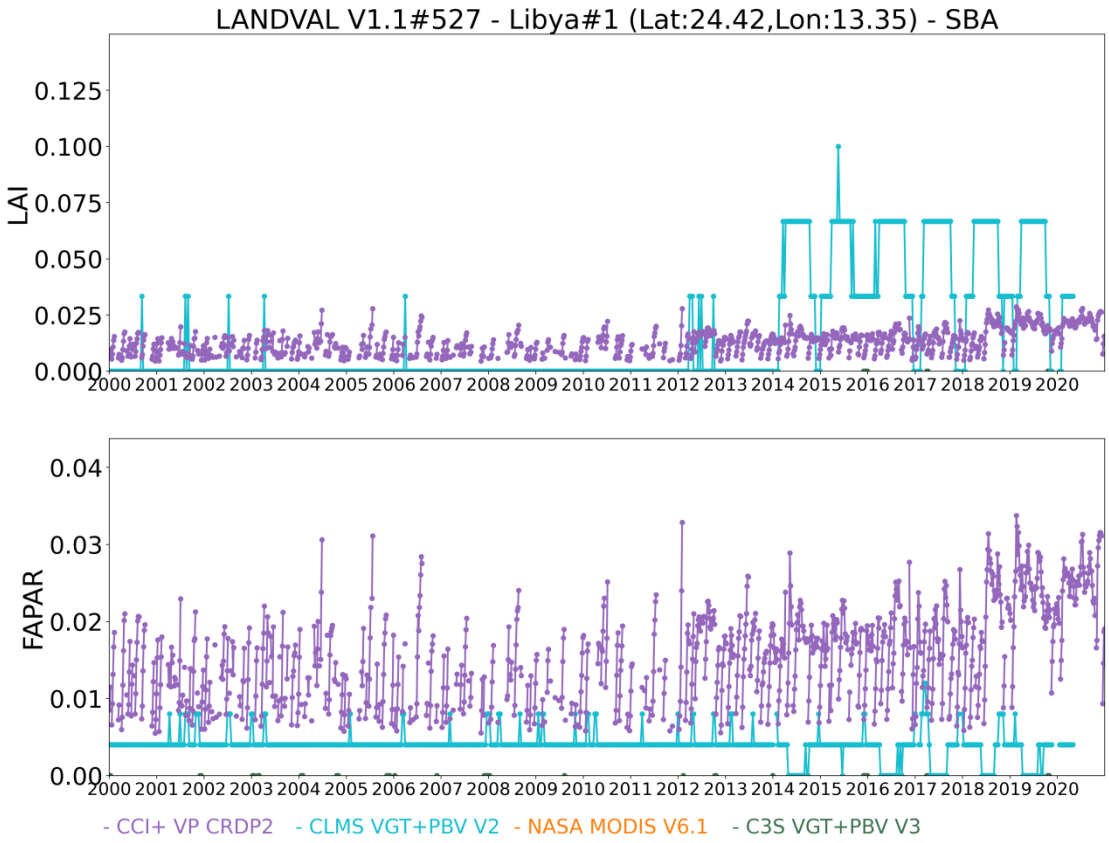
LANDVAL V1.1#527 - Libya#1 (Lat:24.42,Lon:13.35) - SBA
LAI
0.125
0.100
0.075
0.050
0.025
0.000
2000 2001 2002 2003 2004 2005 2006 2007 2008 2009 2010 2011 2012 2013 2014 2015 2016 2017 2018 2019 2020
FAPAR
0.04
0.03
0.02
0.01
0.00
2000 2001 2002 2003 2004 2005 2006 2007 2008 2009 2010 2011 2012 2013 2014 2015 2016 2017 2018 2019 2020
- CCI+ VP CRDP2
- CLMS VGT+PBV V2
- NASA MODIS V6.1
- C3S VGT+PBV V3

Annex II: Scatterplot between CCI+ VP and reference satellite products per biome type

CCI+ VP vs. C3S V3

LAI

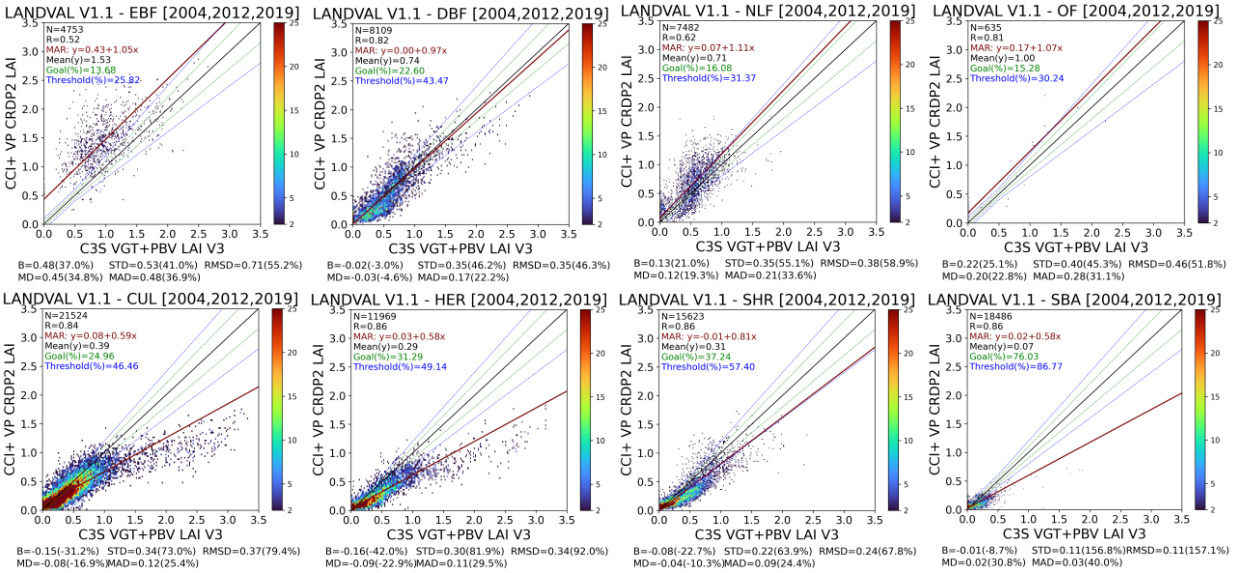

fAPAR

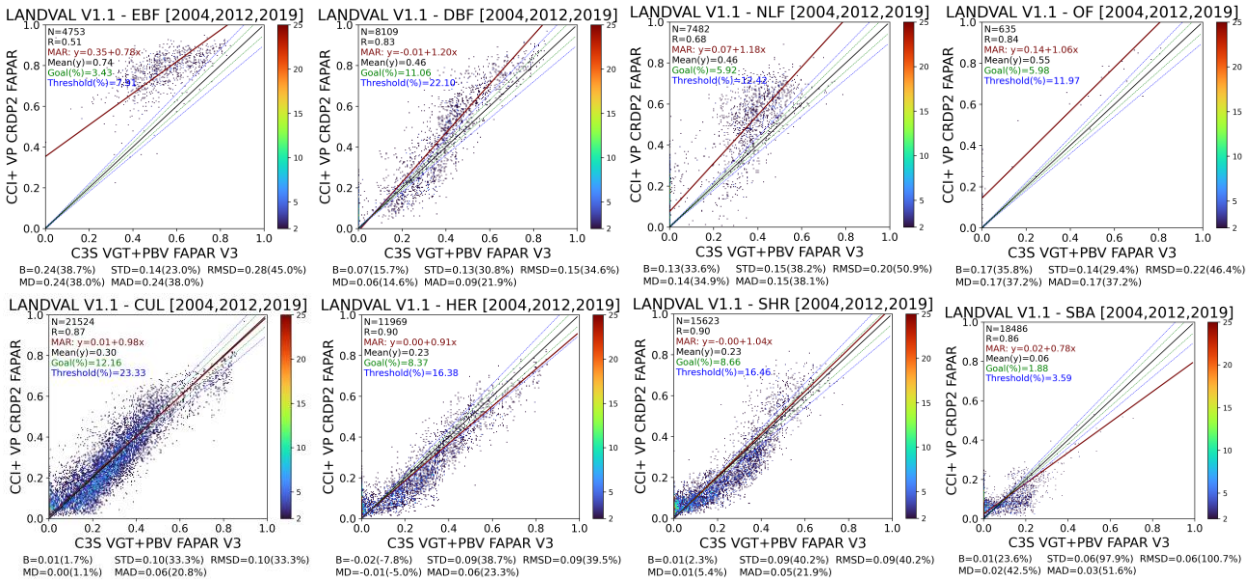

CCI+ VP vs. CLMS V2

fAPAR

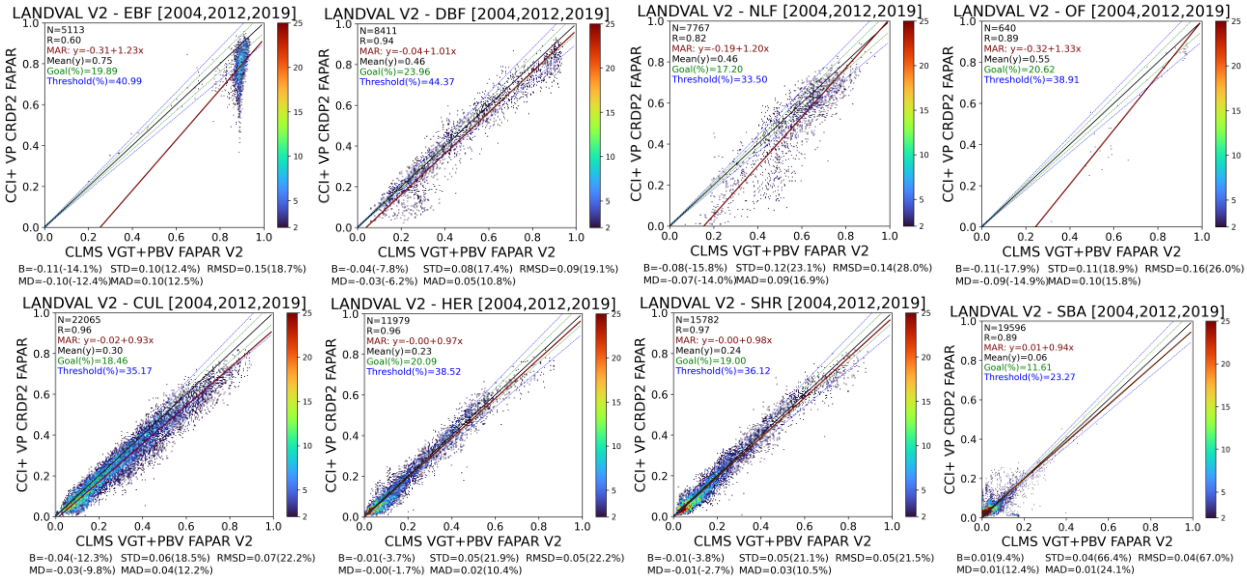

CCI+ VP vs. NASA V6.1

fAPAR

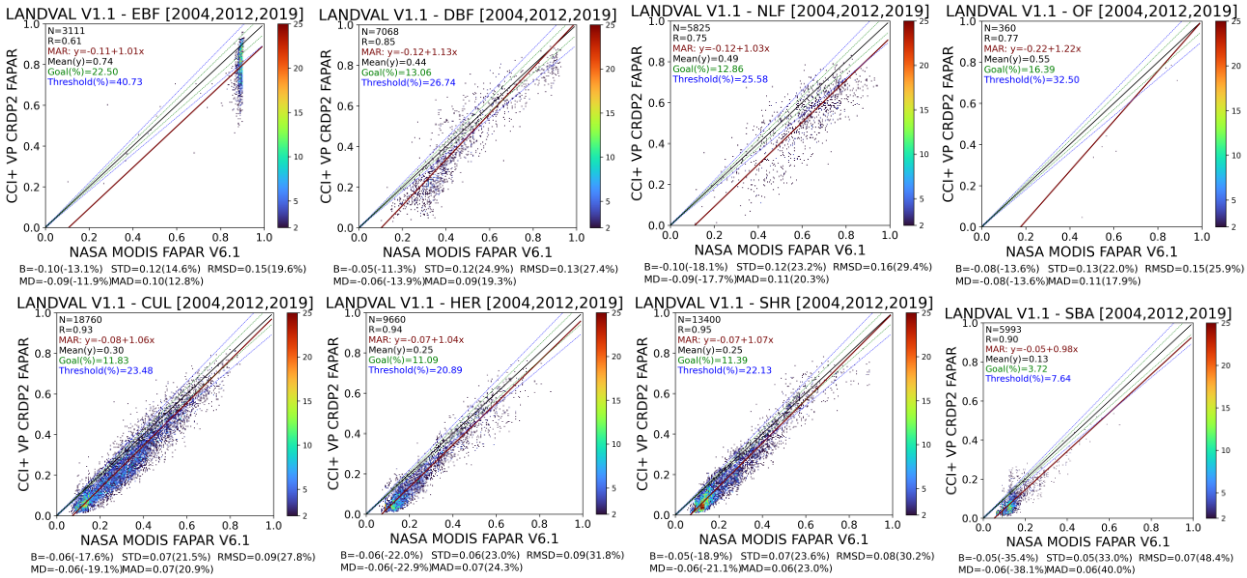

Annex III: Hovmöller plots of the bias with C3S and CLMS fAPAR and over LANDVAL V1.1 sites for BQ retrievals

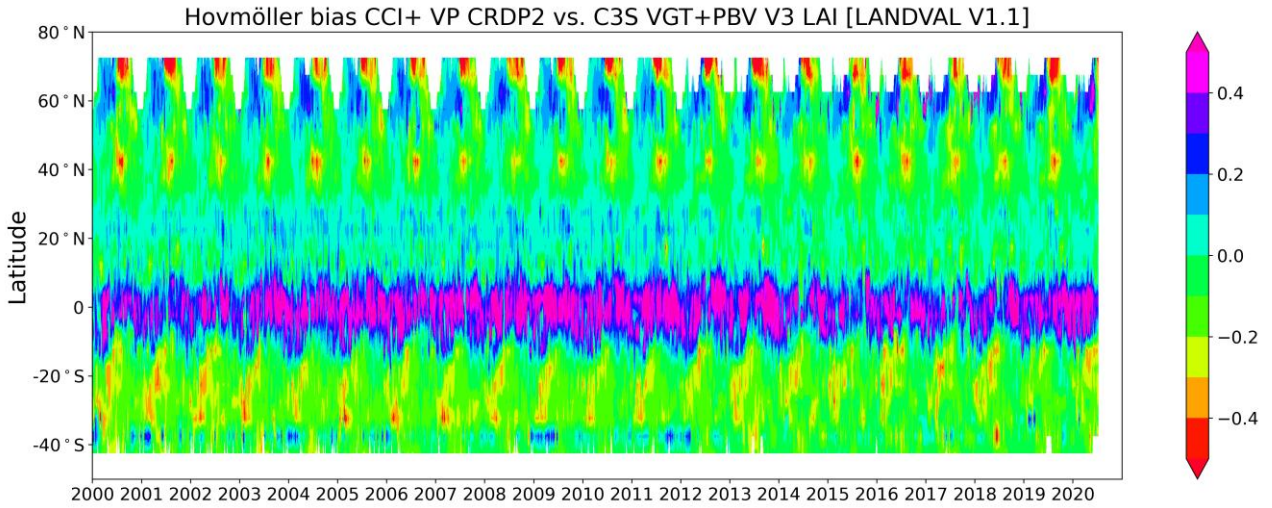

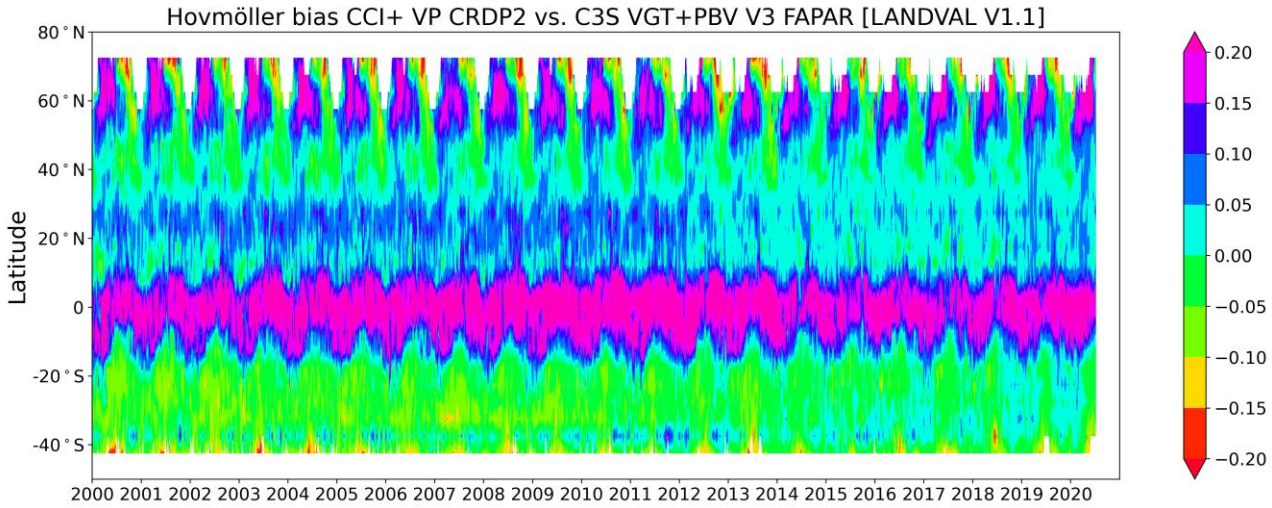

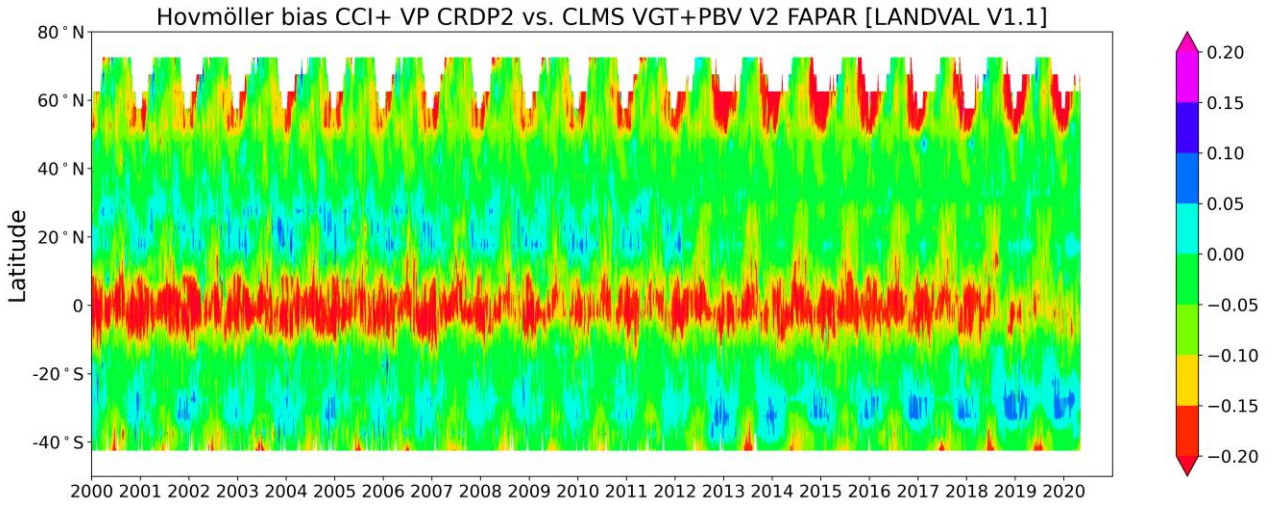

Annex IV: CRDP-2 LAI and fAPAR mean values per biome type across relevant sensor periods

CRDP-2 LAI mean values over BQ pixels LANDVAL V1.1 sites per biome, across relevant sensor periods. N_{mean} stands for number of samples used to estimate the mean, median and percentiles over the relevant periods. N_{tot} stands for total number of best quality observations.

		2000-2007	2008-2011	2012-2017	2018-2020
EBF	N_{mean} /N_{tot}	512/17450	365/16021	438/16853	220/9524
	Mean	1.28	1.35	1.40	1.61
	Median	1.27	1.35	1.39	1.62
	P5	1.05	1.11	1.14	1.38
	P95	1.54	1.64	1.68	1.85
DBF	N_{mean} /N_{tot}	512/20274	365/16876	438/20207	220/10629
	Mean	0.63	0.68	0.72	0.83
	Median	0.55	0.55	0.60	0.69
	P5	0.38	0.37	0.37	0.42
	P95	0.99	1.12	1.20	1.47
NLF	N_{mean} /N_{tot}	512/23317	365/18766	438/21147	220/10859
	Mean	0.51	0.53	0.60	0.62
	Median	0.41	0.43	0.51	0.53
	P5	0.23	0.24	0.26	0.27
	P95	1.00	1.03	1.10	1.19
OF	N_{mean} /N_{tot}	512/1693	365/1480	438/1971	220/986
	Mean	0.73	0.75	0.84	0.91
	Median	0.55	0.60	0.61	0.62
	P5	0.10	0.10	0.12	0.12
	P95	1.75	1.77	1.92	2.11
CUL	N_{mean} /N_{tot}	512/53003	365/41985	438/52520	220/27190
	Mean	0.34	0.37	0.39	0.45
	Median	0.33	0.36	0.37	0.44
	P5	0.21	0.22	0.25	0.30
	P95	0.50	0.57	0.60	0.65
HER	N_{mean} /N_{tot}	512/30362	365/24005	438/28809	220/14847
	Mean	0.25	0.26	0.29	0.33
	Median	0.24	0.24	0.28	0.32
	P5	0.16	0.15	0.18	0.20
	P95	0.37	0.39	0.42	0.47
SHR	N_{mean} /N_{tot}	512/39344	365/30353	438/36370	220/18979
	Mean	0.29	0.30	0.33	0.38
	Median	0.30	0.30	0.34	0.38
	P5	0.22	0.24	0.28	0.31
	P95	0.36	0.36	0.39	0.45
SBA	N_{mean} /N_{tot}	512/39563	365/32141	438/49511	220/26040
	Mean	0.06	0.06	0.06	0.07
	Median	0.06	0.05	0.05	0.06
	P5	0.04	0.04	0.04	0.04
	P95	0.09	0.08	0.09	0.11
FLO	N_{mean} /N_{tot}	512/6710	365/5633	438/6891	220/3562
	Mean	0.41	0.40	0.39	0.43
	Median	0.40	0.40	0.39	0.43
	P5	0.28	0.28	0.27	0.30
	P95	0.58	0.52	0.53	0.56

CRDP-2 fAPAR mean values over BQ pixels LANDVAL V1.1 sites per biome, across relevant sensor periods. N_{mean} stands for number of samples used to estimate the mean, median and percentiles over the relevant periods. N_{tot} stands for total number of best quality observations.

		2000-2007	2008-2011	2012-2017	2018-2020
EBF	N_{mean} /N_{tot}	512/17450	365/16021	438/16853	220/9524
	Mean	0.68	0.70	0.71	0.76
	Median	0.68	0.70	0.72	0.76
	P5	0.61	0.64	0.65	0.70
	P95	0.74	0.76	0.77	0.80
DBF	N_{mean} /N_{tot}	512/20724	365/16876	438/20207	220/10629
	Mean	0.41	0.43	0.45	0.48
	Median	0.38	0.39	0.42	0.46
	P5	0.28	0.28	0.28	0.30
	P95	0.56	0.60	0.63	0.68
NLF	N_{mean} /N_{tot}	512/23317	365/18766	438/21147	220/10859
	Mean	0.36	0.37	0.37	0.38
	Median	0.32	0.33	0.32	0.34
	P5	0.20	0.21	0.19	0.20
	P95	0.60	0.62	0.64	0.66
OF	N_{mean} /N_{tot}	512/1693	365/1480	438/1971	220/986
	Mean	0.44	0.44	0.46	0.48
	Median	0.41	0.42	0.41	0.44
	P5	0.10	0.11	0.12	0.12
	P95	0.80	0.80	0.82	0.86
CUL	N_{mean} /N_{tot}	512/53003	365/41985	438/52520	220/27190
	Mean	0.27	0.29	0.30	0.33
	Median	0.26	0.28	0.29	0.33
	P5	0.18	0.19	0.21	0.24
	P95	0.37	0.40	0.42	0.44
HER	N_{mean} /N_{tot}	512/30362	365/24005	438/28809	220/14847
	Mean	0.20	0.21	0.23	0.25
	Median	0.19	0.19	0.22	0.24
	P5	0.14	0.14	0.16	0.17
	P95	0.28	0.29	0.32	0.34
SHR	N_{mean} /N_{tot}	512/39344	365/30353	438/36370	220/18979
	Mean	0.22	0.23	0.25	0.27
	Median	0.22	0.23	0.25	0.27
	P5	0.18	0.19	0.21	0.24
	P95	0.26	0.26	0.28	0.31
SBA	N_{mean} /N_{tot}	512/39563	365/32141	438/49511	220/26040
	Mean	0.06	0.06	0.05	0.06
	Median	0.06	0.05	0.05	0.06
	P5	0.04	0.04	0.04	0.04
	P95	0.08	0.08	0.08	0.08
FLO	N_{mean} /N_{tot}	512/6710	365/5633	438/6891	220/3562
	Mean	0.31	0.30	0.29	0.31
	Median	0.31	0.30	0.360	0.32
	P5	0.24	0.23	0.22	0.24
	P95	0.38	0.36	0.36	0.38

Annex V: Temporal evolution of bias between CRDP-2 and MODIS fAPAR products evaluated over LANDVAL V1.1 sites best quality per biome type

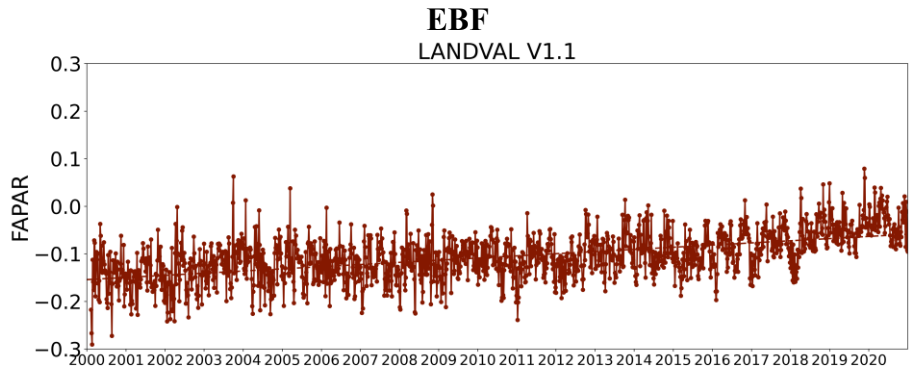

- CCI+ VP CRDP2 vs. NASA MODIS V6.1 (Slope/year:4.5e-03) p-value=0.000 Mann-Kendall result: increasing

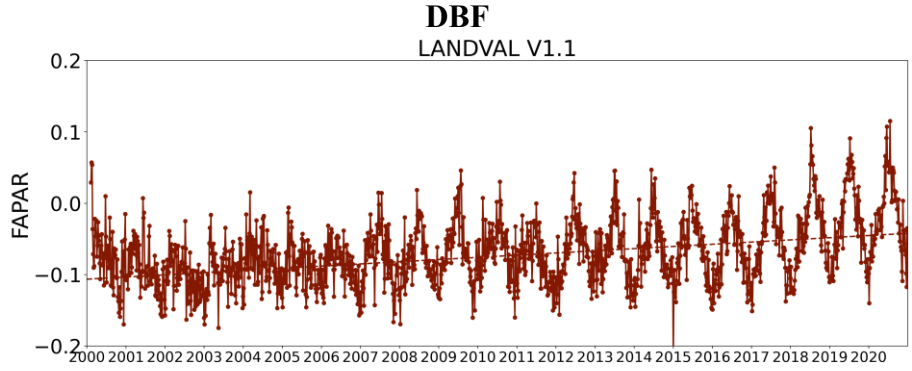

- CCI+ VP CRDP2 vs. NASA MODIS V6.1 (Slope/year:3.1e-03) p-value=0.000 Mann-Kendall result: increasing

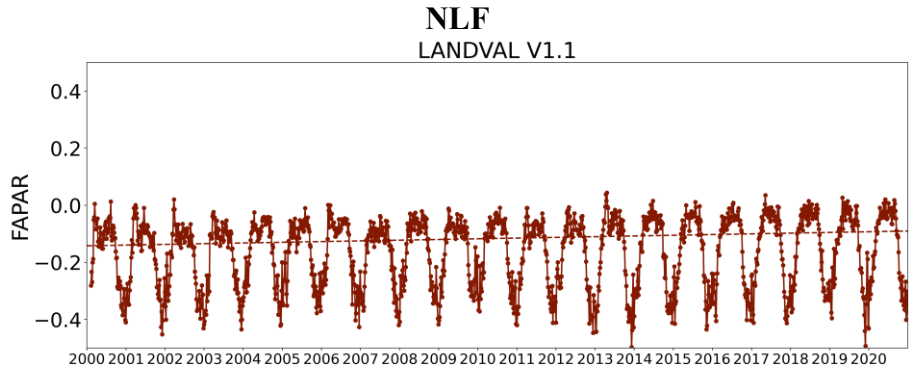

- CCI+ VP CRDP2 vs. NASA MODIS V6.1 (Slope/year:2.5e-03) p-value=0.000 Mann-Kendall result: increasing

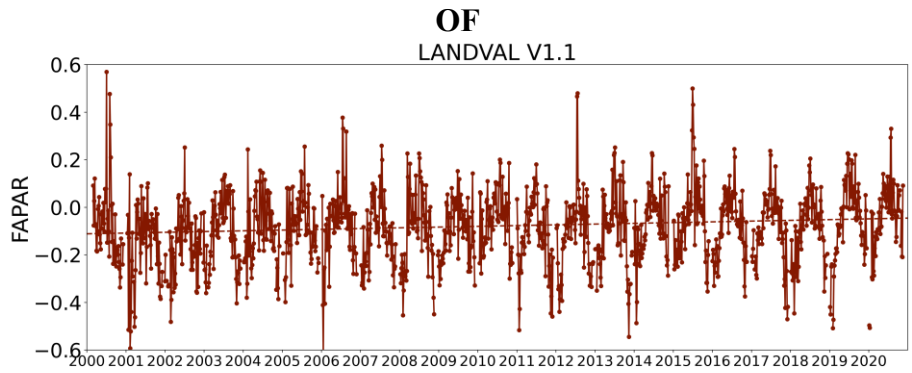

- CCI+ VP CRDP2 vs. NASA MODIS V6.1 (Slope/year:3.1e-03) p-value=0.000 Mann-Kendall result: increasing

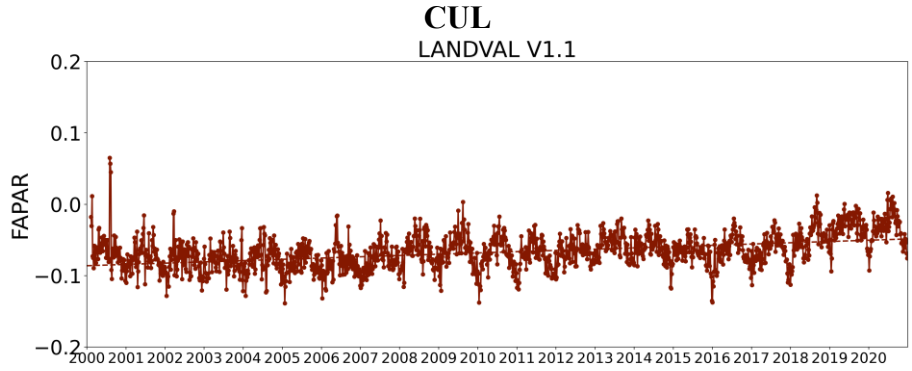

- CCI+ VP CRDP2 vs. NASA MODIS V6.1 (Slope/year:1.8e-03) p-value=0.000 Mann-Kendall result: increasing

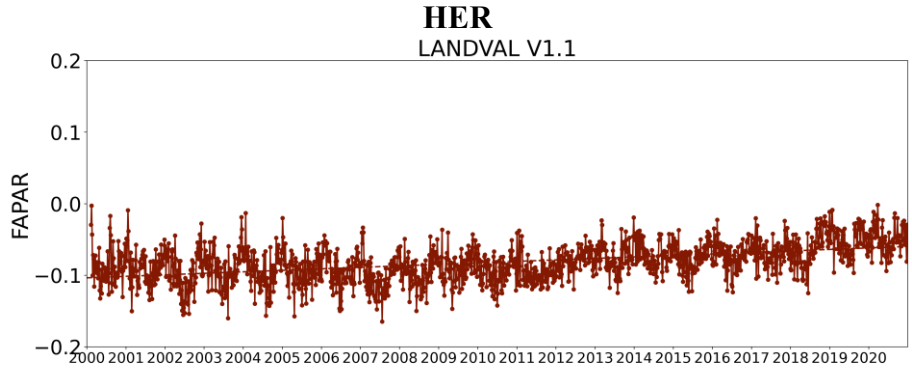

- CCI+ VP CRDP2 vs. NASA MODIS V6.1 (Slope/year:2.1e-03) p-value=0.000 Mann-Kendall result: increasing

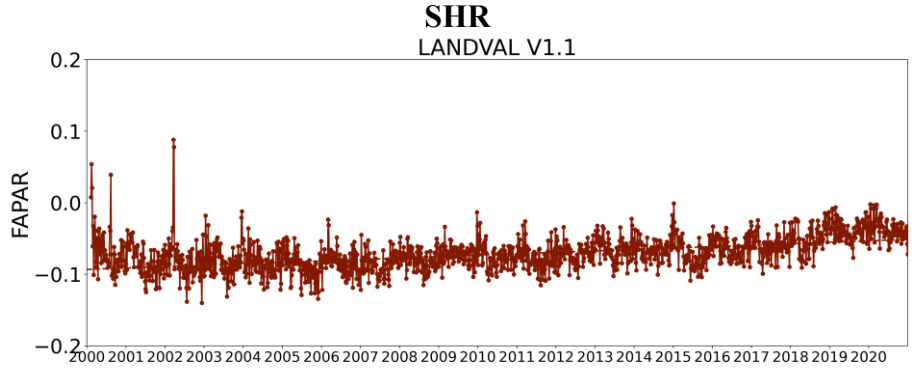

- CCI+ VP CRDP2 vs. NASA MODIS V6.1 (Slope/year:2.0e-03) p-value=0.000 Mann-Kendall result: increasing

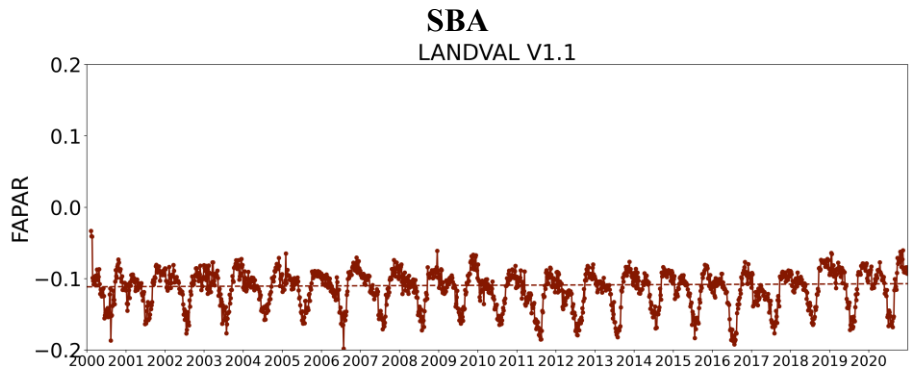

- CCI+ VP CRDP2 vs. NASA MODIS V6.1 (Slope/year:2.1e-04) p-value=0.013 Mann-Kendall result: increasing

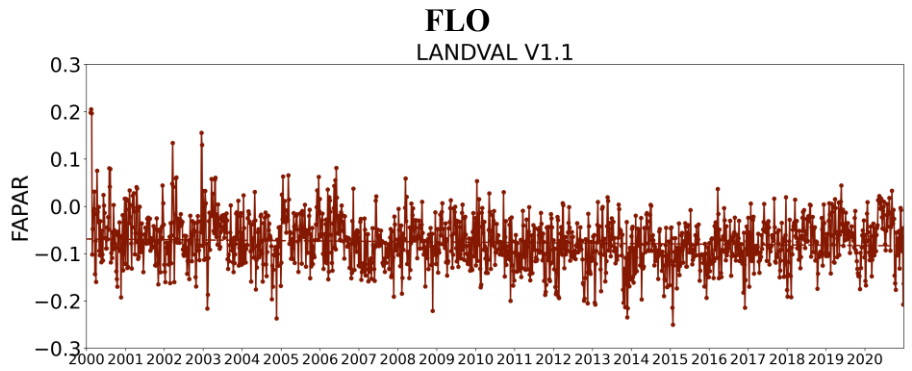

- CCI+ VP CRDP2 vs. NASA MODIS V6.1 (Slope/year:-6.9e-04) p-value=0.003 Mann-Kendall result: decreasing

Annex VI: CRDP-2 vs CRDP-1 LAI, fAPAR product intercomparison